

UCLA

UCLA Electronic Theses and Dissertations

Title

Somatosensory Neuron Subtypes and Sensory Transduction in Larval Zebrafish

Permalink

<https://escholarship.org/uc/item/2tq55242>

Author

Palanca, Ana Marie Silo

Publication Date

2012

Peer reviewed|Thesis/dissertation

UNIVERSITY OF CALIFORNIA

Los Angeles

Somatosensory Neuron Subtypes and Sensory Transduction in Larval Zebrafish

A dissertation submitted in partial satisfaction of the requirements for the degree

Doctor of Philosophy in Molecular, Cell and Developmental Biology

by

Ana Marie Silo Palanca

2012

© Copyright by

Ana Marie Silo Palanca

2012

ABSTRACT OF THE DISSERTATION

Somatosensory Neuron Subtypes and Sensory Transduction in Larval Zebrafish

By

Ana Marie Silo Palanca

Doctor of Philosophy in Molecular, Cell and Developmental Biology

University of California, Los Angeles, 2012

Professor Alvaro Sagasti, Chair

Larval zebrafish are emerging as a model for describing the development and function of simple neural circuits. To analyze somatosensory neuron diversity in larval zebrafish, we identified several enhancers from the zebrafish and pufferfish genomes and used them to create five new reporter transgenes. Sequential deletions of three of these enhancers identified small sequence elements sufficient to drive expression in zebrafish trigeminal and Rohon-Beard (RB) neurons. One of these reporters highlighted a somatosensory neuron subtype that expressed both the *p2rx3a* and *pkcα* genes, as well as a previously described *trpA1b* reporter. To determine whether neurons of this subtype possess characteristic peripheral branching morphologies or central axon projection patterns, we analyzed the morphology of single neurons. Surprisingly, although these analyses revealed diversity in peripheral axon branching and central axon projection, PKCα/*p2rx3a/trpA1b*-expressing RB cells did not possess characteristic

morphological features, suggesting that even within this molecularly defined subtype, individual neurons may possess distinct properties.

Due to their external fertilization, rapid development, and optical clarity, zebrafish larvae are particularly well suited for optogenetic approaches to investigate neural circuit function. Here we demonstrate a procedure for expressing a light-sensitive ion channel in larval zebrafish somatosensory neurons, photo-activating single cells, and recording the resulting behaviors. Specifically, we created a transgene using a somatosensory neuron enhancer to drive the expression of the tagged channelrhodopsin variant, ChEF-tdTomato. Illuminating identified cells in these animals with light from a 473 nm DPSS laser, guided through a fiber optic cable, elicited behaviors that can be recorded with a high-speed video camera and analyzed quantitatively. By introducing a few modifications to previously established methods, this approach was used to elicit behavioral responses from single neurons activated up to at least 4 days post-fertilization (dpf). The new transgenes created in this study will be powerful tools for further characterizing the molecular, morphological, and development diversity of larval somatosensory neurons and in combination with genetic or pharmacological perturbations will be a powerful way to investigate circuit formation and function.

The dissertation of Ana Marie Silo Palanca is approved by

Frank A. Laski

William Lowry

Bennet G. Novitch

Patricia Phelps

Alvaro Sagasti, Committee Chair

University of California, Los Angeles

2012

DEDICATION PAGE

This dissertation is dedicated to my nieces and nephews.

“The higher the goal, the harder the climb, but taken each day, one step at a time. The goal is accomplished, the dream is attained, and the prizes? The wisdom and strength that are gained.”

- American Greeting Cards

TABLE OF CONTENTS

ABSTRACT	ii
COMMITTEE PAGE	iv
DEDICATION PAGE	v
TABLE OF CONTENTS	vi
LIST OF TABLES AND FIGURES	viii
ACKNOWLEDGEMENTS	x
VITA	xi
CHAPTER 1	
Introduction to somatosensation	1
References	16
CHAPTER 2	
New transgenic reporters identify somatosensory neuron subtypes in larval zebrafish ..	26
Introduction	27
Materials and Methods	29
Results	33
Discussion	43
Acknowledgments	46
References	47
Tables and Figures	53
Supplementary Methods	69
Supplementary Tables and Figures	75
CHAPTER 3	
Characterization of TrkA-expressing sensory neurons in larval zebrafish	80
Introduction	81
Materials and Methods	82
Results	85

Discussion	89
Acknowledgments	92
References	93
Tables and Figures	95
 CHAPTER 4	
Optogenetic activation of zebrafish somatosensory neurons using ChEF-tdTomato ...	105
Introduction	106
Procedure	108
Results/Discussion	115
Acknowledgements	117
References	118
Figures	120
 CHAPTER 5	
Concluding remarks	131
References	137

LIST OF TABLES AND FIGURES

CHAPTER 2

Chapter 2 Table 1	53
Chapter 2 Figure 1	54
Chapter 2 Figure 2	55
Chapter 2 Figure 3	57
Chapter 2 Figure 4	59
Chapter 2 Figure 5	61
Chapter 2 Figure 6	63
Chapter 2 Figure 7	65
Chapter 2 Figure 8	67
Chapter 2 Supplementary Figure 1	75
Chapter 2 Supplementary Table 1	77
Chapter 2 Supplementary Table 2	78
Chapter 2 Supplementary Table 3	79

CHAPTER 3

Chapter 3 Figure 1	95
Chapter 3 Figure 2	96
Chapter 3 Table 1	97
Chapter 3 Figure 3	98
Chapter 3 Figure 4	99
Chapter 3 Figure 5	100
Chapter 3 Figure 6	101
Chapter 3 Figure 7	102
Chapter 3 Figure 8	103

CHAPTER 4

Chapter 4 Figure 1	120
Chapter 4 Figure 2	121

Chapter 4 Figure 3	122
Chapter 4 Figure 4	123
Chapter 4 Figure 5	124
Chapter 4 Figure 6	125
Chapter 4 Figure 7	126
Chapter 4 Figure 8	127
Chapter 4 Figure 9	128
Chapter 4 Figure 10	129
Chapter 4 Figure 11	130

ACKNOWLEDGMENTS

I would like to thank my Mom, Dad, Kuya, Ate Amy, Iolo, Anya, Lola and Lolo, for taking care of me. Ate Stella, Ryan, and JP, for always being there. Auntie Helen and Uncle Lito, for never doubting. Yara, Cindy, Marla, Allison, Nancy, Myra, and Muoy, for befriending the shy, studious girl. Adrian, Angelo, James, Mitch and John, for making a good thing better. Yana, Maggie, Faith, Christine, Julie, Jessica, Seanna, Georgeann, Matt, Aya and Xiaoyu, for understanding.

Thank you to the Jacobsen Lab, for providing me with a solid scientific foundation and to the Sagasti Lab, for helping me build upon that foundation.

Chapter 2 is a version of the research article published in *Developmental Neurobiology*, 2012, entitled “New transgenic reporters identify somatosensory neuron subtypes in larval zebrafish” authored by Ana Marie S. Palanca, Sung-Ling Lee, Laura E. Yee, Carlee Joe-Wong, Le A. Trinh, Elizabeth Hiroyasu, Majid Husain, Scott E. Fraser, Matteo Pellegrini and Alvaro Sagasti.

Chapter 4 is a version of the research article submitted and under review in *The Journal of Visualized Experiments*, 2012, entitled “Optogenetic activation of zebrafish somatosensory neurons using ChEF-tdTomato” authored by Ana Marie S. Palanca and Alvaro Sagasti.

Funding for this dissertation was provided by an NRSA award (5F31NS064817) from the NINDS to Ana Marie S. Palanca and grants from the NSF (RIG:0819010) and NIDCR (5R01DE018496) to Alvaro Sagasti.

VITA

Education

- Bachelor's Degree in Molecular, Cell and Developmental Biology, University of California, Los Angeles. September 2001-June 2005.

Research Experience

- Characterization of putative histone methyltransferases (SuvH proteins) and methyl-binding domain proteins in *Arabidopsis thaliana*, June 2003-September 2007.

Publications

- New transgenic reporters identify somatosensory neuron subtypes in larval zebrafish. *Developmental Neurobiology*. August 2012.
- Optogenetic activation of zebrafish somatosensory neurons using ChEF-tdTomato. *Journal of Visualized Experiments*. In review, July 2012.

Oral Presentations

- Department of Molecular, Cell and Developmental Biology Research Conference. Lake Arrowhead, CA. December 2011.
- Department of Molecular, Cell and Developmental Biology Fourth Floor Meeting. UCLA. May 2008, September 2009, November 2010, and February 2012.
- Brain Research Institute Zebrafish Affinity Club. UCLA. March 2011 and February 2012.
- Department of Molecular, Cell and Developmental Biology Graduate Student Seminar. UCLA. May 2009 and June 2011.

Poster Presentations

- EMBO Conference Series on The Assembly and Function of Neuronal Circuits. Ascona, Switzerland. September 2011.

- Department of Molecular, Cell and Developmental Biology Research Conference. Lake Arrowhead, CA. November 2007, November 2008, November 2009, and December 2010.
- 9th International Conference on Zebrafish Development & Genetics. Madison, WI. June 2010.
- 8th International Conference on Zebrafish Development & Genetics. Madison, WI. June 2008.

Teaching Experience

- Teaching Assistant. Neurobiology Course: Neuronal Cell Biology. Marine Biological Laboratory, Woods Hole, MA. July 2011.
- Graduate Teaching Assistant. Life Science 3: Introduction to Molecular Biology. University of California, Los Angeles. Fall 2007 and Fall 2008

Work Experience

- Laboratory Assistant III. Laboratory of Stephen E. Jacobsen. Department of Molecular, Cell and Developmental Biology/Howard Hughes Medical Institute. University of California, Los Angeles. June 2005-September 2006.

Awards, Research Programs and Traineeships

- Ruth L. Kirschstein National Research Service Award Predoctoral Fellowship. August 2009- July 2012.
- Minority Access to Research Careers Undergraduate Student Training in Academic Research Program. June 2003-June 2005.
- UCLA Science, Engineering and Mathematics Summer Program for Undergraduate Research. 2003 and 2004.
- Undergraduate Research Development Stipend Award. January 2003-June 2003.
- CARE Scholars Award. October 2002.
- NIH/CARE BISEP Biomedical Summer Enrichment Program,. June 2002-August 2002.

Chapter 1

Introduction to somatosensation

Touch

Of your five senses (hearing, sight, smell, touch and taste), which could you live without? Conversely, if you had to lose 4 of your 5 senses, which would you keep? When I posed this question to my friends and family, most said that they would give up either their sense of taste or hearing, but could not live without their sense of sight. Before graduate school, I probably would have agreed. However, knowing what I know now, I would still say I could live without the sense of taste, but the one sense I would not give up is touch.

The sense of touch is possibly the most over utilized yet underappreciated sense we have. Touch is not just a casual handshake, a mother's comforting caress, or a friendly hug. It is not just the difference between sand paper and silk. It is the smooth sensation of water as you swim in the ocean, the breeze that cools you down on a hot summer day and the warmth of a fire on a cold winter's night. The sense of touch is what warns you against a hot pan on the stove or even a close encounter with a sharp knife. It tells you when you have been injured and when you have healed. Touch can be calming or catastrophic. It can be reassuring or repulsive. Touch plays an important role in how we feel and what we feel.

Now, think of a world without the sense of touch. Sure, you would not feel the sharp pain of a paper cut or the scorching heat of the summer sun, but you would also miss out on the refreshing feeling of walking into an air-conditioned room, or the softness of a baby's skin. Without the sense of touch, how can you be sure a heat block is hot enough? Or the refrigerator is cold enough? How would you know when you have broken a nail or stubbed your toe? Without the sense of touch, day-to-day tasks would become more difficult, less enjoyable and quite possibly very dangerous.

How do we feel?

Touch sensation is carried out by the somatosensory system and is detected by two major neuronal populations, the trigeminal ganglia in the head and the dorsal root ganglia (DRG) along the spine. The sense of touch can be further divided into three categories: mechanical, thermal and nociceptive. These different sensations are detected by specific sensors and/or receptors associated with each somatosensory neuron. Mechanoreceptors process varying levels of pressure and movement, thermoreceptors detect a range of temperatures, and nociceptors sense noxious or painful stimuli that can be mechanical, thermal or chemical. The ability of specific somatosensory neurons to discriminate and process distinct sensory stimuli is influenced by the territories in which their peripheral arbors innervate the skin, their diameter, the sensory receptors they express and how they connect to the central nervous system (Lumpkin and Caterina, 2007; Marmigère and Ernfors, 2007; Boulais and Misery, 2008).

The anatomy of touch

Characterization of mechanoreceptors started more than a century ago by 19th century anatomists. The most superficial mechanoreceptors, Meissner's corpuscles, are located just below the epidermis and detect light touch (CAUNA and ROSS, 1960). Merkel cells also detect light touch and discriminate texture and shape (Boulais and Misery, 2007). Ruffini endings are located deep within the skin and detect deep, sustained pressure (Halata and Munger, 1981). Pacinian corpuscles are located deeper within the skin and are sensitive to vibration and pressure. These sensory organs are innervated by A β nerve fibers, myelinated low-threshold fibers that are large (6-12 μm) in diameter. Thermosensation is mediated by A δ and C nerve fibers. A δ fibers are lightly myelinated, medium diameter (1-5 μm) neurons while C fibers are unmyelinated,

small diameter (0.2-1.5 μm) neurons. Thermoreceptors detect a range of temperatures, depending on the receptors they express. Nociceptors are mainly high-threshold, unmyelinated C fibers that sense painful or noxious stimuli. Some $\text{A}\beta$ and $\text{A}\delta$ mechanoreceptors are also nociceptive in that they detect significant pressure and other noxious mediators. Thermoreceptive and nociceptive $\text{A}\delta$ and C fibers are mainly free ending somatosensory neurons. These free nerve endings innervate the epidermis and branch within the epidermal layer to create a comprehensive receptive field along the skin (Lumpkin and Caterina, 2007; Boulais and Misery, 2008).

Molecular mechanisms of somatosensation

Detection and transmission of specific sensory stimuli depend on proper development of somatosensory neurons as well as expression of specific sensory molecules. Tropomyosin-related kinase (Trk) receptors recognize specific neurotrophins, secreted growth factors that are capable of eliciting cell survival, differentiation and growth responses in neurons. Three Trk receptors (TrkA, TrkB and TrkC) are expressed in somatosensory neurons and each is responsible for the survival and normal development of a specific subset of sensory neurons (Ernfors et al., 1994; Ernfors et al., 1994; Snider and Silos-Santiago, 1996; Liu and Jaenisch, 2000; Huang and Reichardt, 2001). Different subsets of somatosensory neurons not only express distinct Trk receptors, but the pattern of Trk receptor expression also changes temporally during sensory neurogenesis and differentiation. For example, TrkC neurons appear earliest, increasing in abundance as TrkB neurons appear, followed by a significant decrease in both TrkB and TrkC expressing neurons as TrkA expressing neurons become more prevalent (Rifkin et al., 2000). In the adult somatosensory system, 40-45% of neurons express TrkA, less than 10% express TrkB,

15-20% express TrkC, and the remaining 25-35% of neurons do not express any of the Trk receptors. TrkA positive neurons are the unmyelinated (A δ fiber) and lightly myelinated (C fiber) nociceptive neurons that are predominately medium and small in diameter, respectively. TrkC positive neurons are proprioceptive and are mainly myelinated, large diameter (A β fiber) neurons. TrkB positive neurons are intermediate in cell size, and overlap to some degree with TrkA or TrkC positive populations (Snider and Silos-Santiago, 1996).

Peripheral axon innervation and laminar organization of dorsal root projections also characterize distinct subtypes of somatosensory neurons. Different Trk-expressing DRG neurons project to distinct lamina in the dorsal horn of the spinal cord. TrkA (A δ and C fiber) neurons project to lamina I and II_o (Molliver et al., 1995), whereas TrkB neurons have been shown to project to lamina II_i (Salio et al., 2005) and TrkC neurons project to lamina III, IV and V. The connectivity of these Trk-expressing neurons to specific lamina in the spinal cord suggests that they associate with different downstream neurons, participate in different neural circuits, and are therefore responsible for distinct cognitive and behavioral responses.

Subset specific somatosensory development is dependent on neurotrophin signaling. For example, the TrkA receptor/NGF signaling has been associated with a number of cellular processes including cell survival and neurite outgrowth. In TrkA knockout mice, a subset of DRG neurons do not survive during development (Silos-Santiago et al., 1995; Fagan et al., 1996). To overcome this cell death phenotype, BAX knockout mice were crossed to TrkA knockout mice. BAX transgenics do not undergo apoptosis (Suzuki et al., 2010), thereby circumventing the cell death phenotype in TrkA deficient mice. Double transgenics, deficient for both BAX and TrkA, develop somatosensory neurons, however, these neurons do not express the appropriate nociceptive peptides, nor do they innervate the appropriate peripheral territories

(Patel et al., 2000). Moreover, changes in expression level of TrkA/NGF signaling in humans have been implicated in a number of peripheral neuropathies (Anand, 1995).

The ability of sensory neurons to discriminate particular stimuli depends on expression of appropriate sensory molecules. For example, TrkA positive/nociceptive neurons can be further categorized by the expression of additional genes, such ion channels and neuropeptides. The most widely studied family of ion channels is the transient receptor potential (TRP) channels. Members of the TRP super-family detect a wide range of thermal and chemical stimuli. For example, TRPV receptors detect vanilloid compounds and high temperatures. TRPV1 (formerly VR1 in mammals) is a receptor for capsaicin and temperatures above 43°C while TRPV2 senses noxious temperatures above 52°C and TRPV3 senses warm temperatures between 33-39°C (Julius and Basbaum, 2001; Tominaga and Caterina, 2004; Tominaga, 2007). Cold temperatures, on the other hand, are detected by TRPM8, which is also the receptor for menthol (Bautista et al., 2007; Foulkes and Wood, 2007). Other pungent chemicals such as mustard oil, wasabi, wintergreen and cinnamaldehyde activate TRPA1 (Bandell et al., 2004; Bautista et al., 2006; del Camino et al., 2010), which has also been implicated to play a role in mechanosensation (Corey et al., 2004). Previous studies also suggested that TRPA1 detects cold temperatures (Bandell et al., 2004; Kwan and Corey, 2009), however, recent findings contest this idea (Bautista et al., 2006).

Other well-characterized nociceptive molecules include neuropeptides and P2X receptors. Substance P (SP) and calcitonin gene related peptide (CGRP) are two neuropeptides that function as neurotransmitters in subsets of TrkA-positive neurons (Skofitsch and Jacobowitz, 1985; Oku et al., 1987; Pedersen-Bjergaard et al., 1991; Snider and McMahon, 1998; DeVane, 2001; Orita et al., 2010). They are the main signaling molecules involved in

sensing pain. TrkA knockout mice do not express SP and CGRP (Patel et al., 2000). P2X receptors are ATP-gated ion channels (purinoceptors) (North, 2004). Analysis of the expression patterns of the seven P2X receptors revealed that one member, P2X3, is expressed predominantly in nociceptive neurons and a subset of axon terminals in the dorsal spinal cord (Chen et al., 1995; Bradbury et al., 1998; Xiang et al., 1998), indicating a role in the detection of pain and attracting interest as a target for novel analgesics (Chizh and Illes, 2001).

While the molecular mechanisms of thermosensation and chemosensation have been extensively studied, molecules involved in mechanosensation are less understood. TRP channels, mainly TRPA1 and TRPV4, have been implicated in mammalian mechanotransduction (Mizuno et al., 2003; Suzuki et al., 2003; Suzuki et al., 2003; Corey et al., 2004; Brierley et al., 2009; Kwan et al., 2009). In mice, TRPA1 is expressed at Meissner's corpuscles (Kwan et al., 2009) and TRPV4 is expressed at Ruffini-like endings, Merkel cells and Meissner's corpuscles (Suzuki et al., 2003). Furthermore, knockout mice of both TRPA1 and TRPV4 result in increased response threshold to strong mechanical stimuli (Suzuki et al., 2003; Kwan et al., 2009). Genetic screens in *C. elegans* identified acid-sensing ion channels (ASICs), an H⁺-gated subset of the degenerin/epithelial Na⁺ channel (DEG/ENaC) superfamily, as putative molecules for mechanosensation (Goodman et al., 2002). In mice, ASIC1, ASIC2 and ASIC3 are expressed in A β and A δ fibers. ASIC1 and ASIC3 are also expressed in C fibers. ASIC1 and ASIC2 are associated with Pacinian corpuscles in humans (Montaño et al., 2009; Calavia et al., 2010), while ASIC2 and ASIC 3 expression is also found at Meissner's corpuscles, Merkel cells and free nerve endings (Price et al., 2001). Knockout mice of each of these genes, however, show subtle to no change in mechanosensory sensitivity (Price et al., 2001; Price et al., 2004; Roza et al., 2004; Page et al., 2005). Possible redundancy of function prompted Kang, et al to

create an ASIC1/ASIC2/ASIC3 triple knockout. Surprisingly, the triple knockout showed an increase in cutaneous mechanosensitivity, suggesting that ASICs are involved in mechanosensation, but that they do not directly transduce mechanical stimuli (Kang et al., 2012). This wide array of molecular markers emphasizes the complexity of somatosensory neuron specification in vertebrate models.

Peripheral neuropathies

Defects in any sensory component can result in a range of debilitating disorders collectively known as peripheral neuropathies. Two categories of peripheral neuropathies are hyperalgesia, an increased sensitivity to pain and hypoalgesia, a heightened threshold for normally painful stimuli. Peripheral neuropathies can occur as secondary effects of various disorders and/or their treatments, such as with diabetes and HIV, while in many cases, they are idiopathic.

A world of pain

Hyperalgesia, a heightened sensitivity to painful or noxious stimuli and allodynia, a painful response to a normally innocuous stimulus, takes many forms (LaMotte et al., 1991; LaMotte et al., 1992; Shu and Mendell, 1999). Allodynias can be categorized into three main types: static mechanical allodynia, dynamic mechanical allodynia and thermal allodynia. Static mechanical allodynia refers to pain caused by light touch or pressure. Dynamic mechanical allodynia refers to pain caused by light touch or pressure. Thermal allodynia refers to pain from normally mild hot or cold stimuli. For example, extensive exposure of the skin to ultraviolet (UV) irradiation, also known as sunburn, often leads to increased sensitivity of the affected

region to certain stimuli. While putting on a shirt would normally be painless, performing the same task over a sunburn could be extremely painful. Fibromyalgia is a common syndrome that is associated with long-term, body-wide pain and tenderness in the joints, muscles, tendons and other soft tissues. This disorder is common among women between the ages of 20 and 50 and the cause is unknown (Price and Staud, 2005; Staud, 2007; Staud, 2009; Staud, 2011).

A world without pain

Most people would describe pain as an unpleasant feeling. However, the ability to perceive pain is the body's way of preventing further or more harmful injury and it is important for basic survival. Congenital insensitivity to pain with anhidrosis (CIPA), also called hereditary sensory and autonomic neuropathy (HSAN) type IV, is a rare autosomal recessive peripheral neuropathy. This disorder has been linked to mutations in TrkA (or NTRK1) that affects A δ and C fiber development (Indo et al., 1996). Patients born with CIPA can sense touch and pressure but cannot sense pain and also have problems with thermoregulation. In young CIPA patients, self-mutilation occurs as early as infancy, leading to extensive skin ulcers, bone fractures and joint malformations (Manor et al., 2012; Prashanth and Kamate, 2012). In patients that survive past childhood, daily tasks present life-threatening obstacles and they often experience trauma, bone fractures and osteomyelitis as a result of their insensitivity to pain (Labib et al., 2011). Without the ability to feel pain, it is difficult to determine whether something is harmful or if one has already been injured.

Peripheral diabetic neuropathy (PDN) occurs in at least 50% of diabetic patients in the United States. According to the National Diabetes Statistics, 2011 provided by the National Institute of Diabetes and Digestive and Kidney Diseases (NIDDK), diabetes affects 25.8 million

people of all ages in the United States. Approximately 60% of people with diabetes suffer from mild to severe forms of nervous system damage, including impaired sensation in the hands or feet. Diabetic neuropathies are also the leading cause for non-traumatic lower-limb amputations (<http://diabetes.niddk.nih.gov/dm/pubs/statistics/>).

A better understanding of the molecular mechanism underlying somatosensation, and pain in particular, would provide entry points for therapeutic intervention of many peripheral neuropathies. Extensive research has gone into cataloguing different subtypes of sensory neurons based on their molecular profiles. However, the mechanisms by which sensory neuron subtypes identify, process and transmit different kinds of sensory information are still under investigation. Disease based trials of therapeutic drugs have advanced the treatment of certain peripheral neuralgias, but because somatosensory cells are molecularly and functionally heterogeneous, effective treatments for one neuropathic disorder will not necessarily have the same affect for other disorders. Therefore, treating these disorders will require understanding how different sensory subtypes are determined and how they process and discriminate distinct sensory inputs.

Somatosensation in early mammalian development

Somatosensation is important very early in development. Observations in twin pregnancies provide evidence that tactile sensation first arises at approximately 7 weeks of gestation and develops from anterior to posterior (Lowery et al., 2007; Salihagić Kadić and Predojević, 2012). It is difficult to determine to what level an infant may sense and process its surroundings, yet it is evident that the sense of touch arises very early in development.

Somatosensation in other organisms

More extensive studies in mammalian systems have been difficult to pursue due to the invasiveness of prenatal analyses and limitations of *in vivo* experimentation. These issues have provided an entry point for extensive research in other organisms. The conservation of sensory function and homology of many sensory genes across several model organisms, in addition to the availability of more efficient genetic tools, has led to breakthroughs using genetic manipulation and *in vivo* analyses in other vertebrate and invertebrate organisms.

The process by which sensory neurons develop and determine their peripheral territories has been widely studied in leech, *Drosophila* and *Xenopus* larvae. In these organisms, each peripheral sensory neuron arborizes in a discrete region of the skin. Often, mutually repulsive interactions between developing peripheral arbors are used to limit arborization, allowing each sensory neuron to innervate discrete territories with minimal overlap. This process, by which mutually exclusive territories are formed, is referred to as “tiling”. Studies in both invertebrates and vertebrates have shown that different types of sensory neurons tile independently of one another. In leech, three functionally distinct types of sensory neurons, called touch (T), pressure (P) and nociceptive (N) neurons, tile independently. When either N or T cells were specifically ablated, the receptive territories of other neurons of that specific subclass expanded, but not those of the other subclasses (Blackshaw et al., 1982). Similarly, in *Drosophila*, morphologically distinct sensory neuron subtypes tile independently of one another. *Drosophila* dendritic arborization (da) neurons have been classified into four subclasses (Class I, II, III, and IV) based on the increasing complexity of their branching patterns. Peripheral arbors of different classes of dda neurons overlap extensively, but there is little dendritic overlap among cells of the same

morphological class, suggesting that distinct classes of sensory neurons only recognize axons of the same class (Grueber et al., 2002; Grueber et al., 2003; Grueber and Jan, 2004). Subtype-specific ablation of Class IV ddaC sensory neurons resulted in only ddaC neurons innervating the voided territory, while other da neurons were unaffected (Sugimura et al., 2003).

Subclass-specific tiling also occurs among vertebrate somatosensory neurons. For example, studies in *Xenopus* larvae suggest that competitive interactions among similar sensory neuron types determine the pattern of arborization. One functionally distinct subclass of *Xenopus* trigeminal neurons, known as Type I “movement” detectors inhibit swimming behavior and their peripheral arbors have many fine branches with numerous large varicosities, whereas Type II “rapid transient” detectors stimulate behavior and their peripheral arbors have few relatively straight branches with elongated varicosities (Roberts, 1980; Kitson and Roberts, 1983). Type I “movement detectors,” repel each other at the dorsal midline, limiting their territories to the ipsilateral side of the head, whereas Type II “rapid transient detectors,” often cross the midline (Kitson and Roberts, 1983). Together, these studies show that specific subtypes of sensory neurons tile independently of one another, and use different strategies for selecting their receptive territories.

Somatosensation in zebrafish

Current studies have made considerable advances in the identification of sensory neuron subtypes based on their molecular and functional characteristics. However, little is known about how these different subtypes are optimized to recognize specific stimuli and elicit distinct behaviors. Zebrafish have three populations of peripheral sensory neurons in zebrafish. Trigeminal (TG) sensory neurons that innervate the head, a transient population of Rohon-Beard

(RB) neurons that innervate the body, and dorsal root ganglia (DRG) neurons that replace RB neurons later in development (Kimmel et al., 1990).

Five Trk receptors have been identified in zebrafish, based on homology to mammalian counterparts. Northern blot analysis and *in situ* hybridization showed, respectively, that each Trk receptor has distinct temporal and anatomical expression patterns. Early expression of TrkC1 and TrkC2 during embryo development parallels the temporal expression pattern of TrkC in other vertebrate systems (Martin et al., 1995). In addition, expression patterns revealed by *in situ* hybridization provide evidence that TrkC1 and TrkC2 define two separate neuron populations (Martin et al., 1998).

Somatosensory neuron subtypes can be further characterized by expression of different nociceptive genes. Phylogenetic analysis of TRP homologues across vertebrate systems identified six TRP channels in zebrafish (Saito and Shingai, 2006). A *trpA1b* BAC transgenic line has been shown to mark a subset of peripheral sensory neurons in zebrafish (Pan et al., 2012). *In situ* hybridization of other molecular markers, such as *p2rx3a* and *p2rx3b* has also identified subpopulations of peripheral sensory neurons (Norton et al., 2000; Kucenas et al., 2006). Little is known regarding how expression of zebrafish Trk receptors and TRP channels, as well as other sensory neuron specific genes, overlap with one another, and thus how many molecular subclasses exist.

Zebrafish peripheral sensory neurons select their territories via neuron-neuron interactions. Without competition from neighboring neurons, a single neuron is capable of elaborating its arbors beyond its normal boundaries (Sagasti et al., 2005). *In vivo* time-lapse confocal imaging of fluorescently labeled sensory neurons in live zebrafish suggested that repulsive interactions between neurons direct territory selection. Developing peripheral sensory

arbors are often reluctant to cross over one another. Comparing encounters between growing branches of a single peripheral axon (isoneuronal) versus neuron-neuron interactions within and between ganglia revealed that isoneuronal interactions display a higher frequency (84%) of repulsion, compared to that of heteroneuronal interactions (50%). Interestingly, observations of interactions between pairs of neurons showed that they either consistently repelled or consistently ignored each other. These findings suggest that neuron-neuron interactions play an important role in peripheral arbor territory selection, that these subsets of sensory neurons tile independently of one another, and that there are at least two distinct subtypes of sensory neurons in larval zebrafish (Sagasti et al., 2005).

Behavioral response to somatosensory stimuli in zebrafish larvae

Zebrafish larvae are an excellent model for studying simple behaviors. Zebrafish can perform several distinguishable motor responses, such as fast versus slow swimming and various turning behaviors, which may indicate activation of specific sensory neurons (Budick and O'Malley, 2000). Three types of behavior develop sequentially in zebrafish embryos: spontaneous contractions, metronome-like side-to-side contractions of the tail that appear at 17 hours post-fertilization (hpf); response to touch, contralateral contractions when touched on the head or tail, develops at 21 hpf; and swimming, a net movement of the entire embryo of at least one body length, appears at 26 hpf. After 27 hpf, the escape response becomes distinct. Touching the head results in a full coiling response, whereas touching the tail elicits a partial coil and a brief spurt of swimming (Saint-Amant and Drapeau, 1998). Additional variations in swimming behavior include swimming at various speeds, struggling and the startle response (Liu and Westerfield, 1988). These distinct motor behaviors serve as putative indicators of behaviors

elicited by activation of distinct sensory neuron subtypes.

The central axons of zebrafish trigeminal and RB neurons project into the central nervous system (CNS). These projections connect to the bilateral Mauthner cells, a pair of giant reticulospinal neurons with their cell bodies in the hindbrain (Kimmel et al., 1990). The Mauthner cell is considered a command neuron that, together with two other pairs of segmental homologs (MiDcm2 and MiDcm3), mediates a classic escape response (Gahtan and Baier, 2004). Differential patterns of activation of these three neurons correlate with different magnitudes of coiling in response to touch. Touching the head activates all three cell types and elicits a $\sim 128^\circ$ escape behavior, whereas touching the tail activates only the Mauthner cell, resulting in a $\sim 90^\circ$ escape response (Liu and Fetcho, 1999).

The Mauthner cell has long been considered the mediator for the C-start escape behavior in zebrafish (Korn and Faber, 2005). Increasing evidence, however, points to the existence of a Mauthner-independent escape response. Studies in zebrafish with a lesion caudal to the hindbrain, as well as fish with ablated Mauthner cells have provided evidence for a non-Mauthner mediated escape behavior (Liu and Fetcho, 1999; Downes and Granato, 2006; Kohashi and Oda, 2008; Burgess et al., 2009; Liu et al., 2012). Current advancements in genetic manipulations and optogenetics are making it possible to piece together these findings and identify specific neural networks in zebrafish larvae (Douglass et al., 2008; Lin et al., 2009).

References

- Anand P. 1995. Nerve growth factor regulates nociception in human health and disease. *Br J Anaesth* 75:201-208.
- Bandell M, Story GM, Hwang SW, Viswanath V, Eid SR, Petrus MJ, Earley TJ, Patapoutian A. 2004. Noxious cold ion channel TRPA1 is activated by pungent compounds and bradykinin. *Neuron* 41:849-857.
- Bautista DM, Jordt SE, Nikai T, Tsuruda PR, Read AJ, Poblete J, Yamoah EN, Basbaum AI, Julius D. 2006. TRPA1 mediates the inflammatory actions of environmental irritants and proalgesic agents. *Cell* 124:1269-1282.
- Bautista DM, Siemens J, Glazer JM, Tsuruda PR, Basbaum AI, Stucky CL, Jordt SE, Julius D. 2007. The menthol receptor TRPM8 is the principal detector of environmental cold. *Nature* 448:204-208.
- Blackshaw SE, Nicholls JG, Parnas I. 1982. Expanded receptive fields of cutaneous mechanoreceptor cells after single neurone deletion in leech central nervous system. *J Physiol* 326:261-268.
- Boulais N, Misery L. 2007. Merkel cells. *J Am Acad Dermatol* 57:147-165.
- Boulais N, Misery L. 2008. The epidermis: a sensory tissue. *Eur J Dermatol* 18:119-127.
- Bradbury EJ, Burnstock G, McMahon SB. 1998. The expression of P2X3 purinoreceptors in sensory neurons: effects of axotomy and glial-derived neurotrophic factor. *Mol Cell Neurosci* 12:256-268.
- Brierley SM, Hughes PA, Page AJ, Kwan KY, Martin CM, O'Donnell TA, Cooper NJ, Harrington AM, Adam B, Liebrechts T, Holtmann G, Corey DP, Rychkov GY, Blackshaw

- LA. 2009. The ion channel TRPA1 is required for normal mechanosensation and is modulated by algescic stimuli. *Gastroenterology* 137:2084-2095.e2083.
- Budick SA, O'Malley DM. 2000. Locomotor repertoire of the larval zebrafish: swimming, turning and prey capture. *J Exp Biol* 203:2565-2579.
- Burgess HA, Johnson SL, Granato M. 2009. Unidirectional startle responses and disrupted left-right co-ordination of motor behaviors in robo3 mutant zebrafish. *Genes Brain Behav* 8:500-511.
- Calavia MG, Montañó JA, García-Suárez O, Feito J, Guervós MA, Germanà A, Del Valle M, Pérez-Piñera P, Cobo J, Vega JA. 2010. Differential localization of Acid-sensing ion channels 1 and 2 in human cutaneous pacinian corpuscles. *Cell Mol Neurobiol* 30:841-848.
- CAUNA N, ROSS LL. 1960. The fine structure of Meissner's touch corpuscles of human fingers. *J Biophys Biochem Cytol* 8:467-482.
- Chen CC, Akopian AN, Sivilotti L, Colquhoun D, Burnstock G, Wood JN. 1995. A P2X purinoceptor expressed by a subset of sensory neurons. *Nature* 377:428-431.
- Chizh BA, Illes P. 2001. P2X receptors and nociception. *Pharmacol Rev* 53:553-568.
- Corey DP, García-Añoveros J, Holt JR, Kwan KY, Lin SY, Vollrath MA, Amalfitano A, Cheung EL, Derfler BH, Duggan A, Géléoc GS, Gray PA, Hoffman MP, Rehm HL, Tamasauskas D, Zhang DS. 2004. TRPA1 is a candidate for the mechanosensitive transduction channel of vertebrate hair cells. *Nature* 432:723-730.
- del Camino D, Murphy S, Heiry M, Barrett LB, Earley TJ, Cook CA, Petrus MJ, Zhao M, D'Amours M, Deering N, Brenner GJ, Costigan M, Hayward NJ, Chong JA, Fanger CM,

- Woolf CJ, Patapoutian A, Moran MM. 2010. TRPA1 contributes to cold hypersensitivity. *J Neurosci* 30:15165-15174.
- DeVane CL. 2001. Substance P: a new era, a new role. *Pharmacotherapy* 21:1061-1069.
- Douglass AD, Kraves S, Deisseroth K, Schier AF, Engert F. 2008. Escape behavior elicited by single, channelrhodopsin-2-evoked spikes in zebrafish somatosensory neurons. *Curr Biol* 18:1133-1137.
- Downes GB, Granato M. 2006. Supraspinal input is dispensable to generate glycine-mediated locomotive behaviors in the zebrafish embryo. *J Neurobiol* 66:437-451.
- Ernfors P, Lee KF, Jaenisch R. 1994. Mice lacking brain-derived neurotrophic factor develop with sensory deficits. *Nature* 368:147-150.
- Ernfors P, Lee KF, Kucera J, Jaenisch R. 1994. Lack of neurotrophin-3 leads to deficiencies in the peripheral nervous system and loss of limb proprioceptive afferents. *Cell* 77:503-512.
- Fagan AM, Zhang H, Landis S, Smeyne RJ, Silos-Santiago I, Barbacid M. 1996. TrkA, but not TrkC, receptors are essential for survival of sympathetic neurons in vivo. *J Neurosci* 16:6208-6218.
- Foulkes T, Wood JN. 2007. Mechanisms of cold pain. *Channels (Austin)* 1:154-160.
- Gahtan E, Baier H. 2004. Of lasers, mutants, and see-through brains: functional neuroanatomy in zebrafish. *J Neurobiol* 59:147-161.
- Goodman MB, Ernstrom GG, Chelur DS, O'Hagan R, Yao CA, Chalfie M. 2002. MEC-2 regulates *C. elegans* DEG/ENaC channels needed for mechanosensation. *Nature* 415:1039-1042.
- Grueber WB, Jan LY, Jan YN. 2002. Tiling of the *Drosophila* epidermis by multidendritic sensory neurons. *Development* 129:2867-2878.

- Grueber WB, Jan YN. 2004. Dendritic development: lessons from *Drosophila* and related branches. *Curr Opin Neurobiol* 14:74-82.
- Grueber WB, Ye B, Moore AW, Jan LY, Jan YN. 2003. Dendrites of distinct classes of *Drosophila* sensory neurons show different capacities for homotypic repulsion. *Curr Biol* 13:618-626.
- Halata Z, Munger BL. 1981. Identification of the Ruffini corpuscle in human hairy skin. *Cell Tissue Res* 219:437-440.
- Huang EJ, Reichardt LF. 2001. Neurotrophins: roles in neuronal development and function. *Annu Rev Neurosci* 24:677-736.
- Indo Y, Tsuruta M, Hayashida Y, Karim MA, Ohta K, Kawano T, Mitsubuchi H, Tonoki H, Awaya Y, Matsuda I. 1996. Mutations in the TRKA/NGF receptor gene in patients with congenital insensitivity to pain with anhidrosis. *Nat Genet* 13:485-488.
- Julius D, Basbaum AI. 2001. Molecular mechanisms of nociception. *Nature* 413:203-210.
- Kang S, Jang JH, Price MP, Gautam M, Benson CJ, Gong H, Welsh MJ, Brennan TJ. 2012. Simultaneous disruption of mouse ASIC1a, ASIC2 and ASIC3 genes enhances cutaneous mechanosensitivity. *PLoS One* 7:e35225.
- Kimmel CB, Hatta K, Metcalfe WK. 1990. Early axonal contacts during development of an identified dendrite in the brain of the zebrafish. *Neuron* 4:535-545.
- Kitson DL, Roberts A. 1983. Competition during innervation of embryonic amphibian head skin. *Proc R Soc Lond B Biol Sci* 218:49-59.
- Kohashi T, Oda Y. 2008. Initiation of Mauthner- or non-Mauthner-mediated fast escape evoked by different modes of sensory input. *J Neurosci* 28:10641-10653.

- Korn H, Faber DS. 2005. The Mauthner cell half a century later: a neurobiological model for decision-making? *Neuron* 47:13-28.
- Kucenas S, Soto F, Cox JA, Voigt MM. 2006. Selective labeling of central and peripheral sensory neurons in the developing zebrafish using P2X(3) receptor subunit transgenes. *Neuroscience* 138:641-652.
- Kwan KY, Corey DP. 2009. Burning cold: involvement of TRPA1 in noxious cold sensation. *J Gen Physiol* 133:251-256.
- Kwan KY, Glazer JM, Corey DP, Rice FL, Stucky CL. 2009. TRPA1 modulates mechanotransduction in cutaneous sensory neurons. *J Neurosci* 29:4808-4819.
- Labib S, Adnane Berdai M, Abourazzak S, Hida M, Harandou M. 2011. Congenital insensitivity to pain with anhidrosis: report of a family case. *Pan Afr Med J* 9:33.
- LaMotte RH, Lundberg LE, Torebjörk HE. 1992. Pain, hyperalgesia and activity in nociceptive C units in humans after intradermal injection of capsaicin. *J Physiol* 448:749-764.
- LaMotte RH, Shain CN, Simone DA, Tsai EF. 1991. Neurogenic hyperalgesia: psychophysical studies of underlying mechanisms. *J Neurophysiol* 66:190-211.
- Lin JY, Lin MZ, Steinbach P, Tsien RY. 2009. Characterization of engineered channelrhodopsin variants with improved properties and kinetics. *Biophys J* 96:1803-1814.
- Liu DW, Westerfield M. 1988. Function of identified motoneurons and co-ordination of primary and secondary motor systems during zebra fish swimming. *J Physiol* 403:73-89.
- Liu KS, Fetcho JR. 1999. Laser ablations reveal functional relationships of segmental hindbrain neurons in zebrafish. *Neuron* 23:325-335.

- Liu X, Jaenisch R. 2000. Severe peripheral sensory neuron loss and modest motor neuron reduction in mice with combined deficiency of brain-derived neurotrophic factor, neurotrophin 3 and neurotrophin 4/5. *Dev Dyn* 218:94-101.
- Liu YC, Bailey I, Hale ME. 2012. Alternative startle motor patterns and behaviors in the larval zebrafish (*Danio rerio*). *J Comp Physiol A Neuroethol Sens Neural Behav Physiol* 198:11-24.
- Lowery CL, Hardman MP, Manning N, Hall RW, Anand KJ, Clancy B. 2007. Neurodevelopmental changes of fetal pain. *Semin Perinatol* 31:275-282.
- Lumpkin EA, Caterina MJ. 2007. Mechanisms of sensory transduction in the skin. *Nature* 445:858-865.
- Manor E, Joshua BZ, Levy J, Brennan PA, Bodner L. 2012. Pathological fracture of the mandible in a paediatric patient with congenital insensitivity to pain with anhidrosis (CIPA). *J Craniomaxillofac Surg*.
- Marmigère F, Ernfors P. 2007. Specification and connectivity of neuronal subtypes in the sensory lineage. *Nat Rev Neurosci* 8:114-127.
- Martin SC, Marazzi G, Sandell JH, Heinrich G. 1995. Five Trk receptors in the zebrafish. *Dev Biol* 169:745-758.
- Martin SC, Sandell JH, Heinrich G. 1998. Zebrafish TrkC1 and TrkC2 receptors define two different cell populations in the nervous system during the period of axonogenesis. *Dev Biol* 195:114-130.
- Mizuno A, Matsumoto N, Imai M, Suzuki M. 2003. Impaired osmotic sensation in mice lacking TRPV4. *Am J Physiol Cell Physiol* 285:C96-101.

- Molliver DC, Radeke MJ, Feinstein SC, Snider WD. 1995. Presence or absence of TrkA protein distinguishes subsets of small sensory neurons with unique cytochemical characteristics and dorsal horn projections. *J Comp Neurol* 361:404-416.
- Montaño JA, Calavia MG, García-Suárez O, Suarez-Quintanilla JA, Gálvez A, Pérez-Piñera P, Cobo J, Vega JA. 2009. The expression of ENa(+)/C and ASIC2 proteins in Pacinian corpuscles is differently regulated by TrkB and its ligands BDNF and NT-4. *Neurosci Lett* 463:114-118.
- North RA. 2004. P2X3 receptors and peripheral pain mechanisms. *J Physiol* 554:301-308.
- Norton WH, Rohr KB, Burnstock G. 2000. Embryonic expression of a P2X(3) receptor encoding gene in zebrafish. *Mech Dev* 99:149-152.
- Oku R, Satoh M, Fujii N, Otaka A, Yajima H, Takagi H. 1987. Calcitonin gene-related peptide promotes mechanical nociception by potentiating release of substance P from the spinal dorsal horn in rats. *Brain Res* 403:350-354.
- Orita S, Ohtori S, Nagata M, Horii M, Yamashita M, Yamauchi K, Inoue G, Suzuki M, Eguchi Y, Kamoda H, Arai G, Ishikawa T, Miyagi M, Ochiai N, Kishida S, Takaso M, Aoki Y, Takahashi K. 2010. Inhibiting nerve growth factor or its receptors downregulates calcitonin gene-related peptide expression in rat lumbar dorsal root ganglia innervating injured intervertebral discs. *J Orthop Res* 28:1614-1620.
- Page AJ, Brierley SM, Martin CM, Price MP, Symonds E, Butler R, Wemmie JA, Blackshaw LA. 2005. Different contributions of ASIC channels 1a, 2, and 3 in gastrointestinal mechanosensory function. *Gut* 54:1408-1415.
- Pan YA, Choy M, Prober DA, Schier AF. 2012. Robo2 determines subtype-specific axonal projections of trigeminal sensory neurons. *Development* 139:591-600.

- Patel TD, Jackman A, Rice FL, Kucera J, Snider WD. 2000. Development of sensory neurons in the absence of NGF/TrkA signaling in vivo. *Neuron* 25:345-357.
- Pedersen-Bjergaard U, Nielsen LB, Jensen K, Edvinsson L, Jansen I, Olesen J. 1991. Calcitonin gene-related peptide, neurokinin A and substance P: effects on nociception and neurogenic inflammation in human skin and temporal muscle. *Peptides* 12:333-337.
- Prashanth GP, Kamate M. 2012. A case of hereditary sensory autonomic neuropathy type IV. *Ann Indian Acad Neurol* 15:134-136.
- Price DD, Staud R. 2005. Neurobiology of fibromyalgia syndrome. *J Rheumatol Suppl* 75:22-28.
- Price MP, McIlwrath SL, Xie J, Cheng C, Qiao J, Tarr DE, Sluka KA, Brennan TJ, Lewin GR, Welsh MJ. 2001. The DRASIC cation channel contributes to the detection of cutaneous touch and acid stimuli in mice. *Neuron* 32:1071-1083.
- Price MP, Thompson RJ, Eshcol JO, Wemmie JA, Benson CJ. 2004. Stomatin modulates gating of acid-sensing ion channels. *J Biol Chem* 279:53886-53891.
- Rifkin JT, Todd VJ, Anderson LW, Lefcort F. 2000. Dynamic expression of neurotrophin receptors during sensory neuron genesis and differentiation. *Dev Biol* 227:465-480.
- Roberts A. 1980. The function and role of two types of mechanoreceptive "free" nerve endings in the head skin of amphibian embryos. *Journal of Comparative Physiology* 135:341-348.
- Roza C, Puel JL, Kress M, Baron A, Diochot S, Lazdunski M, Waldmann R. 2004. Knockout of the ASIC2 channel in mice does not impair cutaneous mechanosensation, visceral mechanonociception and hearing. *J Physiol* 558:659-669.
- Sagasti A, Guido MR, Raible DW, Schier AF. 2005. Repulsive interactions shape the morphologies and functional arrangement of zebrafish peripheral sensory arbors. *Curr Biol* 15:804-814.

- Saint-Amant L, Drapeau P. 1998. Time course of the development of motor behaviors in the zebrafish embryo. *J Neurobiol* 37:622-632.
- Saito S, Shingai R. 2006. Evolution of thermoTRP ion channel homologs in vertebrates. *Physiol Genomics* 27:219-230.
- Salihagić Kadić A, Predojević M. 2012. Fetal neurophysiology according to gestational age. *Semin Fetal Neonatal Med*.
- Salio C, Lossi L, Ferrini F, Merighi A. 2005. Ultrastructural evidence for a pre- and postsynaptic localization of full-length trkB receptors in substantia gelatinosa (lamina II) of rat and mouse spinal cord. *Eur J Neurosci* 22:1951-1966.
- Shu XQ, Mendell LM. 1999. Neurotrophins and hyperalgesia. *Proc Natl Acad Sci U S A* 96:7693-7696.
- Silos-Santiago I, Molliver DC, Ozaki S, Smeyne RJ, Fagan AM, Barbacid M, Snider WD. 1995. Non-TrkA-expressing small DRG neurons are lost in TrkA deficient mice. *J Neurosci* 15:5929-5942.
- Skofitsch G, Jacobowitz DM. 1985. Calcitonin gene-related peptide coexists with substance P in capsaicin sensitive neurons and sensory ganglia of the rat. *Peptides* 6:747-754.
- Snider WD, McMahon SB. 1998. Tackling pain at the source: new ideas about nociceptors. *Neuron* 20:629-632.
- Snider WD, Silos-Santiago I. 1996. Dorsal root ganglion neurons require functional neurotrophin receptors for survival during development. *Philos Trans R Soc Lond B Biol Sci* 351:395-403.
- Staud R. 2007. Treatment of fibromyalgia and its symptoms. *Expert Opin Pharmacother* 8:1629-1642.

- Staud R. 2009. Chronic widespread pain and fibromyalgia: two sides of the same coin? *Curr Rheumatol Rep* 11:433-436.
- Staud R. 2011. Peripheral pain mechanisms in chronic widespread pain. *Best Pract Res Clin Rheumatol* 25:155-164.
- Sugimura K, Yamamoto M, Niwa R, Satoh D, Goto S, Taniguchi M, Hayashi S, Uemura T. 2003. Distinct developmental modes and lesion-induced reactions of dendrites of two classes of *Drosophila* sensory neurons. *J Neurosci* 23:3752-3760.
- Suzuki H, Aoyama Y, Senzaki K, Vincler M, Wittenauer S, Yoshikawa M, Ozaki S, Oppenheim RW, Shiga T. 2010. Characterization of sensory neurons in the dorsal root ganglia of Bax-deficient mice. *Brain Res* 1362:23-31.
- Suzuki M, Mizuno A, Kodaira K, Imai M. 2003. Impaired pressure sensation in mice lacking TRPV4. *J Biol Chem* 278:22664-22668.
- Suzuki M, Watanabe Y, Oyama Y, Mizuno A, Kusano E, Hirao A, Ookawara S. 2003. Localization of mechanosensitive channel TRPV4 in mouse skin. *Neurosci Lett* 353:189-192.
- Tominaga M. 2007. Nociception and TRP channels. *Handb Exp Pharmacol*:489-505.
- Tominaga M, Caterina MJ. 2004. Thermosensation and pain. *J Neurobiol* 61:3-12.
- Xiang Z, Bo X, Burnstock G. 1998. Localization of ATP-gated P2X receptor immunoreactivity in rat sensory and sympathetic ganglia. *Neurosci Lett* 256:105-108.

Chapter 2

New transgenic reporters identify somatosensory neuron subtypes in larval zebrafish

Introduction

Somatosensation is carried out by a variety of specialized populations of sensory neurons that detect different types of thermal, chemical and mechanical touch stimuli (Lumpkin and Caterina, 2007; Marmigère and Ernfors, 2007). Innervation of the skin by somatosensory neurons occurs very early in development, allowing animals to detect touch even at embryonic stages (Davies and Lumsden, 1984; Moore and Munger, 1989; Kimmel et al., 1990; Saint-Amant and Drapeau, 1998; Sagasti et al., 2005). The degree of heterogeneity among somatosensory neurons at early embryonic and larval stages has not been fully characterized, but distinct types of neurons can be distinguished by both function and axon morphology. For example, *Xenopus* trigeminal neurons that innervate the head, fall into two functionally, anatomically and physiologically distinct types: Type I “movement” detectors inhibit swimming behavior and their peripheral arbors have many fine branches with numerous large varicosities, whereas Type II “rapid transient” detectors stimulate behavior and their peripheral arbors have few relatively straight branches with elongated varicosities (Roberts, 1980; Hayes and Roberts, 1983).

Zebrafish are an ideal model for studying early stages of somatosensory neuron development and function due to their external fertilization, rapid development, and optical clarity, but the heterogeneity of their embryonic and larval somatosensory neurons have not been well characterized. Zebrafish possess three populations of somatosensory neurons: trigeminal neurons that innervate the head, Rohon-Beard (RB) neurons that innervate the body at early larval stages, and dorsal root ganglia (DRG) neurons that innervate the body at later stages. Several observations suggest that embryonic and larval zebrafish possess multiple subtypes of somatosensory neurons. First, the cutaneous axons of trigeminal and RB neurons display a broad spectrum of peripheral axon branching patterns, which might reflect multiple subclasses with

distinct morphologies (Sagasti et al., 2005). Second, populations of trigeminal peripheral axon arbors appear to “tile” the skin independently of one another: Although the territories of all arbors are limited by repulsion, individual arbors only repel a subset of others (Sagasti et al., 2005). Third, distinct patterns of varicosities can be distinguished in the central axons of individual classes of trigeminal neurons, likely reflecting distinct synaptic patterns (Pan et al., 2012). Fourth, electrophysiological and molecular analyses have revealed that sodium currents in different populations of RB neurons rely on different sodium channels (Pineda et al., 2006). Finally, several genes, such as *protein kinase C alpha (pkcα)* (Slatter et al., 2005; Patten et al., 2007), the ATP-gated ion channel *p2rx3a* (Boué-Grabot et al., 2000; Norton et al., 2000; Appelbaum et al., 2007) and the chemosensory ion channel *trpA1b* (Caron et al., 2008; Pan et al., 2012) are expressed in subpopulations of zebrafish trigeminal and RB neurons. Nonetheless, co-expression between most of these molecules has largely not been examined, so these observations have yet to cohere into a clear picture of the diversity among these neurons.

Fluorescent transgenic reporters have made it possible to study somatosensory neurons in live zebrafish larvae. The most commonly used reporters for these neurons utilize enhancers cloned from genomic regions near the *islet1* and *islet2b* genes to drive expression of a fluorescent protein (Higashijima et al., 2000; Uemura et al., 2005; Pittman et al., 2008). These enhancers have generally been thought to drive expression in all zebrafish somatosensory neurons, although one report suggests that a transgenic line using an *islet1* enhancer may mark a subset of neurons (Pan et al., 2012). While these reporters have been useful for characterizing sensory neuron development, their presumed pan-neuronal labeling limits their utility for studying sensory neuron subtypes. Furthermore, several of these reporters use the Gal4-VP16/UAS system, which amplifies expression and allows combinatorial versatility (Köster and

Fraser, 2001), but also attracts methylation (Goll et al., 2009), leading to variegated expression. Fluorescence expression in subsets of somatosensory neurons has been achieved with reporters for *trpA1b* and *p2rx3b* that were made by recombining fluorescent proteins into bacterial artificial chromosomes (BACs) (Kucenas et al., 2006; Pan et al., 2012), but such reporters are rare, can be laborious to create, and their relation to other reporters has yet to be fully assessed.

To initiate a systematic analysis of subtype-specific transgenes, we have created several reporters using enhancers from neurotrophin receptors and ion channels. Defining enhancer sequences that control expression of these reporters could help identify transcriptional pathways regulating somatosensory neuron development. Subtype-specific transgenic reporters will also be useful tools for characterizing somatosensory neuron diversity. These new fluorescent reporters will make it possible to test whether different axon morphologies are optimized for specific somatosensory functions and for characterizing neural circuitry controlling behavioral responses to touch stimuli.

Materials and Methods

Fish strains and transgenic lines

Embryos were raised at 28.5°C on a 14 hr/10 hr light/dark cycle. All experiments were approved by the Chancellor's Animal Research Care Committee at the University of California, Los Angeles.

Expression analysis of transgenes was performed in wild-type AB or *Gt(T2KSAG)^{j1229a}* (Burgess et al., 2009) fish. Stable transgenic lines were created with the Tol2 transposase system (Kawakami, 2004). Supplementary Table 1 summarizes all the transgenic lines used in this study, as well as the transgenes used for transient transgenesis. Although transgenic lines

were not mapped, expression from all lines segregated in a Mendelian manner, indicating that they integrated into single genomic loci.

Cloning/ Transgenes

Enhancer regions of somatosensory neuron specific genes were amplified from genomic DNA of the zebrafish *Danio rerio* or the pufferfish *Fugu rubripes* by PCR (Table 1). These enhancer regions were initially cloned into Gal4:GFP-pBSK vectors by PCR amplification using primers with restriction sites incorporated into the flanking sequences. Subsequent subcloning and promoter dissection of these elements was performed using the Multi-Site Gateway Cloning System (Invitrogen, 12537-023) in combination with the Tol2 Gateway System developed by the Chien Lab (Kwan et al., 2007). Briefly, genomic sequences were PCR amplified with primers containing attB sites and recombined into pDONR P4-P1R, creating 5' DONR plasmids. The binomial enhancers, E1b:Gal4-VP16:pA,14XUAS:E1b and E1b:LexA-VP16:pA,4xLexAop:E1b were cloned into pDONR 221 to make middle elements. Reporter genes, EGFP, mCherry and KikGR were cloned into pDONR P2R-P3 to make 3' elements. Reporter transgenes were created by recombination of different sets of pDONR elements using LR Clonase II Plus (Invitrogen, 12538120). Reporter function of each transgene was tested by injection into wildtype embryos. PCR primers used for amplifying genomic fragments are listed in Supplementary Table 2.

Transient analysis of reporter transgenes and confocal imaging

Zebrafish embryos were injected at the 1-cell stage with approximately 2 nl of 50 ng/ul plasmid DNA, raised in a 28.5°C incubator and treated with phenylthiourea (PTU) at 24 hpf to

block pigmentation. Larvae were screened for fluorescence between 24 and 72 hpf using a Zeiss Discovery.V12 SteREO fluorescence dissecting scope.

For confocal imaging, fish were anesthetized with 0.02% tricaine and mounted in 1.2% low melt agarose (Promega, V2111). Fluorescence was imaged with a Zeiss LSM 510 confocal microscope using a 488 nm laser line for GFP/YFP/Citrine, 633 nm for Cy5 and 543 nm for mCherry/DsRed/Rhodamine. Images were taken with a 20x water objective (a 0.7x or 2x optical zoom was used where indicated) and projected from 20-50 optical sections of ~3 μm intervals.

Photoconversion of KikGR protein

Photoconversion of KikGR protein was performed using a Discovery.V12 SteREO fluorescence dissecting scope with a UV filter. Larvae were exposed to UV light for 5 minutes or until all neurons were photoconverted from green to red. Neurons were photoconverted in 24-hour intervals, subsequent to confocal imaging. Photoconverted larvae were raised at 28.5°C, in the dark, until imaging the following day.

Morphological analysis of peripheral axons

High-resolution (1024x1024 pixels) confocal images of single neurons were collected as described above. Using NeuroLucida tracing software, axons were traced in three dimensions; the primary axon projecting from the cell body to the first branch point in the skin was excluded from the analysis. Branch length and number for each traced neuron were acquired using NeuroLucidaExplorer software and analyzed with a Matlab program, which is described in detail in Supplementary Materials.

Retrograde labeling of Mauthner cells

Retrograde labeling of Mauthner cells was performed using rhodamine dextran (Invitrogen, 1824) according to established protocols (Fetcho and O'Malley, 1995; Volkmann and Köster, 2007). A filamented glass needle filled with a saturated concentration of rhodamine dextran was used to create a lesion and introduce the dye within the caudal spinal cord of 48 hpf larvae. Larvae were allowed to recover for at least 24 hours at 28.5°C, in the dark, before imaging.

Whole Mount Double Fluorescent In Situ Hybridization and Antibody Staining

Embryos were fixed in 4% paraformaldehyde/PBS overnight at 4°C and permeabilized with proteinase K prior to antibody staining and/or in situ hybridization with standard protocols (Boué-Grabot et al., 2000; Slatter et al., 2005) (<https://wiki.zfin.org/display/prot/Thisse+Lab+-+In+Situ+Hybridization+Protocol+-+2010+update>). Antibody staining was performed with primary antibodies (PKC α , GFP/YFP/Citrine and mCherry) (1:500) incubated overnight at 4°C followed by incubation with AlexaFluor secondary antibodies (488 anti-mouse and 568 anti-rabbit for GFP, YFP and citrine expressing transgenics or 568 anti-mouse and 488 anti-rabbit for mCherry expressing transgenics) (1:1000) at 4°C overnight (Supplementary Table 3). Specificity of the PKC α antibody staining was verified with co-expression analysis, as shown in Figure 7. Supplementary Table 3 summarizes the antibodies used in this study. For fluorescent *in situ* hybridization, embryos were incubated with DIG labeled riboprobe (*p2rx3a* or *trkA*) and visualized using Cy5-Tyramide amplification (1:100) (Perkin Elmer, NEL752001KT). Embryos were mounted dorsally and imaged using confocal microscopy as described above.

Results

Zebrafish and pufferfish genomic sequences drive transgene expression in trigeminal and RB neurons

To analyze the development and diversity of somatosensory neurons in larval zebrafish, we created a library of transgenic reporters by cloning zebrafish (*Danio rerio*) and pufferfish (*Fugu rubripes*) genomic regions from upstream of neurotrophin receptors and ion channels (ATP-gated channels and Trp channels) and used them to drive expression of GFP (Table 1, Figure 1). To ensure robust reporter expression and allow for potential co-expression of effector genes, these candidate enhancers were subcloned upstream of the Gal4-VP16 transcriptional activator; on the same plasmid, multiple copies of the Gal4 upstream activation sequence (14xUAS) were used to drive GFP expression (Figure 1A) (Köster and Fraser, 2001). For comparison, we also created similar transgenes using two previously identified somatosensory-specific enhancers from the *islet1* gene, *isl1(ss)* and *CREST3* (Higashijima et al., 2000; Uemura et al., 2005). Similar to the *islet1* enhancers, several of the cloned candidate sequences (from the *trpAla*, *Fru.trkA*, *Fru.trkB*, *Fru.trkC* and *Fru.p2x3-2* genes) drove GFP expression primarily in zebrafish trigeminal (Figure 1B-H) and RB (Figure 1B'-H') neurons. Many of these reporters were also consistently expressed in limited populations of additional cells, including muscles or other populations of neurons (Table 1). Stable transgenic reporter lines using several of these enhancers (*isl1(ss)*, *CREST3*, *Fru.trkA*, and *Fru.p2x3-2*) exhibited similar patterns of fluorescence, confirming the reliability of the transient transgenic approach for characterizing expression.

Using transient transgenesis, we analyzed the onset of fluorescence in somatosensory neurons to determine whether these reporters exhibited differences in temporal expression. The

zebrafish *isll(ss)* enhancer drove expression earliest, turning on at approximately the 13 somites (som) stage, before somatosensory neurons have projected central and peripheral axons. Expression from *CREST3* and *trpA1a* enhancer-driven reporters was first visible at the 17 somites stage, *Fru.p2x3-2* enhancer-driven expression began at the 20 somites stage, *Fru.trkA* enhancer-driven expression began at 28 hours post-fertilization (hpf) and *Fru.trkC* enhancer-driven expression began at 30 hpf (Figure 2A).

Determining when enhancer activity ceased was more difficult than determining when it turned on, since mRNA and proteins can perdure for many hours. We devised a technique using a photoconvertible fluorescent protein to address this issue and used it to characterize *isll(ss)* and *CREST3* enhancer activity. Stable transgenic lines were made using these enhancers to drive expression of KikGR, a photoconvertible fluorescent protein that changes from green to red when exposed to UV light (Tsutsui et al., 2005). KikGR-expressing cells were photoconverted and imaged at daily intervals (Figure 2B). Expression of green fluorescence after photoconversion indicated newly synthesized KikGR; absence of green fluorescence after photoconversion indicated that the enhancer had turned off. With this approach, we found that the *isll(ss)* enhancer drove expression until approximately 54 hpf (Figure 2C-G), while the *CREST3* enhancer continued to be active past 13 days post-fertilization (dpf) in a subset of somatosensory neurons (Figure 2C'-G' and Figure 3A).

Small regulatory regions were sufficient for transgene expression in zebrafish somatosensory neurons

Identifying smaller genomic regions sufficient to drive expression in somatosensory neurons could make enhancers easier to subclone, potentially improve expression specificity or

efficiency, and makes possible the identification of conserved regulatory motifs. To isolate minimal sequences sufficient for somatosensory neuron expression, we performed sequential deletion analysis of the *Fru.trkA*, *Fru.p2x3-2*, and *trpA1a* enhancer regions. Specific regions from within each enhancer sequence were subcloned into fluorescent reporter transgenes (Figure 4A), which were then injected into one-cell stage embryos and monitored for transient expression during the first three days of development. To estimate the relative efficiency of each enhancer, we quantified the number of embryos with fluorescence in somatosensory neurons in each injected clutch (Figure 4).

From an initial ~4 kb [-3939: -1] *Fru.trkA* enhancer region, we isolated a ~1 kb region proximal to the start site [-996: -1] capable of driving expression in somatosensory neurons (Figure 4B). This enhancer was almost twice as efficient as the original ~4 kb sequence (48% vs 25% of embryos with expression), indicating that there may be a negative regulatory element within the distal 3 kb of the original enhancer that reduced its activity. Subsequent deletions within the [-996: -1] fragment decreased its efficiency, with the two shortest sufficient elements [-996: -814] and [-238: -81] driving expression in an average of ~18% and 20% of embryos, respectively. However, when these two minimal regions [-996: -814] and [-238: -81] were combined [-996: -678, -238: -1], they were almost as efficient as the [-996: -1] fragment, indicating that each of the two small regulatory elements were sufficient for somatosensory expression, but sum to achieve optimal expression.

The ~1.6 kb [-1619: -1] *Fru.p2x3-2* enhancer was dissected into several progressively smaller fragments that drove expression in TG and RB neurons (Figure 4C). One of these fragments was 305 bps long [-1036: -731] and drove expression with comparable efficiency to

the full 1.6 kb sequence (65% and 70% of embryos, respectively). A 144 bp fragment [-946: -802] was also sufficient for expression in somatosensory neurons, but was less efficient.

Dissection of the ~5 kb [-4993: -1] *trpA1a* genomic sequence indicated that the ~2 kb furthest from the start site was sufficient to drive expression (Figure 4D). By examining overlapping fragments, we isolated a 941 bp region [-4457: -3517] that was sufficient for expression in somatosensory neurons. However, partially overlapping fragments [-4993: -4003] and [-3873: -3013] were unable to drive expression, indicating that multiple elements are required together. By creating 4 internal deletions of this 941 bp [-4457: -3517] fragment, we found two smaller regions, [-4136: -3946] and [-3946: -3517], that were required but not sufficient to drive robust expression in sensory neurons.

The Fru.p2x3-2 reporter and PKC α gene trap reporter define a somatosensory neuron subset that partially overlaps with neurons expressing a Fru.trkA reporter

PKC α is expressed in approximately 40% of RB neurons in 24 and 48 hpf larvae (Slatter et al., 2005). We obtained a gene trap line with an insertion in the gene encoding PKC α (*PKC α ^{ct7a}*) to examine the relationship between the neurons marked by our reporter lines and PKC α -expressing neurons. In this line, an exon encoding the yellow fluorescent protein, citrine, is integrated between exons 3 and 4 of the PKC α gene, resulting in the expression of a PKC α -citrine fusion protein under the control of the endogenous PKC α transcriptional regulatory elements (Trinh et al., 2011). To determine if expression from *PKC α ^{ct7a}* is confined to a subset of RB neurons, we crossed it to an *isll(ss)* transgenic reporter line, *Tg(isll(ss):Gal4-VP16,14xUAS:DsRed)*. Due to variegation from the Gal4-VP16/UAS system, DsRed in this line is expressed in approximately 74% of RB neurons (as determined by crossing it to a non-Gal4-

VP16/UAS, non-variegated *isl2b:GFP* line) (Figure 5A and F). At 72 hpf, 41% of RB neurons in the *isl1(ss)* reporter line also expressed citrine from the *PKC α^{ct7a}* gene trap line, and 56% expressed DsRed only (Figure 5B and F). 3% of the labeled neurons expressed citrine only, which likely represents a population of neurons with silenced DsRed.

The *p2rx3a* gene is also expressed in a subset of somatosensory neurons (Boué-Grabot et al., 2000; Norton et al., 2000; Appelbaum et al., 2007). To create a potential reporter line for the *p2rx3a* gene, we used the *Fru.p2x3-2* enhancer (P3X3-2 is the pufferfish homolog of zebrafish P2rx3a) to drive expression of LexA-VP16 and drove expression of mCherry with the LexA operator (4xLexAop). Using the LexA-VP16/LexAop binary system has the same advantages as the Gal4-VP16/UAS system in terms of amplification and combinatorial versatility, but can be crossed to Gal4-VP16/UAS lines without cross-activating them (Lai and Lee, 2006). Crossing a *Fru.p2x3-2* reporter line, *Tg(Fru.p2x3-2[-1036,-731]:LexA-VP16,4xLexAop:mCherry)*, to the *isl2b:GFP* line revealed that the *Fru.p2x3-2* reporter labeled approximately 30% of RB neurons (Figure 5C and F). To determine the relationship between the *Fru.p2x3-2* reporter and *PKC α^{ct7a}* neurons, we crossed the two lines together (Figure 5D). Strikingly, citrine and mCherry expression almost completely coincided, with 96% of RB neurons expressing both (Figure 5F). Thus, an RB neuron subtype, comprising approximately 30-40% of the population, is marked by expression of both the *Fru.p2x3-2* reporter line and *PKC α^{ct7a}* .

This subtype of RB neurons persists until at least 16 dpf (Figure 3B-E), well beyond the time when RB neurons are thought to disappear, consistent with previous reports that *PKC α* -expressing RB neurons are present until at least 2 weeks post-fertilization (Slatter et al., 2005; Patten et al., 2007). RB neurons in fish and amphibians degenerate during larval stages and their function is replaced by DRG neurons. It has been reported that most (Williams et al., 2000;

Svoboda et al., 2001), or at least a subset (Reyes et al., 2004), of RB neurons degenerate in zebrafish between 2 and 4 dpf. We did not detect widespread RB neuron degeneration within the first five days of development with any of our reporter transgenes, and found that at least some RB neurons persisted for at least two weeks in several transgenic lines (Figure 3). This observation is consistent with previous studies (Metcalf et al., 1990; Slatter et al., 2005; Patten et al., 2007; O'Brien et al., 2012), suggesting that RB neuron degeneration in zebrafish might be more limited, or occur at later stages, than previously thought.

Like the *p2rx3a* gene, the *trkA* gene is also expressed in a subpopulation of larval zebrafish somatosensory neurons (Martin et al., 1995; Pan et al., 2012). We hypothesized that reporters using the *Fru.trkA* enhancer would highlight this subtype, allowing us to assess its relationship to the *Fru.p2x3-2* reporter-expressing subpopulation. We made three *Fru.trkA* transgenes using the Gal4-VP16/UAS system and one using the LexA-VP16/LexAop system to drive expression of different reporter genes. All of these lines were extensively variegated, but unfortunately, without the use of these amplification systems, the expression from this enhancer was very weak (data not shown). A line using *Fru.trkA* to drive expression of a YFP-tagged version of the light activated ChannelRhodopsin-2 (ChR2-YFP), *Tg(Fru.trkA:Gal4-VP16,14xUAS:ChR2-YFP)*, was the least variegated, so we crossed it to the *Fru.p2x3-2* reporter line (Figure 5E). Fluorescence expression in the *Fru.trkA* reporter line partially overlapped with the subset labeled by the *Fru.p2x3-2* reporter line. Although variegation made it difficult to analyze neurons that were not labeled by the *Fru.trkA* reporter line, it was clear that only about half of the neurons expressing this reporter also expressed the *Fru.p2x3-2* reporter line, which is not highly variegated (see below), indicating that it marks a different, perhaps broader, set of neurons than the *Fru.p2x3-2/PKC α^{ct7a}* reporters (Figure 5F).

Morphological variation in peripheral and central arbors of RB neurons does not correlate with subtype reporters

Having identified PKC α /*p2rx3a*-expressing RB neurons as a distinct subtype, we hypothesized that these neurons might display a characteristic peripheral axon branching morphology optimized for their sensory properties or a distinct central connectivity pattern dictating their behavioral function. To test the possibility of the former, we examined confocal images of single neurons expressing different transgenic reporters (using the *isll(ss)*, *Fru.trkA*, *Fru.trkC* or *Fru.p2x3-2* enhancers) in 72 hpf transient transgenic embryos (Figure 1B'-H'). Peripheral arbors of neurons labeled by each transgene did not exhibit dramatically distinct morphologies, like those that distinguish sensory subtypes in *Xenopus* (Hayes and Roberts, 1983) or *Drosophila* (Grueber et al., 2003) larvae. However, to assess morphology more objectively, we manually traced arbors of many single neurons arborizing over the central trunk with NeuroLucida tracing software (MicroBrightField), allowing us to extract quantitative information about each arbor. To compare arbors we created a Matlab program that generated a hierarchically clustered dendrogram reflecting the degree of morphological similarity between each pair of axons, based on branch length and number for each branch order. The algorithm reliably segregated most trigeminal and RB arbors into different groups and grouped arbors of the same neurons traced by different experimenters, giving us confidence that the method accurately distinguishes peripheral axons (Supplementary Figure 1A-A'). This program segregated RB arbors into five major clusters, but neurons labeled by different transgenes fell into multiple clusters, indicating substantial morphological diversity within each population of RB neurons labeled by these transgenic reporters (Supplementary Figure 1B-F). This

quantitative analysis confirmed our qualitative impression that peripheral arbors marked by different transgenes do not exhibit dramatic morphological distinctions, but does not preclude the possibility that other more subtle features could distinguish these arbors.

The central axons of somatosensory neurons connect to downstream neurons in the central nervous system (CNS) to elicit behavioral responses. In zebrafish larvae, touch elicits a stereotypical C-start escape response (Saint-Amant and Drapeau, 1998; Drapeau et al., 2002). This response has been attributed to the direct activation of a well-characterized pair of reticulospinal interneurons that form in rhombomere 4 of the hindbrain, called Mauthner cells, by RB neurons (Korn and Faber, 2005; Kohashi and Oda, 2008). However, touch can elicit an escape response in the absence of the Mauthner cells (Liu and Fetcho, 1999; Burgess et al., 2009), or even the entire hindbrain (Downes and Granato, 2006), suggesting that RB neurons can connect directly to spinal cord circuits.

We hypothesized that subtypes of RB neurons might connect to distinct circuits, as has been suggested for trigeminal neurons (Pan et al., 2012). To characterize central axon projections of RB neurons, we imaged single neurons in transient transgenics while simultaneously visualizing the Mauthner cells by dye-filling (Fetcho and O'Malley, 1995; Volkmann and Köster, 2007) or with a transgenic line, *Gt(T2KSAG)^{j1229a}* (Burgess et al., 2009) (Figure 6A-B and D-D', respectively). Surprisingly, the central projections of most RB neurons failed to contact the Mauthner cell dendrite, instead terminating either in the caudal hindbrain or within the spinal cord (Figure 6B). Both Mauthner- and non-Mauthner dendrite-contacting neurons were situated all along the rostral-caudal extent of the spinal cord, though Mauthner dendrite-contacting RB neurons appeared to be more abundant in the rostral spinal cord (Figure 6C). Failure to contact

the Mauthner dendrite was not due to delayed outgrowth, since these axons never grew further into the hindbrain (Figure 6D and D').

The majority of RB neurons labeled by all of the examined transgenes (using the *isl1(ss)*, *CREST3*, *Fru.p2x3-2* and *Fru.trkA* enhancers) failed to contact the Mauthner cell dendrite (Figure 6E and data not shown). Notably, neurons labeled by the *Fru.p2x3-2* reporter displayed a similar distribution of central axon termination patterns as axons labeled by the *isl1(ss)* and *CREST3* enhancer-driven reporters, indicating that although PKC α /*p2rx3a*-expressing neurons define a distinct RB subtype, neurons within that subtype can exhibit different termination patterns.

Fluorescent transgenes reflect endogenous gene expression

To determine whether the subtypes of neurons identified with our reporters reflect endogenous gene expression and thus truly distinct molecular subtypes of somatosensory neurons, we examined endogenous protein or mRNA expression in our reporter lines (Figure 7). Double antibody staining for PKC α protein and GFP in the *isl2b:GFP* line confirmed that PKC α -expressing neurons make up a subpopulation of RB neurons (Figure 7D and G). Staining for endogenous PKC α and for citrine in *PKC α ^{ci7a}* verified that the gene trap line faithfully labels all PKC α -expressing RB neurons at 72 hpf (Figure 7A and G). As expected, PKC α and mCherry antibody staining in the *Fru.p2x3-2* reporter line, *Tg(Fru.p2x3-2[-1036, -731]:LexA-VP16,4xLexAop:mCherry)*, revealed that most PKC α -expressing neurons (89%) are labeled by the *Fru.p2x3-2* reporter line (Figure 7E, G).

Fluorescent *in situ* hybridization (FISH) for *p2rx3a* (previously reported as *p2x3*, *p2rx3* and *p2x3.1*) and antibody staining for mCherry in 72 hpf *Tg(Fru.p2x3-2[-1036, -731]:LexA-*

VP16,4xLexAop:mCherry) larvae revealed that 92% of *p2rx3a*-expressing neurons also expressed the *Fru.p2x3-2* reporter, indicating that transgene expression faithfully recapitulated endogenous expression but was silenced in, at most, 10% of *p2rx3a*-expressing neurons. At 54 hpf, a larger proportion of neurons stained with the *p2rx3a* mRNA probe failed to express the reporter (20-35%, data not shown), perhaps reflecting cross-hybridization with the *p2rx3a* ortholog, *p2rx3b*, since increasing the hybridization temperature reduced the number of neurons that did not co-express the transcript and the reporter.

To characterize *trkA* (also known as *ntrk1*) expression in the *Fru.trkA* reporter line, *Tg(Fru.trkA:Gal4-VP16,14xUAS:Chr2-YFP)*, we performed FISH for *trkA* mRNA and antibody staining for YFP at 32 hpf, when gene expression appeared to be highest. 60% of neurons expressing *trkA* mRNA also expressed YFP, but few YFP-expressing neurons failed to express *trkA* (Figure 7C and G). This result confirms that the *Fru.trkA* reporter line is variegated (YFP was silenced in ~40% of *trkA* neurons), but also that expression from the transgene faithfully reflects endogenous *trkA* expression.

To determine the relationship between the PKC α /*p2rx3a* subtype of RB neurons and expression in previously published *p2rx3b:EGFP* and *trpA1b:EGFP* BAC reporter lines, we performed double antibody staining for GFP and endogenous PKC α in 72 hpf larvae from each of these BAC reporter lines. Approximately 56% of *p2rx3b:EGFP*-expressing RB neurons also expressed PKC α (Figure 8A and B), indicating that PKC α /*p2rx3a*-expressing neurons are a subset of *p2rx3b:EGFP*-expressing neurons. This finding also suggests that *p2rx3b:EGFP* is expressed in most, if not all, RB neurons. In contrast, expression of the *trpA1b:EGFP* BAC reporter completely overlapped with PKC α -expressing RB neurons. We have thus identified a subtype of RB neurons expressing three different transgenic reporter lines

(*PKC α /p2rx3a/trpA1b*) and accurately reflecting the expression of genes involved in sensory signal transduction.

Discussion

New enhancers and transgenic reporters for studying zebrafish somatosensory neurons

To sense diverse touch stimuli, vertebrate somatosensation is carried out by several functionally and molecularly distinct sensory neuron subtypes. Although less well characterized, multiple somatosensory neuron subtypes likely exist even at early embryonic stages. Despite having morphologically similar cutaneous endings (O'Brien et al., 2012), subpopulations of RB neurons in larval zebrafish differentially express genes such as *pkc α* , *p2rx3a* and specific sodium channels (Boué-Grabot et al., 2000; Norton et al., 2000; Slatter et al., 2005; Pineda et al., 2006; Appelbaum et al., 2007; Patten et al., 2007). To characterize the morphology, function and connectivity of larval zebrafish somatosensory neuron subpopulations we created several new reporter transgenes that express fluorescent proteins in these neurons using enhancers from neurotrophin receptors and ion channels. Some of the enhancers were cloned from the pufferfish genome, which we used because its more compact genome made it easier to identify regulatory elements. The fact that these enhancers drove expression in the expected neuronal populations indicates that they contain conserved regulatory elements, at least among teleost fish. By dissecting these enhancer sequences and performing expression analysis, we identified several compact sequences (<200 bp) that are sufficient and/or required for somatosensory neuron expression, making them excellent starting points for identifying transcriptional regulatory motifs. Given their portability, strong expression, and temporal variability, these new enhancers

and reporters will be useful tools for developmental and functional studies of zebrafish somatosensory neurons.

RB neurons possess diverse peripheral axon morphologies and central axon termination patterns, even within molecularly distinct subtypes

Different axon morphologies may be optimized for the sensation of particular kinds of stimuli. In *Drosophila* and *Xenopus*, the complexity of cutaneous neurite branches defines functionally distinct somatosensory neuron subtypes (Hayes and Roberts, 1983; Grueber et al., 2003). Zebrafish trigeminal and RB neurons display a spectrum of arbor morphologies, prompting us to hypothesize that branching morphology is characteristic of RB subtypes as well. Analysis of branching morphology of RB neurons labeled by reporters driven by the *isll(ss)*, *Fru.trkA*, *Fru.trkC* and *Fru.p2x3-2* enhancers grouped axon arbors into five categories. However, most of these reporters were found in all five categories, potentially implying that branching morphology may be a stochastically determined property unrelated to sensory function.

Central axon termination patterns determine the potential neural circuits that a particular sensory neuron can activate. Touch usually elicits an escape response in larval zebrafish, but kinematically distinct patterns of escape can be distinguished (Saint-Amant and Drapeau, 1998; Liu and Fetcho, 1999; Drapeau et al., 2002; Burgess et al., 2009; Liu et al., 2012), implying that different circuits underlie them. The Mauthner cell is the central component of the classic escape response circuit (Liu and Fetcho, 1999; Korn and Faber, 2005; Kohashi and Oda, 2008). It was therefore surprising to find that the majority of RB neurons visualized with any of our transgenic reporters failed to contact the Mauthner cell dendrite, terminating instead within the spinal cord

or caudal hindbrain. Touch can elicit escape responses in the absence of Mauthner cells (Liu and Fetcho, 1999; Burgess et al., 2009), or even of the entire hindbrain (Downes and Granato, 2006), implying that RB neurons must also connect to local spinal circuits. Mauthner-independent escape responses have a substantially slower latency than the classic escape response (Liu and Fetcho, 1999; Kohashi and Oda, 2008; Burgess et al., 2009), suggesting that non-Mauthner-contacting RB cells may elicit those slow responses. If that is the case, activating individual neurons within this class might elicit distinct behaviors. The new transgenic enhancers presented here provide valuable tools for addressing this hypothesis and for comprehensively analyzing the sensory and behavioral functions of subtypes of somatosensory neuron in larval zebrafish.

A somatosensory neuron subtype is defined by PKC α and p2rx3a expression

Analysis of the PKC α^{ct7a} gene trap line, the *Fru.p2x3-2* reporter line and the *trpA1b:EGFP* BAC transgenic line revealed that they highlight the same population of RB neurons and faithfully reflect endogenous expression of PKC α and *p2rx3a*, thus defining a molecularly distinct somatosensory neuron subtype. To our knowledge, this is the first report of a somatosensory neuron subtype in zebrafish defined by more than one reporter or gene. In different experiments the percentage of RB neurons highlighted by these two reporters ranged from 30-50%, likely reflecting variability from animal to animal, but nonetheless consistent with previous reports that PKC α is expressed in ~40% of RB neurons (Slatter et al., 2005; Patten et al., 2007). PKC α is a kinase that functions in diverse signaling pathways, P2rx3a is an ATP-gated ion channel involved in nociception, and TrpA1b is a channel that is activated by pungent chemicals (Caron et al., 2008; Prober et al., 2008; Pan et al., 2012). This expression pattern suggests that these cells likely detect distinct nociceptive somatosensory stimuli and possess

unique physiological properties. Since they likely detect distinct stimuli, the peripheral arbors of PKC α /*p2rx3a/trpA1b*-expressing neurons likely “tile” the skin independently of other RB neurons, so that animals can sense each modality throughout their body. This prediction remains to be tested, but our previous observation that each zebrafish trigeminal axon arbor repels approximately half of its neighboring arbors is consistent with this model (Sagasti et al., 2005).

Acknowledgements

I would like to thank Lindsey Mork for initial cloning of zebrafish enhancers, Holly Vu for tracing neurons, Hillary McGraw for advice on *trkA in situ* hybridization, Michael Granato for the *Gt(T2KSAG)^{j1229a}* line, Alex Schier for the *Tg(trpA1b:EGFP)* line, Mark Voight for the *Tg(p2rx3b:EGFP)* line, Matt Veldman, Ann Cavanaugh and Kevin Mouillesseaux for technical advice and members of the Sagasti Lab for comments on the manuscript. Funds were provided by an NRSA (5F31NS064817) to AMSP from the NINDS and grants from the NSF (RIG:0819010) and NIDCR (5R01DE018496) to AS.

References

- Appelbaum L, Skariah G, Mourrain P, Mignot E. 2007. Comparative expression of p2x receptors and ecto-nucleoside triphosphate diphosphohydrolase 3 in hypocretin and sensory neurons in zebrafish. *Brain Res* 1174:66-75.
- Boué-Grabot E, Akimenko MA, Séguéla P. 2000. Unique functional properties of a sensory neuronal P2X ATP-gated channel from zebrafish. *J Neurochem* 75:1600-1607.
- Burgess HA, Johnson SL, Granato M. 2009. Unidirectional startle responses and disrupted left-right co-ordination of motor behaviors in robo3 mutant zebrafish. *Genes Brain Behav* 8:500-511.
- Caron SJ, Prober D, Choy M, Schier AF. 2008. In vivo birthdating by BAPTISM reveals that trigeminal sensory neuron diversity depends on early neurogenesis. *Development* 135:3259-3269.
- Davies A, Lumsden A. 1984. Relation of target encounter and neuronal death to nerve growth factor responsiveness in the developing mouse trigeminal ganglion. *J Comp Neurol* 223:124-137.
- Downes GB, Granato M. 2006. Supraspinal input is dispensable to generate glycine-mediated locomotive behaviors in the zebrafish embryo. *J Neurobiol* 66:437-451.
- Drapeau P, Saint-Amant L, Buss RR, Chong M, McDearmid JR, Brustein E. 2002. Development of the locomotor network in zebrafish. *Prog Neurobiol* 68:85-111.
- Fetcho JR, O'Malley DM. 1995. Visualization of active neural circuitry in the spinal cord of intact zebrafish. *J Neurophysiol* 73:399-406.
- Goll MG, Anderson R, Stainier DY, Spradling AC, Halpern ME. 2009. Transcriptional silencing and reactivation in transgenic zebrafish. *Genetics* 182:747-755.

- Grueber WB, Ye B, Moore AW, Jan LY, Jan YN. 2003. Dendrites of distinct classes of *Drosophila* sensory neurons show different capacities for homotypic repulsion. *Curr Biol* 13:618-626.
- Hayes BP, Roberts A. 1983. The anatomy of two functional types of mechanoreceptive 'free' nerve-ending in the head skin of *Xenopus* embryos. *Proc R Soc Lond B Biol Sci* 218:61-76.
- Higashijima S, Hotta Y, Okamoto H. 2000. Visualization of cranial motor neurons in live transgenic zebrafish expressing green fluorescent protein under the control of the islet-1 promoter/enhancer. *J Neurosci* 20:206-218.
- Kawakami K. 2004. Transgenesis and gene trap methods in zebrafish by using the Tol2 transposable element. *Methods Cell Biol* 77:201-222.
- Kimmel CB, Hatta K, Metcalfe WK. 1990. Early axonal contacts during development of an identified dendrite in the brain of the zebrafish. *Neuron* 4:535-545.
- Kohashi T, Oda Y. 2008. Initiation of Mauthner- or non-Mauthner-mediated fast escape evoked by different modes of sensory input. *J Neurosci* 28:10641-10653.
- Korn H, Faber DS. 2005. The Mauthner cell half a century later: a neurobiological model for decision-making? *Neuron* 47:13-28.
- Kucenas S, Soto F, Cox JA, Voigt MM. 2006. Selective labeling of central and peripheral sensory neurons in the developing zebrafish using P2X(3) receptor subunit transgenes. *Neuroscience* 138:641-652.
- Kwan KM, Fujimoto E, Grabher C, Mangum BD, Hardy ME, Campbell DS, Parant JM, Yost HJ, Kanki JP, Chien CB. 2007. The Tol2kit: a multisite gateway-based construction kit for Tol2 transposon transgenesis constructs. *Dev Dyn* 236:3088-3099.

- Köster RW, Fraser SE. 2001. Tracing transgene expression in living zebrafish embryos. *Dev Biol* 233:329-346.
- Lai SL, Lee T. 2006. Genetic mosaic with dual binary transcriptional systems in *Drosophila*. *Nat Neurosci* 9:703-709.
- Liu KS, Fetcho JR. 1999. Laser ablations reveal functional relationships of segmental hindbrain neurons in zebrafish. *Neuron* 23:325-335.
- Liu YC, Bailey I, Hale ME. 2012. Alternative startle motor patterns and behaviors in the larval zebrafish (*Danio rerio*). *J Comp Physiol A Neuroethol Sens Neural Behav Physiol* 198:11-24.
- Lumpkin EA, Caterina MJ. 2007. Mechanisms of sensory transduction in the skin. *Nature* 445:858-865.
- Marmigère F, Ernfors P. 2007. Specification and connectivity of neuronal subtypes in the sensory lineage. *Nat Rev Neurosci* 8:114-127.
- Martin SC, Marazzi G, Sandell JH, Heinrich G. 1995. Five Trk receptors in the zebrafish. *Dev Biol* 169:745-758.
- Metcalfe WK, Myers PZ, Trevarrow B, Bass MB, Kimmel CB. 1990. Primary neurons that express the L2/HNK-1 carbohydrate during early development in the zebrafish. *Development* 110:491-504.
- Moore SJ, Munger BL. 1989. The early ontogeny of the afferent nerves and papillary ridges in human digital glabrous skin. *Brain Res Dev Brain Res* 48:119-141.
- Norton WH, Rohr KB, Burnstock G. 2000. Embryonic expression of a P2X(3) receptor encoding gene in zebrafish. *Mech Dev* 99:149-152.

- O'Brien GS, Rieger S, Wang F, Smolen GA, Gonzalez RE, Buchanan J, Sagasti A. 2012. Coordinate development of skin cells and cutaneous sensory axons in zebrafish. *J Comp Neurol* 520:816-831.
- Pan YA, Choy M, Prober DA, Schier AF. 2012. Robo2 determines subtype-specific axonal projections of trigeminal sensory neurons. *Development* 139:591-600.
- Patten SA, Sihra RK, Dhama KS, Coutts CA, Ali DW. 2007. Differential expression of PKC isoforms in developing zebrafish. *Int J Dev Neurosci* 25:155-164.
- Pineda RH, Svoboda KR, Wright MA, Taylor AD, Novak AE, Gamse JT, Eisen JS, Ribera AB. 2006. Knockdown of Nav1.6a Na⁺ channels affects zebrafish motoneuron development. *Development* 133:3827-3836.
- Pittman AJ, Law MY, Chien CB. 2008. Pathfinding in a large vertebrate axon tract: isotypic interactions guide retinotectal axons at multiple choice points. *Development* 135:2865-2871.
- Prober DA, Zimmerman S, Myers BR, McDermott BM, Kim SH, Caron S, Rihel J, Solnica-Krezel L, Julius D, Hudspeth AJ, Schier AF. 2008. Zebrafish TRPA1 channels are required for chemosensation but not for thermosensation or mechanosensory hair cell function. *J Neurosci* 28:10102-10110.
- Reyes R, Haendel M, Grant D, Melancon E, Eisen JS. 2004. Slow degeneration of zebrafish Rohon-Beard neurons during programmed cell death. *Dev Dyn* 229:30-41.
- Roberts A. 1980. The function and role of two types of mechanoreceptive "free" nerve endings in the head skin of amphibian embryos. *Journal of Comparative Physiology* 135:341-348.

- Sagasti A, Guido MR, Raible DW, Schier AF. 2005. Repulsive interactions shape the morphologies and functional arrangement of zebrafish peripheral sensory arbors. *Curr Biol* 15:804-814.
- Saint-Amant L, Drapeau P. 1998. Time course of the development of motor behaviors in the zebrafish embryo. *J Neurobiol* 37:622-632.
- Slatter CA, Kanji H, Coutts CA, Ali DW. 2005. Expression of PKC in the developing zebrafish, *Danio rerio*. *J Neurobiol* 62:425-438.
- Svoboda KR, Linares AE, Ribera AB. 2001. Activity regulates programmed cell death of zebrafish Rohon-Beard neurons. *Development* 128:3511-3520.
- Trinh IA, Hochgreb T, Graham M, Wu D, Ruf-Zamojski F, Jayasena CS, Saxena A, Hawk R, Gonzalez-Serricchio A, Dixon A, Chow E, Gonzales C, Leung HY, Solomon I, Bronner-Fraser M, Megason SG, Fraser SE. 2011. A versatile gene trap to visualize and interrogate the function of the vertebrate proteome. *Genes Dev* 25:2306-2320.
- Tsutsui H, Karasawa S, Shimizu H, Nukina N, Miyawaki A. 2005. Semi-rational engineering of a coral fluorescent protein into an efficient highlighter. *EMBO Rep* 6:233-238.
- Uemura O, Okada Y, Ando H, Guedj M, Higashijima S, Shimazaki T, Chino N, Okano H, Okamoto H. 2005. Comparative functional genomics revealed conservation and diversification of three enhancers of the *isl1* gene for motor and sensory neuron-specific expression. *Dev Biol* 278:587-606.
- Volkman K, Köster RW. 2007. In vivo retrograde labeling of neurons in the zebrafish embryo or larva with rhodamine dextran. *CSH Protoc* 2007:pdb.prot4832.

Williams JA, Barrios A, Gatchalian C, Rubin L, Wilson SW, Holder N. 2000. Programmed cell death in zebrafish rohn beard neurons is influenced by TrkC1/NT-3 signaling. *Dev Biol* 226:220-230.

Figures

Table 1. Enhancer regions from the zebrafish and pufferfish genomes drive reporter expression in somatosensory neurons. Enhancer regions were isolated by cloning sequences upstream of the translational start site (ATG) of indicated genes (Enhancers) of indicated lengths (Size, in base pairs) from the genomes of either zebrafish or pufferfish (Origin). All sequences drove expression in trigeminal and Rohon-Beard neurons (TG and RB); a few drove expression in additional tissues, such as muscle and other neurons (Expression). Expression analysis of all transgenes was performed with transient transgenesis, as described in the text. In some cases stable transgenic lines (*) verified expression specificity. Shaded rows indicate previously reported enhancers.

Enhancer	Size (bp)	Origin	Expression
<i>isl1(ss)</i>	4200	zebrafish	TG, RB, other neurons*
<i>CREST3</i>	868	zebrafish	TG, RB, DRG*
<i>trpA1a</i>	5019	zebrafish	TG, RB, lateral line
<i>trkA</i>	3939	pufferfish	TG, RB*
<i>trkB</i>	4017	pufferfish	TG, RB, other neurons
<i>trkC</i>	3936	pufferfish	TG, RB, other neurons, muscle
<i>p2x3-2</i>	1620	pufferfish	TG, RB, muscle*

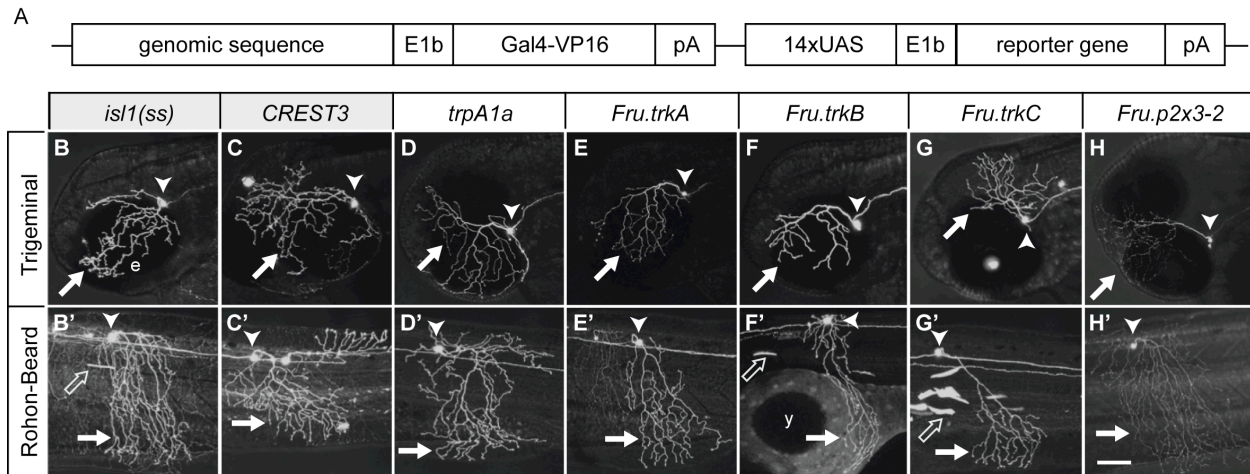
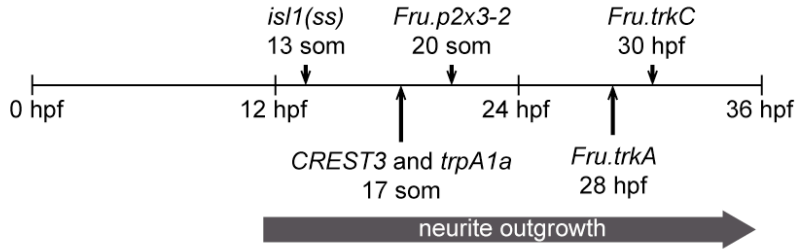


Figure 1. New transgenes drive expression in zebrafish somatosensory neurons. (A) Design of transgenic reporters: Genomic sequences containing somatosensory-specific enhancers drove the Gal4-VP16 transcriptional activator; on the same plasmid 14 copies of the Gal4 upstream activation sequence (14xUAS) were used to drive GFP. The adenovirus E1b minimal promoter was placed upstream of both Gal4-VP16 and the reporter gene. An SV40 polyadenylation sequence was placed 3' to both Gal4-VP16 and the reporter gene to signal transcription termination. (B-H') Transgenes were transiently expressed in zebrafish larvae and imaged by confocal microscopy at 72 hpf. Both zebrafish and pufferfish (*Fru*) genomic enhancer sequences drove expression of fluorescent reporters in zebrafish trigeminal (B-H) and Rohon-Beard (B'-H') neurons. Anterior is left and dorsal is up in all images. The eye (e) and yolk (y) are indicated. Arrowheads point to cell bodies; arrows point to peripheral arbors; empty arrows point to muscle. Scale bar, 100 μ m.

A. Initial onset of transgene expression



B. Approach for determining duration of transgene activity

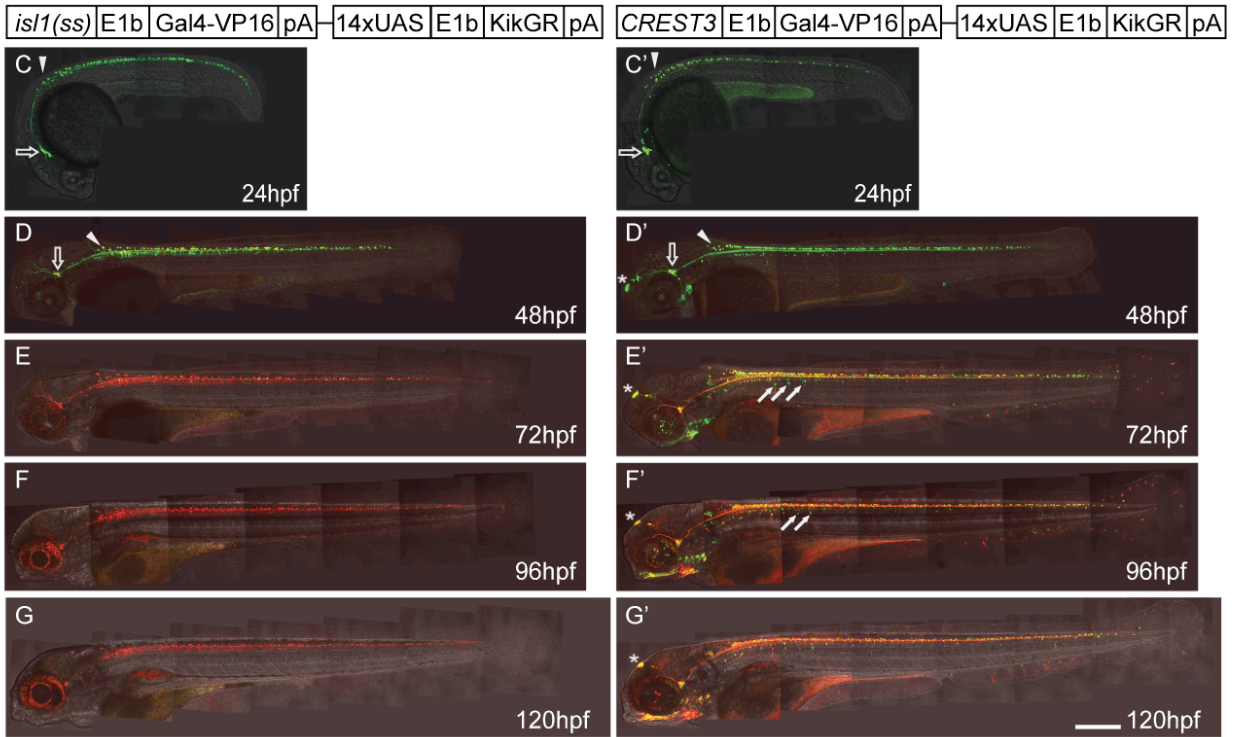
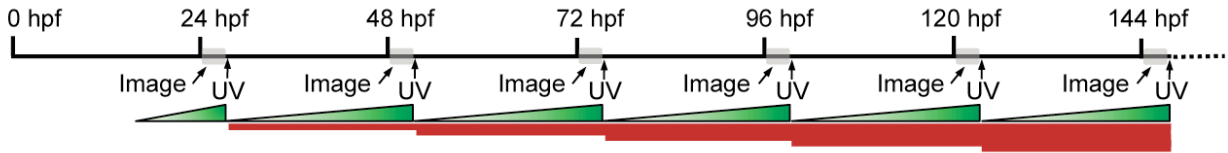


Figure 2. Different transgenes have distinct temporal expression patterns. (A) Onset of gene expression as determined by transient transgenesis. Transgenes with indicated enhancers driving GFP (see Figure 1) were injected into embryos at the one-cell stage. Embryos were raised at 28.5°C and staged according to somite (som) number and hours post fertilization (hpf). Initial observation of GFP expression was recorded: Expression driven by the *isll(ss)* enhancer was the earliest at 13 som, followed by *CREST3* and *trpA1a* enhancer-driven expression at 17 som, *Fru.p2x3-2* enhancer-driven expression at 20 som, *Fru.trkA* enhancer-driven expression at 28 hpf and *Fru.trkC* enhancer-driven expression at 30 hpf. (B) The duration of *isll(ss)* and *CREST3* enhancer activity was determined by daily photoconversion and imaging of KikGR expression. Green fluorescence indicated newly synthesized KikGR (active promoter, new neuron), red fluorescence indicated older/photoconverted KikGR (inactive promoter, old neuron) and yellow indicated neurons expressing both forms of KikGR (active promoter, old neuron). (C-G) The *isll(ss)* enhancer was active from 14 hpf until approximately 54 hpf. (C'-G') Enhancer activity in sensory neurons lasted until at least 14 dpf (see Figure 3). Confocal images were taken with a 20x objective and 0.7x optical zoom; anterior is left and dorsal is up. Empty arrows indicate the trigeminal ganglia, arrowheads point to anterior RB neurons, filled arrows are DRGs and asterisks are located near a population of anterior neurons. Scale bar, 300 μm.

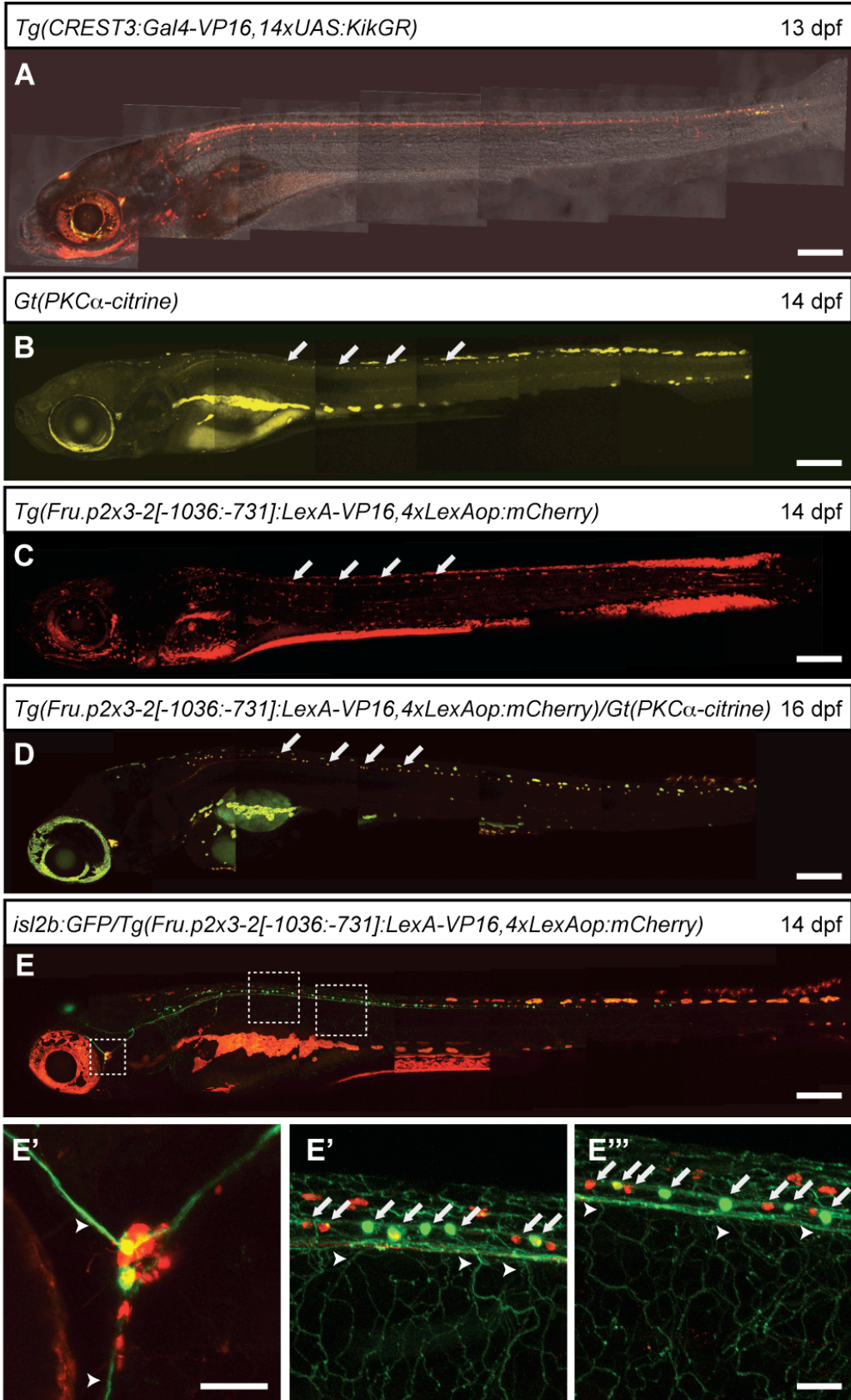


Figure 3. Rohon-Beard neurons persist in 2-week-old larvae. Somatosensory neurons in (A) *CREST3*, (B) *PKC α^{ct7a}* , (C) *Fru.p2x3-2*, (D) *Fru.p2x3-2/PKC α^{ct7a}* and (E) *isl2b/Fru.p2x3-2* transgenic fish were visible until at least two weeks post-fertilization. Confocal images were taken with a 20x objective; anterior is left and dorsal is up. (E'-E''') Magnified images of various regions outlined in E. Trigeminal neurons are shown in E' and RB neurons in E'' and E'''. Arrows point to individual RB neuron cell bodies. Arrowheads in E'-E''' point to RB neuron peripheral arbors. Scale bar, 200 μm in A-E and 50 μm in E'-E'''.

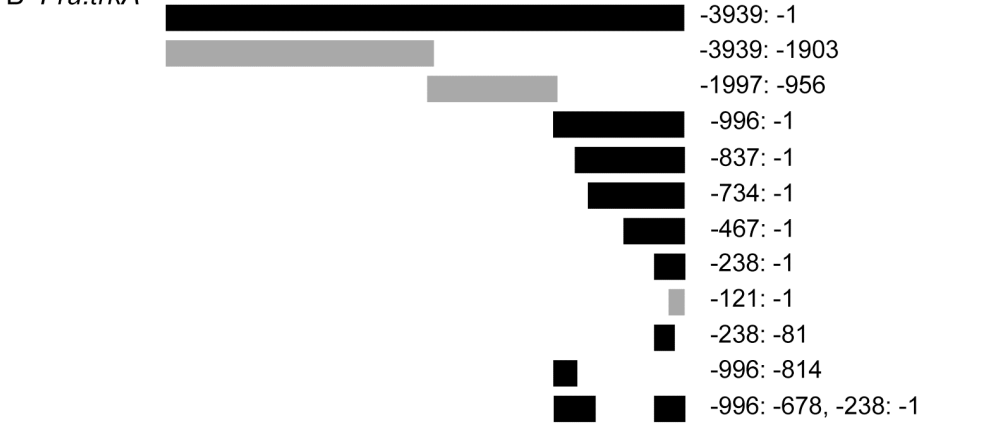

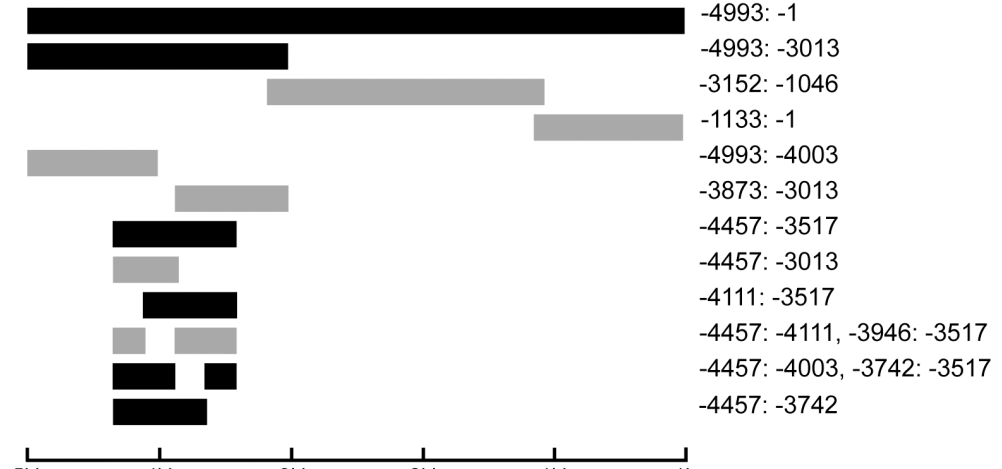
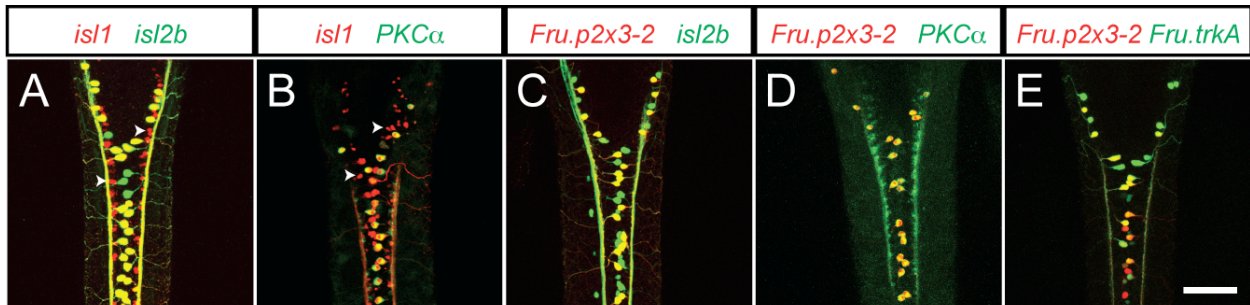
A	
<p>B <i>Fru.trkA</i></p>  <p> -3939: -1 -3939: -1903 -1997: -956 -996: -1 -837: -1 -734: -1 -467: -1 -238: -1 -121: -1 -238: -81 -996: -814 -996: -678, -238: -1 </p>	<p>% embryos with expression</p> <p>25% none none 48% 30% 32% 28% 17% none 20% 17% 43%</p>
<p>C <i>Fru.p2x3-2</i></p>  <p> -1619: -1 -1619: -974 -1036: -1 -1036: -479 -510: -109 -168: -1 -1036: -731 -751: -479 -1036: -926 -822: -606 -946: -802 </p>	<p>70% none 55% 59% none none 65% none none none 24%</p>
<p>D <i>trpA1a</i></p>  <p> -4993: -1 -4993: -3013 -3152: -1046 -1133: -1 -4993: -4003 -3873: -3013 -4457: -3517 -4457: -3013 -4111: -3517 -4457: -4111, -3946: -3517 -4457: -4003, -3742: -3517 -4457: -3742 </p> <p>-5kb -4kb -3kb -2kb -1kb -1bp</p>	<p>+ + none none none none 60% none 70% none 50% +</p>

Figure 4. Identification of minimal regulatory elements sufficient for transgene expression in zebrafish trigeminal and Rohon-Beard neurons. (A) Transgenes were constructed by cloning genomic sequences upstream of Gal4-VP16,14xUAS:GFP or LexA-VP16,4xLexAop:mCherry (the E1b promoter and SV40 pA sequence were used as indicated). (B) Two fragments of the *Fru.trkA* enhancer, each less than 200 bp, were sufficient to drive expression in sensory neurons, though both together were required to drive expression at levels similar to the ~1 kb fragment [-996: -1]. (C) A 144 bp fragment [-946: -802] of the *Fru.p2x3-2* enhancer sequence was sufficient to drive expression in somatosensory neurons, though its efficiency was lower than that of a 305 bp fragment [-1036: -731]. (D) The *trpA1a* enhancer sequence was divided into 4 functional elements. The right column indicates the percent of embryos with expression within a clutch. (+) in (D) indicates qualitatively similar expression from each transgene, though this was not quantitatively measured.



F Co-expression of stable transgenic lines

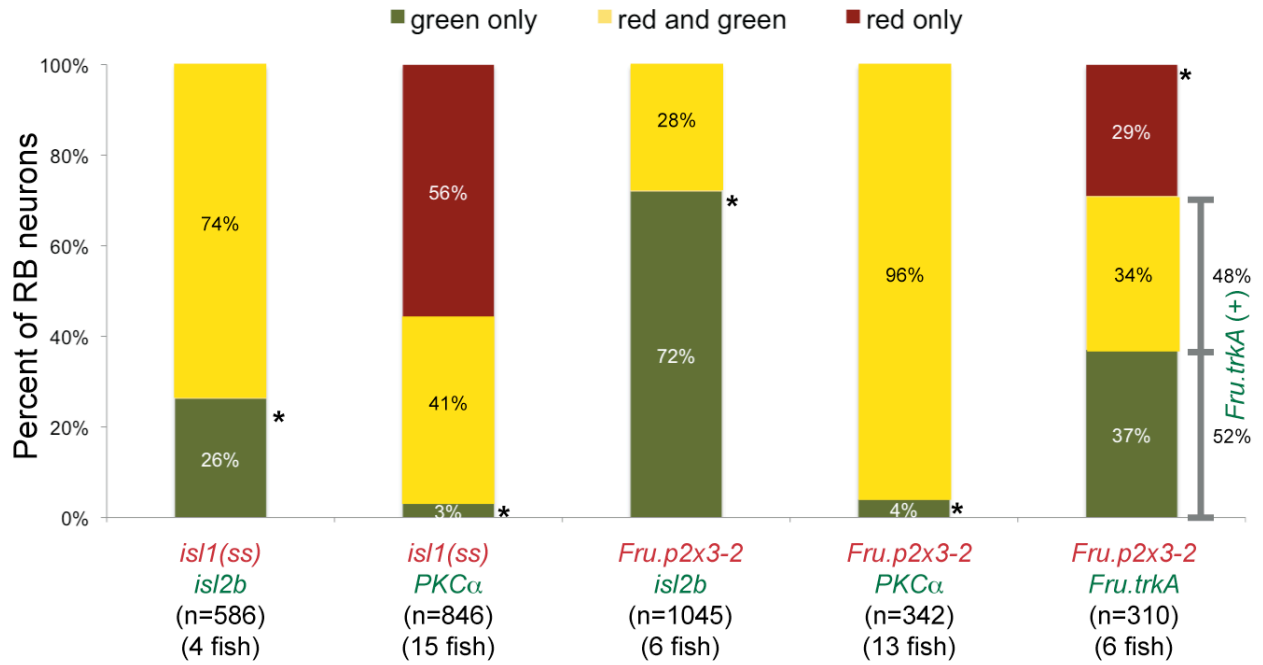


Figure 5. The PKC α^{ct7a} gene trap line and a transgenic reporter using a *Fru.p2x3-2* enhancer label the same subset of Rohon-Beard neurons. (A-E) Transgenic lines, each using the indicated enhancers to drive expression of different fluorescent proteins, were crossed to compare their expression patterns. (A) Crossing *Tg(is11(ss):Gal4-VP16,14xUAS:DsRed)* to *Tg(-17.6isl2b:GFP)* allowed us to estimate the degree of variegation caused by the Gal4/UAS system: The *isl2b* (GFP) and *is11(ss)* (DsRed) enhancers are thought to drive expression in all somatosensory neurons, however the *is11(ss)* reporter line was expressed in only 74% of *isl2b:GFP* RB neurons (co-expression shown in yellow), suggesting that in the *is11(ss)* line the Gal4/UAS system was silenced in ~25% of RB neurons. Small lateral DsRed-labeled cells (indicated by arrowheads) are not RB neurons. (B) The PKC α^{ct7a} line labeled ~40% the RB neurons labeled by the variegated *is11(ss)* reporter line. (C) The *Fru.p2x3-2* reporter line labeled approximately a third of all RB neurons labeled by *isl2b:GFP*. (D) The *Fru.p2x3-2* reporter line was expressed in the same population of RB neurons as the PKC α^{ct7a} line. (E) Approximately 50% of RB neurons labeled by the *Fru.trkA* reporter line overlapped with the *Fru.p2x3-2* reporter line. Dorsal confocal images were taken of the anterior spinal cord with a 20x objective; anterior is up. Scale bar, 100 μ m. (F) Quantification of co-expression between transgenic lines. n = total number of RB neurons. Asterisks indicate categories that may underestimate co-expression due to variegation in some reporter lines.

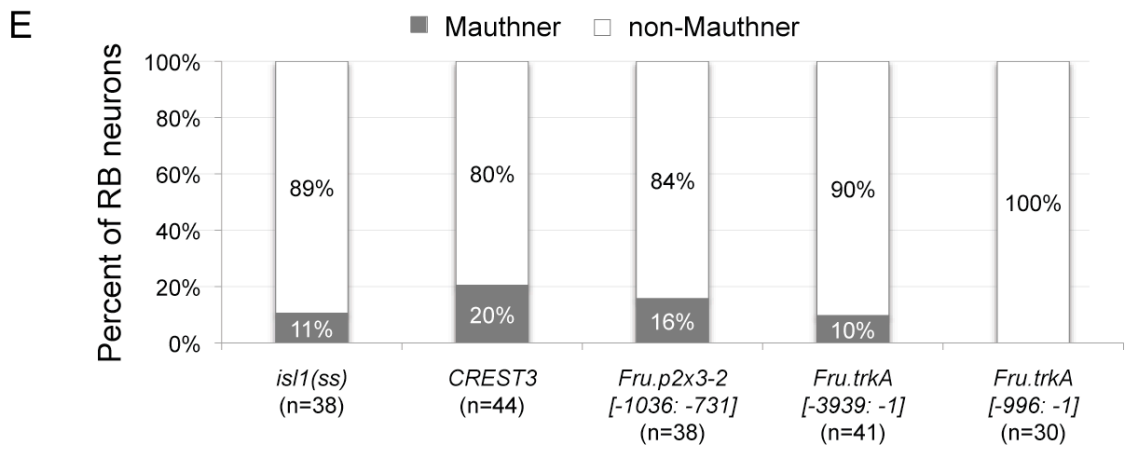
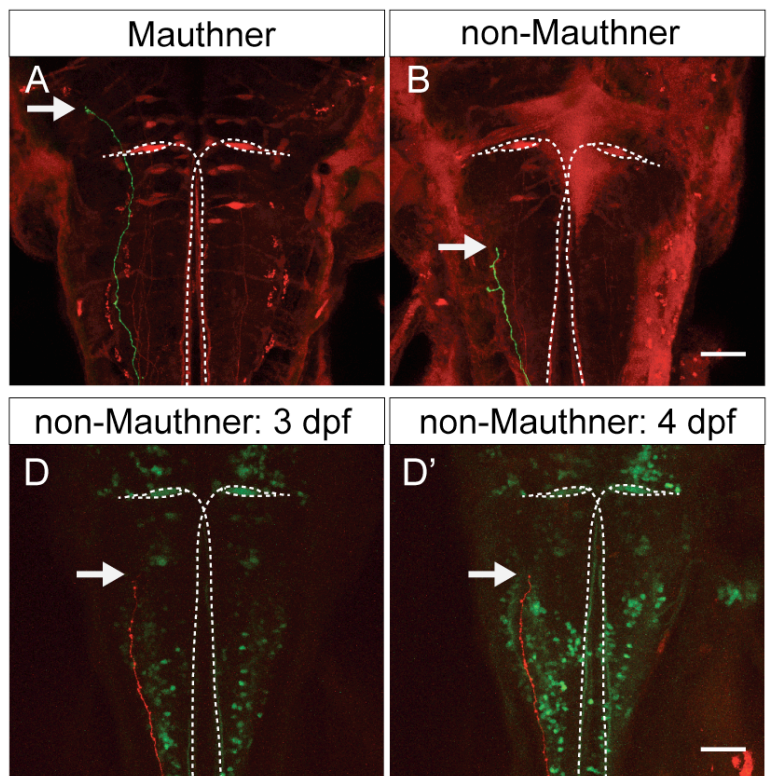
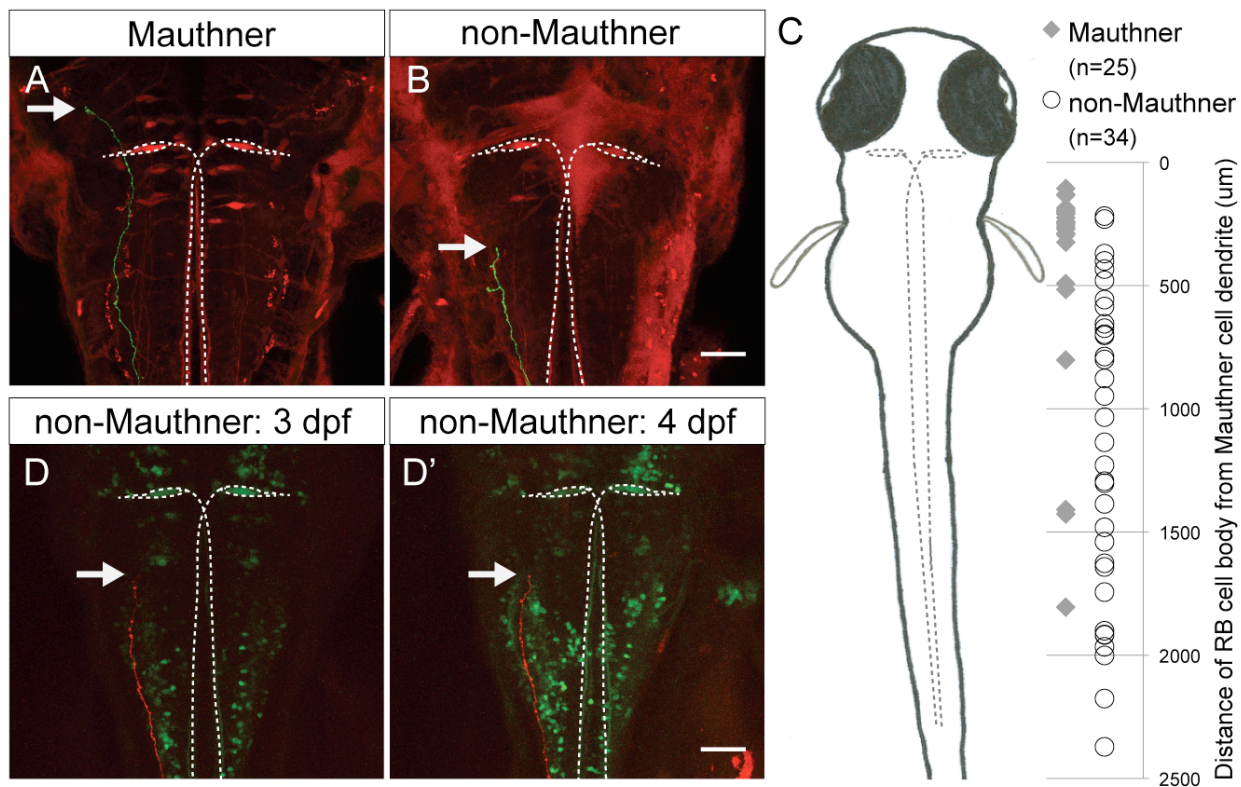


Figure 6. Rohon-Beard central projections either contact or fail to contact the Mauthner cell dendrite. (A-B) Dorsal confocal images of 72 hpf larvae show two patterns of central projection termination. Some RB central projections contacted the Mauthner cell dendrite (labeled by retrograde dye-filling) (Mauthner) (A), whereas others terminated caudal to the Mauthner cell dendrite (non-Mauthner) (B). Arrows indicate the rostral termini of RB central axons. The Mauthner cells are outlined. Scale bar, 50 μ m. (C) The position of a neuron's cell body along the rostral-caudal axis did not dictate whether or not its central projection contacted the Mauthner cell dendrite. (D and D') Failure to contact the Mauthner cell dendrite was not due to slow RB central axon growth. Confocal images of a non-Mauthner contacting RB neuron (red) in the *Gt(T2KSAG)^{j1229a}* gene trap line taken at 3 and 4 dpf. Scale bar, 50 μ m. (E) All transgenes primarily labeled non-Mauthner dendrite contacting RB neurons. n = total number of RB neurons.

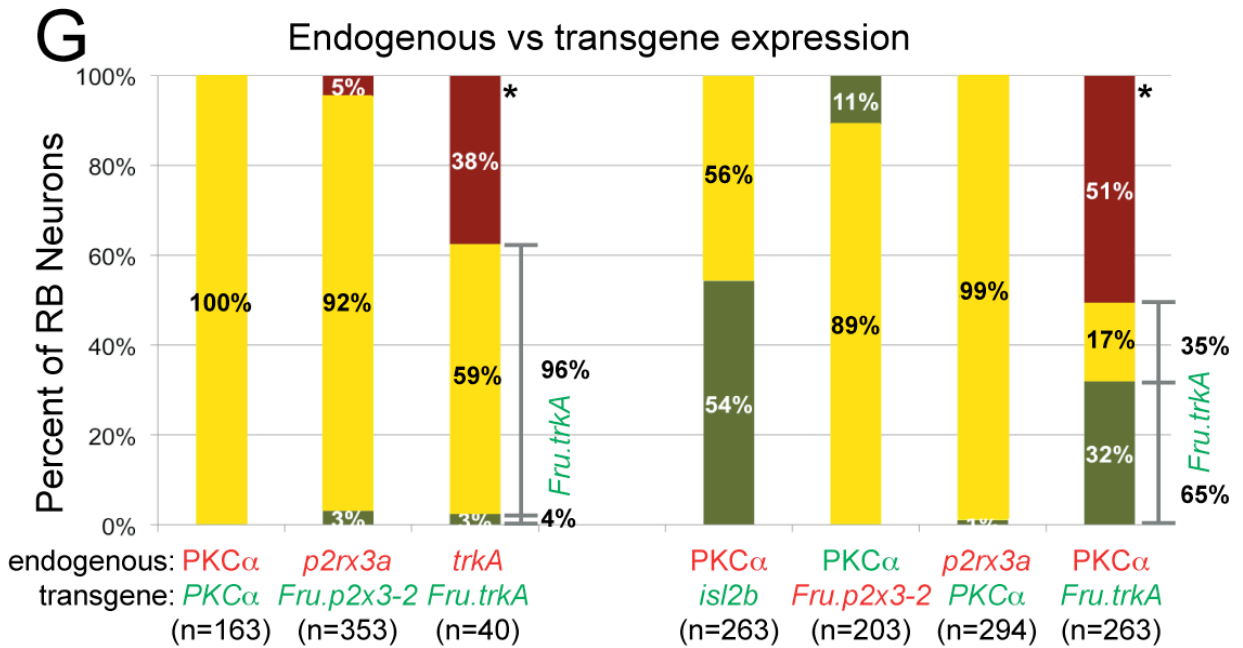
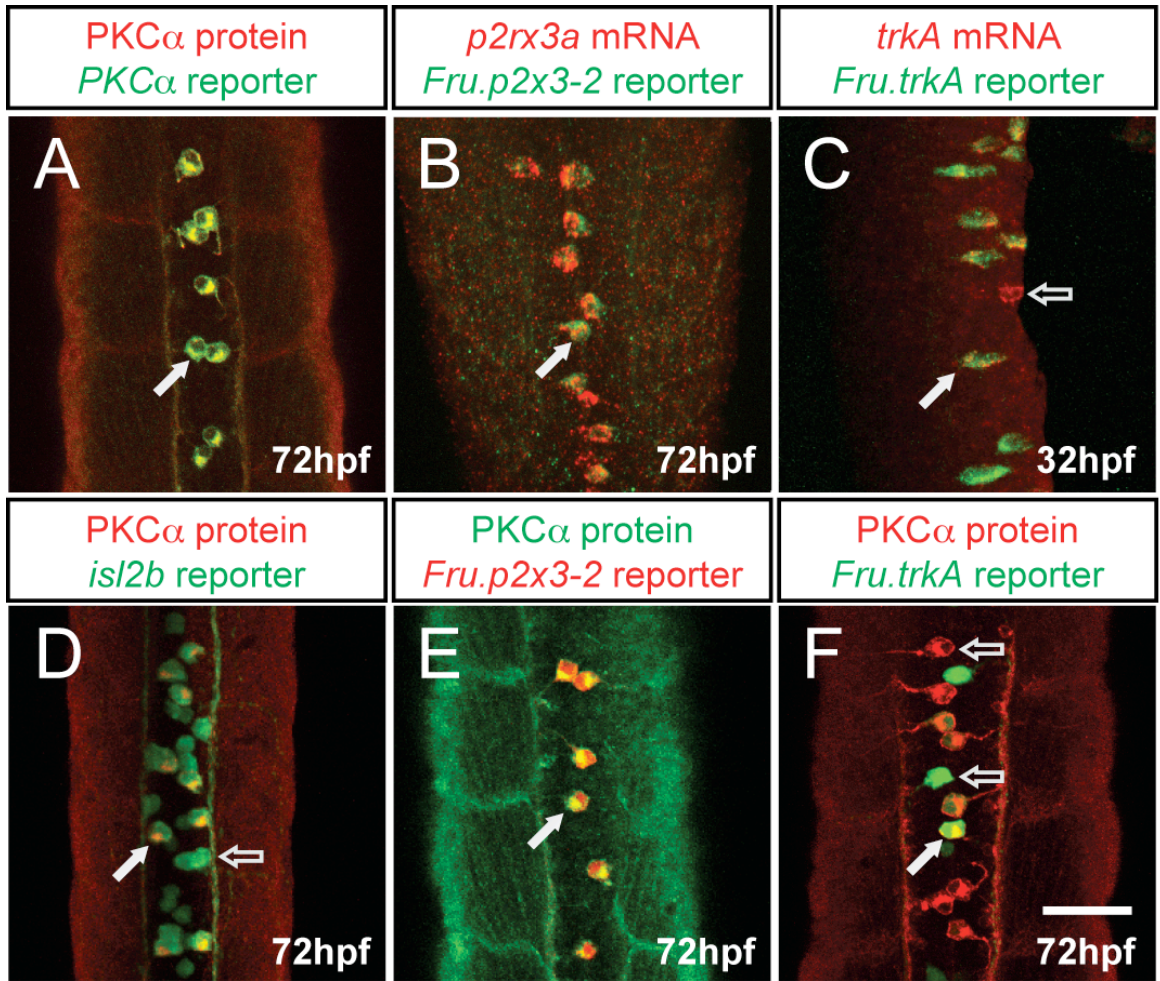
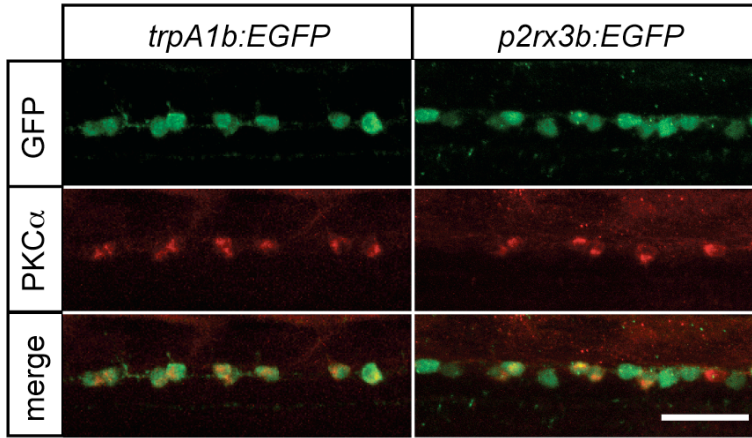


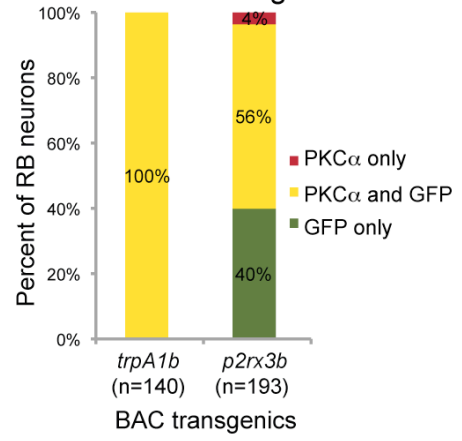
Figure 7. Fluorescent transgenic reporters accurately reflect endogenous gene expression.

(A, D-F) Whole mount double antibody staining for endogenous protein expression and transgene-driven fluorescent protein expression. (B and C) Fluorescent *in situ* hybridization for endogenous mRNA and antibody staining for transgene-driven fluorescent protein expression. The label above each panel indicates the endogenous protein or mRNA visualized and the transgene enhancer used. Filled arrows indicate cells co-expressing the transgene and protein or mRNA; open arrows indicate cells expressing only one or the other. Confocal images of the dorsal spinal cord were taken with a 20x objective and a 2x optical zoom; anterior is up. Scale bar, 50 μ m. (G) Quantification of co-expression between transgene and endogenous genes. The PKC α ^{ct7a} line faithfully labeled all (100%) cells expressing PKC α protein, the *Fru.p2x3-2* reporter line labeled most (92%) *p2rx3a* mRNA-expressing neurons and the *Fru.trkA* reporter line labeled the majority (60%) of *trkA* expressing neurons. Note that many neurons expressing *trkA* mRNA did not express the reporter, indicating variegation. PKC α protein was expressed in 46% of the total (*isl2b:GFP*-expressing) RB neuron population. PKC α endogenous expression almost perfectly co-labeled neurons marked by the *Fru.p2x3-2* reporter line and vice versa. Expression of the PKC α protein only partially overlapped with *Fru.trkA* reporter line expression, as expected from analyzing transgene co-expression (Figure 5). Due to variegation of the transgene (indicated by the asterisk) the number of neurons expressing PKC α protein only is an overestimate. n = total number of RB neurons.

A



B Co-expression of PKC α and BAC transgenic lines



C Molecular Subtypes

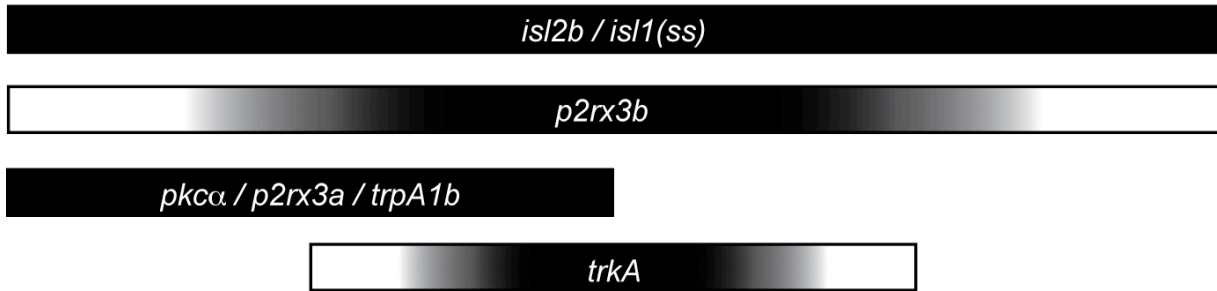


Figure 8. Transgenic lines label molecular subtypes of somatosensory neurons. (A) Antibody staining for PKC α (red) and GFP (green) in 72 hpf *trpA1b:GFP* and *p2rx3b:GFP* BAC transgenic lines. Confocal images of the spinal cord were taken with a 20x objective and a 2x optical zoom; lateral images, anterior is left and dorsal is up. Scale bar, 50 μ m. (B) 100% of *trpA1b:GFP* RB neurons expressed PKC α . Approximately 56% of *p2rx3:GFP* RB neurons also expressed PKC α . n = number of RB neurons. (C) Model for zebrafish larval RB neuron subtypes: *isl2b* and *isl1(ss)* highlight all RB somatosensory neurons. *p2rx3b:GFP* expression labels most, if not all, RB neurons. PKC, *p2rx3a* and *trpA1b:GFP* are co-expressed in a distinct population of neurons that make up approximately 40% of all RB neurons. TrkA-expressing neurons partially overlap with the PKC α /*p2rx3a* subtype.

Supplementary Methods

Extracting Data from NeuroLucida Explorer

Individual neurons were traced in 3 dimensions using NeuroLucida software. Data from each traced image was extracted using NeuroLucida Explorer. Running the Segment analysis generated an Excel table showing, among other characteristics, the branch order and length of each segment. Branches were ordered in this matrix so that the bottom-most branch shown was the root branch, from beginning to the first node. The next branch up was a branch of order 2, off of the root branch. The next one shown was a branch of order 3, and so on. Upon encountering a branch of order x with a normal ending (i.e., one that did not split further), the program went back to the nearest node y . The next segment displayed was the other branch of order x that originated at y . After encountering the next ending, the program went back to the nearest node from which there was an un-displayed branch and displayed that branch. The values for length and branch order of each segment were copied, preserving the original order in Excel, into a new worksheet, which was then saved as a .csv file. The data also went into a spreadsheet titled worksheet Data.xls. Both the .csv file and the spreadsheet were labeled with the name of the tracing. (The contents of the Data.xls spreadsheet do not matter; however, the name of the spreadsheet must match the name of the .csv file.) All the data was then imported into a Matlab program we developed called Comparing_Distance_Matrices3.

Creating the Distance Matrix

After importing the Excel data, a distance matrix was created for each using the Matlab function DistanceMatrixFinal. Given a branch A and its order x , the distance from branch A to a branch B of order y (assuming without loss of generality that B is above A in the Excel table) is

the sum of the lengths of the branches between B and A. The Excel table was used to extract the lengths of these branches for any given branches A and B. The start of the root branch, every node, and every ending on the neuron was counted as a point and numbered. The start of the root branch is 1, the end of the root branch 2, the ends of the second-order branches 3 and 4, and so forth. Each entry (i, j) of the final distance matrix represents the distance between points i and j in that particular tracing. A more detailed description of the methodology in creating this distance matrix follows.

When the Excel data was imported into DistanceMatrixFinal, it was flipped vertically, so that the last row of the table was the first row of the input matrix, the second-to-last row of the table was the second row of the input matrix, and so on. To find the branches between branches A and B, it was assumed first that B was below A in the input matrix (i.e., B was above A in the Excel table). First, considering the case where there was no branch of order less than A's between A and B. The lengths of the relevant branches were extracted assuming that every branch between A and B in the tracing must be between A and B in the table and have an order between x and y . The relevant branch for each of these orders is the one closest to A in the matrix. These lengths were then grouped together in a three-dimensional matrix R . Given a branch i of order x and a branch j (above i) of order y , $R(i, j, :)$ contains the lengths of each branch of order between x and y that is closest to row i in the Excel matrix.

The matrix T that contains the distance matrix, formed by summing the entries in each $R(i, j, :)$. As stated above, the start of the root branch, every node, and every ending on the neuron was counted as a point, so the # of points = 1 + # of branches. Initially, the point at the end of the branch in row i was assigned to be represented by the $i+1$ th row/column in the distance matrix. Point 1 was the start of the root branch. The upper half of T was formed by

summing the $(i, j, :)$ entries of R and assigning that value to the $(i, j+1)$ entry of T . The diagonal was assigned to be all zeros, because the distance between a point and itself is zero. In the case where going from point x to point y meant “backtracking” along a branch of lower order, $T(x, y)$ was assigned to be zero, to be corrected as described below.

If there was a branch between the i th and j th rows with order less than the order of the j th row, then $R(i, j, :)$ also represented the lengths of the branches between i and j . However, a slightly more complicated method was necessary to find these branches. The lengths of those branches between branch i and the branch of minimum order between i and j (call it branch k) were found using the same method as mentioned above for branches where no backtracking was necessary. The same was done for the branches between branches i and k . All of these branches were then entered into $R(i, j, :)$. The sum of the entries in $R(i, j, :)$ was then assigned to $T(i+1, j+1)$. The upper half of T was then complete, and the lower half formed by assigning $T(i, j)$ to equal $T(j, i)$.

Finally, the numbers of the points in the tracing were reassigned, shuffling T . The start of the root branch was point 1. The end of the root branch was point 2, the ends of the second-order branches 3 and 4, and so forth, as described above. The new number of each point was found and assigned the old entry of T to its new coordinates.

Comparing the Distance Matrices

`Comparing_Distance_Matrices3` takes the tracings and compares each pair of them to generate a correlation coefficient. All correlation coefficients were put in a matrix, where each (i, j) entry is the correlation coefficient between matrices i and j . The correlation between a matrix and itself is 1, and all other coefficients range from 0 to the ratio of the sizes of the

matrices. The matrices are numbered according to the order of their spreadsheets in Data.xls. Only the upper half of the correlation coefficient matrix was computed, since the (i, j) and the (j, i) correlation coefficients should be the same, the lower half of the matrix was assigned to be the upper half reflected over the diagonal. Each pair of matrices was compared by randomly choosing and shuffling rows and columns in a Monte Carlo simulation. To fix the primary branch (i.e., the first row and column for each matrix), we replace rTest1 in the program with rTest2. The program does this for a chosen number of iterations (this analysis was performed with 2500, 3000, 5000, 10000 iterations) and outputs the maximum global correlation coefficient. Each coefficient is then multiplied by the ratio of the sizes of the distance matrices being compared. The size of the distance matrix depends directly on the number of branches in the tracing, so this variable as well as the branch length is considered in the analysis.

Constructing the Dendrogram

Once the matrix of correlation coefficients was computed, Matlab was used to find the Euclidean distances between each pair of coefficients in the correlation coefficient matrix. Next, Matlab clustered these pairs, treating each row of the coefficient matrix as a row of observations (the coefficient when matrix i is compared with matrix 1, when compared with matrix 2, etc.). Thus, each row vector i “represents” the matrix i . Three different methods of clustering the pairs were used. The unweighted average distance used the average distance between all pairs of objects in the two clusters being combined. These clusters may be single or already-combined row vectors. The weighted average method does the same, only using weighted instead of unweighted averages (the distances are weighted by the size of the clusters being combined). Ward’s method uses the incremental sum-of-squares, meaning the increase in the total sum of squares as a result of joining the two clusters. The sum of squares is defined as the sum of the

squares of the distance between all entries in the row vector and the centroid of that vector.

Each of these methods produced a matrix that Matlab converted to a dendrogram with at most thirty leaf nodes; since this analysis had seventy tracings, several nodes represented more than one distance matrix. The indexing of the dendrogram function was used to determine the names of the tracings whose distance matrices were represented by each node.

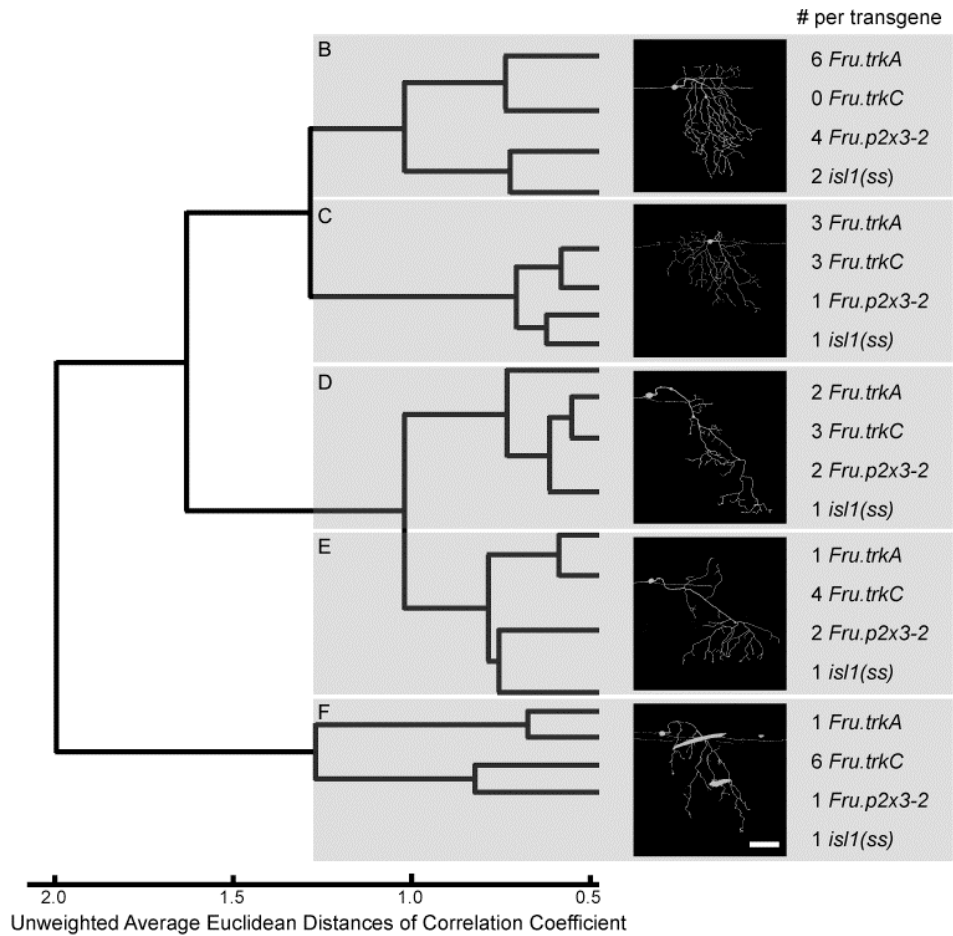
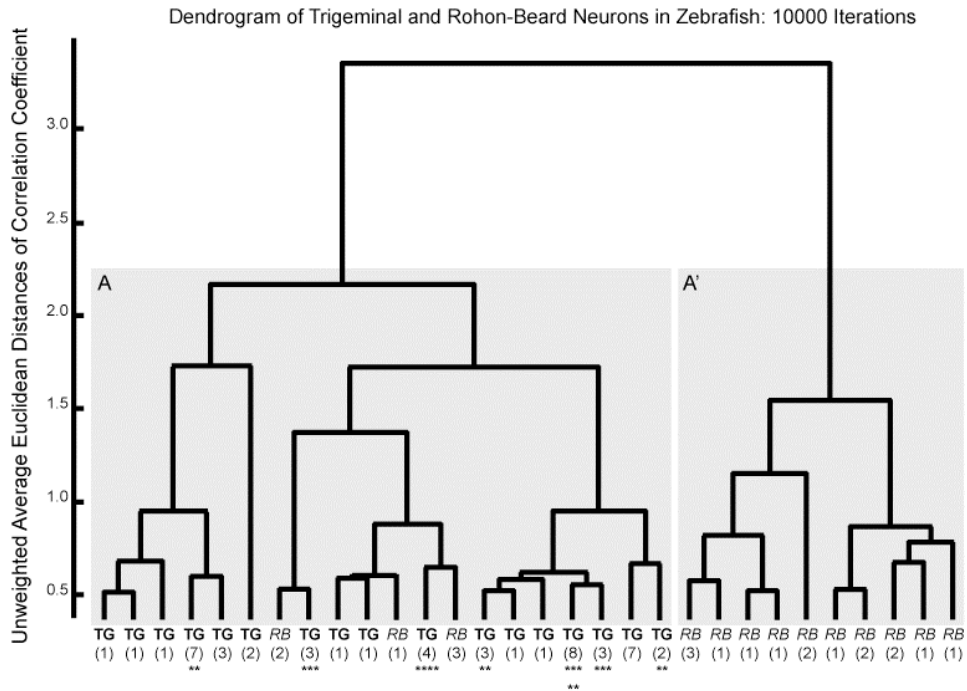
Brief Summary of Results

Given the similarity between the correlation coefficient matrices produced, the number of iterations did not appear to be important. The correlations between the matrices all rounded to 0.99, except for those involving the 5000-iteration matrix (0.93, 0.90, and 0.95) and were probably smaller because the 5000-iteration matrix was larger than the other correlation matrices (since the 5000 analysis included 5 secondary trees).

The Ward method seemed to be slightly better for producing dendrograms. Both the average and unweighted average methods clustered up to eight matrices into one node, for every number of iterations. However, the Ward method clustered a maximum of six matrices per node for the 2500 and 3000 iterations, eight for the 5000 iterations, and only five for the 10000 iterations. This difference is likely not too important, though clustering too many matrices per node indicates more random clustering, since one would expect fairly even clustering.

One of the controls to test this program's accuracy was separating Rohon-Beard and trigeminal neurons. All of the dendrograms divided the tracings overall into two classes, which generally conformed to the Rohon-Beard/trigeminal division. There was some overlap, but it appeared to be fairly consistent between all of the dendrograms.

Another control was analyzing different tracings of the same neuron to see how similar they would be. Most of these tracings were consistently clustered together; for example, KikGR_Tg-8's different tracings were clustered together in nearly all of the dendrograms, and were in adjacent clusters for the other dendrograms. KikGR_Tg-9 had similar results. Some different tracings of the same neuron did not appear together; this may be due to error on the tracer's part. For example, KikGR_Tg-6A and M always were clustered together, but KikGR_Tg-6C was always in a separate cluster.



Supplementary Figure 1. Categorization of peripheral axon morphology by branch number and length. Trigeminal (A) and Rohon-Beard (A') neurons cluster separately. Y-axis represents relative distance between groups. Asterisks represent the number of times the same neuron, traced by different experimenters, appears in a cluster. (B-F) Peripheral axons of single RB neurons labeled by transient transgenesis using reporter transgenes with *Fru.trkA*, *Fru.trkC*, *Fru.p2x3-2* or *isl1(ss)* enhancer sequences were hand-traced with NeuroLucida Software and analyzed based on branch number and length for each branch order. Peripheral axons of individual neurons segregated into 5 main categories from more complex (B) to less complex (F). Representative lateral confocal images of 72 hpf RB neurons are shown for each group. Dorsal is up; anterior is right. The number of RB arbors from each transgene within each category is reported on the right. Scale on bottom represents relative distance between categories. Scale bar, 100 μ m.

Supplementary Table 1: List of transgenic/gene trap lines and other transgenes.

Transgenic/Gene trap lines	Allele numbers
<i>Tg(isl1:Gal4-VP16,UAS:EGFP)</i> , previously <i>sensory:GFP</i>	zf154
<i>Tg(isl1:Gal4-VP16,UAS:dsRed)</i> , previously <i>sensory:DsRed</i>	Zf234
<i>Tg(isl1(ss):Gal4-VP16,14xUAS:KikGR)</i>	LA203
<i>Tg(CREST3:Gal4-VP16,14xUAS:EGFP)</i>	LA204
<i>Tg(CREST3:Gal4-VP16,14xUAS:KikGR)</i>	LA205
<i>Tg(Fru.trkA:Gal4-VP16,14xUAS:ChR2-YFP)</i>	LA206
<i>Tg(Fru.p2x3-2[-1036:-731]:LexA-VP16,4xLexAop:mCherry)</i>	LA207
<i>Tg(-17.6isl2b:GFP)</i>	zc7
<i>Gt(PKCα-citrine)</i> , herein called <i>PKCα^{ct7a}</i>	ct7a
<i>Gt(T2KSAG)</i>	j1229a
<i>Tg(trpA1b:EGFP)</i>	a4593
<i>Tg(p2rx3b:EGFP)</i>	sl1
Additional Transgenes	
<i>CREST3:LexA-VP16,4xLexAop:mCherry</i>	
<i>trpA1a:Gal4-VP16,14xUAS:KikGR</i>	
<i>Fru.trkA:Gal4-VP16,14xUAS:GFP</i>	
<i>Fru.trkA:LexA-VP16,4xLexAop:mCherry</i>	
<i>Fru.trkB:Gal4-VP16,14xUAS:GFP</i>	
<i>Fru.trkC:Gal4-VP16,14xUAS:GFP</i>	
<i>Fru.p2x3-2:Gal4-VP16,14xUAS:GFP</i>	

Supplementary Table 2. List of primers for 5' enhancer elements. Primer name (right column) and primer sequence (left column) are provided for each enhancer sequence. Lower case letters in primer sequence indicate attB sequences, uppercase letters are specific to the enhancer sequence.

Primer name	Primer Sequence
attB4- <i>CREST3</i> Forward	ggggacaactttgtatagaaaagttgGTAACAGGATGTGACACGTCGTCTGC
attB1- <i>CREST3</i> Reverse	ggggactgctttttgtacaaactgGCCTGCTGCTGGTGTCAATTTACTGG
attB4- <i>trpA1a</i> Forward	ggggacaactttgtatagaaaagttgAACCTATTGCACTTGTATCAGCAG
attB1- <i>trpA1a</i> Reverse	ggggactgctttttgtacaaactgGGCCATGAAGAAATTCTGA
attB4- <i>Fru.trkA</i> Forward	ggggacaactttgtatagaaaagttgGTTCCCTCATTGGAACAACACC
attB1- <i>Fru.trkA</i> Reverse	ggggactgctttttgtacaaactgACTGTGCGGAAACAGGACAG
attB4- <i>Fru.trkB</i> Forward	ggggacaactttgtatagaaaagttgTCAAGGCTTTGCTCACATGC
attB1- <i>Fru.trkB</i> Reverse	ggggactgctttttgtacaaactgTTTTGAGGAGCCACAACACTC
attB4- <i>Fru.trkC</i> Forward	ggggacaactttgtatagaaaagttgGACACTGTAATTGCTTCGACTG
attB1- <i>Fru.trkC</i> Reverse	ggggactgctttttgtacaaactgTTTTCTGCAGTGCGTCAGCAG
attB4- <i>Fru.p2x3-2</i> Forward	ggggacaactttgtatagaaaagttgCACCACTTTTCGGAGGTGTCT
attB1- <i>Fru.p2x3-2</i> Reverse	ggggactgctttttgtacaaactgGTCAGTGTGCACCAGAGAGC

Supplementary Table 3: List of antibodies used for whole mount antibody staining.

Primary antibodies	Antigen	Source	Dilution used
PKC α	Peptide mapping at the C-terminus of human PKC α	Rabbit polyclonal antibody from Santa Cruz Biotechnologies, Inc. (sc-208)	1:500
GFP/YFP/Citrine	Full length Aequorea Victoria GFP	Mouse monoclonal antibody from Clontech (Living Colors JL-8)	1:500
DsRed/mCherry	Full-length DsRed2	Mouse monoclonal antibody from Clontech (Living Colors 632393)	1:500

Secondary antibodies	Fluorophore	Source	Dilution used
Goat anti-mouse IgG (H+L)	AlexaFluor 488	Molecular Probes (A11001)	1:1000
Goat anti-mouse IgG (H+L)	AlexaFluor 568	Molecular Probes (A11004)	1:1000
Goat anti-rabbit IgG (H+L)	AlexaFluor 488	Molecular Probes (A11008)	1:1000
Goat anti-rabbit IgG (H+L)	AlexaFluor 568	Molecular Probes (A11011)	1:1000

Chapter 3

Characterization of TrkA-expressing sensory neurons in larval zebrafish

Introduction

TrkA/NGF signaling plays a critical role in proper neuronal development and function (Silos-Santiago et al., 1995; Fagan et al., 1996; Patel et al., 2000). TrkA-expressing neurons have also been classified as the subset of somatosensory neurons responsible for detecting touch (Patapoutian and Reichardt, 2001; Lumpkin and Caterina, 2007). Therefore, this gene serves as a likely candidate for defining a specific functional subset of somatosensory neurons in larval zebrafish. We previously reported that the *Fru.trkA* enhancer labels a subset of zebrafish RB neurons that partially overlap with the PKC α /*p2rx3a/trpA1b*-expressing subset of RB neurons (Palanca et al., 2012). We also showed that the [-996: -1] fragment of the *Fru.trkA* promoter drives expression exclusively in RB neurons with central axons that do not contact the Mauthner cell dendrite, thus identifying a morphologically distinct population of RB neurons. To further characterize the *Fru.trkA*-expressing subset of somatosensory neurons, we sought to identify minimal regulatory elements required for *Fru.trkA* expression, which would provide a starting point for identifying the transcriptional regulatory elements required for somatosensory neuron-specific expression. We first focused on sequences within the *Fru.trkA* [-996, -1] minimal enhancer region and compared it to the minimal enhancer regions of other somatosensory-specific enhancers to identify short consensus sequences of approximately 6-8 bp. We then performed deletion analysis and/or site-directed mutagenesis to identify regulatory elements/putative binding sites required for enhancer expression. From this analysis, we identified several consensus sequences, however while deletion or mutation of some consensus sequences did not abolish enhancer activity we were able to identify a 4 bp sequence that is critical for expression of *Fru.trkA*.

To better understand the function of TrkA in zebrafish somatosensory neurons, we performed morpholino knockdown. Using two different morpholinos, we saw no dramatic effect on RB cell number over time. Nor did it seem to affect peripheral arbor or central axon morphology. We also performed single neuron activation using *Fru.trkA:Gal4:ChR2-YFP* to determine if RB neurons with central projections that contact the Mauthner cell dendrite elicit a distinct behavioral response from RB neurons with central axons that do not contact the Mauthner cell dendrite.

Materials and Methods

In Situ Hybridization

Embryos were fixed in 4% paraformaldehyde/PBS overnight at 4°C and permeabilized with proteinase K prior to *in situ* hybridization with standard protocols (Boué-Grabot et al., 2000; Slatter et al., 2005) (<https://wiki.zfin.org/display/prot/Thisse+Lab+-+In+Situ+Hybridization+Protocol+-+2010+update>). All solutions and washes were performed using Triton X-100 instead of Tween-20. Embryos were incubated with DIG labeled riboprobe for 2 days at 65°C in the dark. The NBT/BCIP color reaction was performed over 2 days at room temperature, with an overnight incubation in NTMT at 4°C between color reactions.

Confocal imaging

Zebrafish embryos were injected at the 1-cell stage with approximately 2 nl of 50 ng/ul plasmid DNA, raised in a 28.5°C incubator and treated with phenylthiourea (PTU) at 24 hpf to block pigmentation. Larvae were screened for fluorescence between 24 and 72 hpf using a Zeiss Discovery.V12 SteREO fluorescence dissecting scope.

For confocal imaging, fish were anesthetized with 0.02% tricaine and mounted in 1.2% low melt agarose (Promega, V2111). Fluorescence was imaged with a Zeiss LSM 510 confocal microscope using a 488 nm laser line for GFP. Images were taken with a 20x water objective and projected from 20-50 optical sections of ~3 μm intervals.

Transgenes

Subcloning and promoter dissection of enhancer elements were performed using the Multi-Site Gateway Cloning System (Invitrogen, 12537-023) in combination with the Tol2 Gateway System developed by the Chien Lab (Kwan et al., 2007). Genomic sequences were PCR amplified with primers containing attB sites and recombined into pDONR P4-P1R, creating 5' DONR plasmids. The binomial enhancer, E1b:Gal4-VP16:pA,14XUAS:E1b, was cloned into pDONR 221 to make a middle element. Reporter genes, EGFP and Chr2-YFP, were cloned into pDONR P2R-P3 to make 3' elements. Reporter transgenes were created by recombination of different sets of pDONR elements using LR Clonase II Plus (Invitrogen, 12538120). Reporter function of each transgene was tested by injection into wildtype embryos. For the duration of each experiment, embryos were raised at 28.5°C on a 14 hr/10 hr light/dark cycle unless otherwise noted.

Site-directed mutagenesis

Single and multiple base pair mutations were performed by mutating base pair(s) within a primer sequence, then amplifying the sequence by PCR. Small deletions were created by designing primers flanking the desired deletion and amplifying outward using PCR. PCR products were ligated and transformed into Top10 Chemically Competent Cells (Invitrogen and

selected on the appropriate media. Clones were sequenced to verify desired mutation prior to analysis.

Morpholinos and RT-PCR

TrkA morpholinos were generated by Gene Tools (Philomath, OR). ATG-MO (5'-GCAGTTATCATTTTCGAATGAATCC-3') and splice-blocking *trkA*-splice2-MO (5'-TCCATAGATGTCTCATGTACCTCCA-3') were diluted to a concentration of 1 mM with ddH₂O. 1-2 nl of diluted morpholino was injected directly into the cell at the 1-cell stage. Morpholino function was verified using RT-PCR. RNA was extracted from 20-30 larvae at indicated time-points using the RNAqueous Kit (Ambion, AM1912). cDNA was synthesized using the RETROscript Kit (Ambion, AM1710). RT-PCR was performed using primer pairs specific to each Exon/Intron or control gene.

List of primers for RT-PCR

Primer Name	Primer sequence
<i>trkA Exon 1</i> Forward	5'- CAGATTCGCTGGATTCATT -3'
<i>trkA Intron 1</i> Reverse	5'- GCAGTTACAGGCCAGAGGAG -3'
<i>trkA Exon 2</i> Forward	5'- CCGACAGTGACCACTCAAGA -3'
<i>trkA Exon 3</i> Reverse	5'- GTGCAGGTTGTCAGCAGAAG -3'
<i>trkA Exon 4</i> Forward	5'- CCAGTGCGGATCATATATCTCAA -3'
<i>trkA Exon 4</i> Reverse	5'- GGGATCAAAAGGATTGTCCA -3'
<i>preproinsulin</i> Forward	5'- GCTCTGTTGGTCCTGTTGGT -3'
<i>preproinsulin</i> Reverse	5'- GGGCAGATTTAGGAGGAAGG -3'
β - <i>actin</i> Forward	5'- TGCTGTTTTCCCCTCCATTG -3'
β - <i>actin</i> Reverse	5'- TTCTGTCCCATGCCAACCA -3'

Activation of single RB neurons expressing Fru.trkA:Gal4:ChR2-YFP

Zebrafish embryos were injected at the 1 cell stage with ~1 pg of plasmid DNA directly into the cell. Embryos were raised at 28.5°C in the dark. Larvae were manually dechorionated and screened for ChR2-YFP expression in single RB neurons at 30 hpf. Larvae were placed in blue water on a slide for free-swimming behavior analysis. Single neuron activation was performed using a 488 nm LED with a lens attachment to create a focal point of approximately 4 mm in diameter. A 5 ms light pulse was delivered with a maximum power of 5 V using a Grass stimulator. Resulting behavior was recorded using a high-speed video camera at a rate of 1000 frames per second (fps).

Results

TrkA is expressed in RB neurons

From our previous study, we determined that *Fru.trkA*-expressing RB cells represent approximately 50% of RB neurons in zebrafish larvae. *In situ* hybridization verified that *trkA* is expressed in a subset of RB neurons. We were also able to determine that *trkA* mRNA expression was strongest/best distinguishable by *in situ* in larvae at 32 hpf (Figure 1).

Fru.trkA-expressing neurons do not contact the Mauthner cell dendrite

We previously reported that approximately 10-20 % of RB neurons contact the Mauthner cell dendrite, whereas 80-90% of RB neurons do not. We also showed that a 1 kb fragment, [-996: -1], of the *Fru.trkA* enhancer drove expression exclusively in neurons with central axons that do not contact the Mauthner cell dendrite. Laser ablation of entire trigeminal ganglia in a

stable transgenic line, *Tg(Fru.trkA:Gal4:ChR2-YFP)*, verified that *Fru.trkA*-expressing RB neurons are non-Mauthner contacting neurons (Figure 2).

Identification of consensus sequences within the Fru.trkA [-996: -1] minimal regulatory region

We previously reported that two fragments of *Fru.trkA* [-996, -1], *Fru.trkA* [-996, -814] and *Fru.trkA* [-238, -81], were sufficient to drive expression in somatosensory neurons, but were together, required for expression comparable to the 1 kb fragment. Using overlap-extension PCR to fuse the *Fru.trkA* [-996, -814] to *Fru.trkA* [-238, -81] and subcloning the fusion fragment into a reporter transgene resulted in a construct that drove GFP expression as strongly as *Fru.trkA* [-996, -1], indicating that *Fru.trkA* [-996, -814] and *Fru.trkA* [-238, -81] may act redundantly to enhance expression. Furthermore, the spacing between these two regions did not seem to affect their function.

Using these two small fragments, *Fru.trkA* [-996, -814] and *Fru.trkA* [-238, -81], and other identified minimal regulatory regions including *trpA1a* [-4136, -3517], *Fru.p2x3-2* [-946, -802], *CREST3* (868 bp) (Uemura *et al.*, 2005) and murine *trkA* (457 bp) (Ma *et al.*, 2000), we performed computational comparisons to search for consensus sequences shared by any two or more of these regions. The program searched for identical sequences of defined lengths (5+ bp) between any two minimal regulatory regions. “Hits” that also appeared in any of three non-somatosensory neuron promoter regions (heart-specific *cardiomyosin light chain 2*, skin-specific *keratin 4* or pancreas-specific *insulin*) were discarded from further study. Consensus sequences that also appeared in the regions of the *Fru.trkA* and *trpA1a* that had no somatosensory neuron enhancer activity were also eliminated. Eighteen consensus sequences were identified (Table 1). Seventeen of these sequences were shared by two minimal regulatory regions, while one

sequence, TCCCACT, was shared by three (*Fru.p2x3-2*, *CREST3* and murine *trkA*). This is consistent with the understanding that there are distinct, yet overlapping populations of somatosensory neurons. Therefore, these consensus sequences may identify subtype-specific, but not pan-somatosensory neuron transcriptional control.

Interestingly, when these consensus sequences were mapped onto the minimal regulatory regions to visualize their spatial relations, six of the consensus sequences common to *Fru.trkA* [-996, -814] and *Fru.trkA* [-238, -81], appeared in the same order, suggesting that somatosensory neuron-specific transcription factor binding sites may also be functionally dependent on relative order (Figure 3).

A 4 bp element within Fru.trkA [-996, -1] is critical for expression in somatosensory neurons

To test whether any of the eighteen consensus sequences were important for enhancer activity, we performed site-directed mutagenesis, mutating 3-4 bps at the center of consensus sequences from purine to pyrimidine, and vice versa. These three mutated minimal regulatory regions were injected into zebrafish embryos, and their expression efficiency was quantified as before.

Mutating a consensus sequence shared by *Fru.trkA* [-238, -81] and *trpA1a* [-4136, -3517], TATTGATTTA, to TATACTATTA in *Fru.trkA* [-238, -81] resulted in a dramatic decrease in efficiency. Expression fell from $20 \pm 2\%$ in the non-mutated element to $2 \pm 1\%$ (Figure 4). This result indicates that the four mutated base pairs, TGAT, comprise at least a part of an enhancer element involved in the regulation of *trkA* expression. This knowledge lays the foundation for teasing apart the various components of transcriptional machinery that drives subtype-specific expression contributing to somatosensory neuron diversity.

TrkA morphants

To determine the function of TrkA in zebrafish somatosensory neurons, we designed morpholinos to perform knockdown analysis. We initially designed three morpholinos, one ATG morpholino and two splice blocking morpholinos (Figure 5). The ATG morpholino actually functioned as a splice blocking morpholino, causing inclusion of Intron 1 in the transcript (Figure 6, A and B). The splice blocking morpholino against the Intron 1-Exon 2 boundary did not affect the *trkA* transcript (data not shown). A splice blocking morpholino against the Exon 2-Intron 2 boundary incorporated Intron 2 in the transcript (Figure 7, A and B). Quantification of RB neurons in different transgenic lines showed no change in RB neuron number between *trkA* morphants and untreated siblings (Figure 6 and 7). Qualitative analysis of peripheral arbor morphologies also showed no significant difference between *trkA* morphants and untreated siblings (data not shown).

Single neuron activation

To determine if RB neurons with distinct central projections elicit different behavioral responses, we devised an optogenetic approach using a transgene expressing the light activated channel, channelrhodopsin 2 fused to YFP (ChR2-YFP) (Figure 8A). Single neuron activation using a blue LED was recorded with a high-speed camera at a rate of 1000 frames per second. Latency from start of the light pulse to start of behavior was calculated for each of the fish recorded. RB neurons with central projections that did not contact the Mauthner cell dendrite had an average latency of 25.5 and 36.0 ms, while the average latency of behavior elicited by a RB neuron with a central axon that presumably contacted the Mauthner cell dendrite was 39.5 ms.

Discussion

In mammals, TrkA-expression is essential for peripheral neuron survival during embryonic development (Silos-Santiago et al., 1995; Fagan et al., 1996; Patel et al., 2000). TrkA-expressing neurons also define a subset of somatosensory neurons that predominantly respond to nociceptive stimuli. In the absence of programmed cell death, TrkA-deficient mice show defects in cutaneous innervation and a deficit in nociceptive molecules, such as CGRP and Substance P (Patel et al., 2000).

The importance of TrkA/NGF signaling in mammalian systems prompted us to characterize this subset of neurons in zebrafish. Since zebrafish respond to touch stimuli and also express TrkA in a subset of somatosensory neurons (Martin et al., 1995; Pan et al., 2012), it is likely that TrkA function in zebrafish would parallel TrkA function in mammals. To verify *trkA* expression in zebrafish, we performed *in situ* hybridization at different stages of development. We discovered that *trkA* mRNA expression is most clearly distinguishable in RB neurons at 32 hpf. However, *in situ* staining is also visible in the central nervous system, and specific regions in the head are not clearly distinguishable. It is likely that *trkA* expression comes on even earlier than this time point, perhaps as early as 24 hpf, as seen by fluorescence expression in one of our stable transgenic lines, *Tg(Fru.trkA:Gal4:ChR2-YFP)* (data not shown). Furthermore, using both transient and stable transgenics, we were able to verify that *trkA*-expressing neurons represent a subpopulation of RB neurons that do not contact the Mauthner cell dendrite, thereby identifying this as a morphologically distinct subset of sensory neurons.

Characterization of a 457 bp *trkA* minimal enhancer in mice identified 6 *cis*-elements involved in expression in DRGs and 2 *cis*-elements required for expression in DRGs. Surprisingly, when we compared this minimal enhancer region to our *Fru.trkA* minimal enhancer

sequences, we were unable to identify consensus *cis*-elements between the sequences. This observation led us to believe that perhaps zebrafish have a completely different transcription regulatory system for expressing specific somatosensory genes. We then compared the *Fru.trkA* minimal enhancers to other zebrafish minimal enhancers such as *CREST3*, *trpA1a* [-4136, -3517] and *Fru.p2x3-2* [-946, -802]. By pair-wise comparisons, we identified 18 short sequences conserved between any 2 elements, 11 of which were in *Fru.trkA*. From these elements, one 4 bp sequence, TGAT, within a 10 bp consensus element was shown to be required for enhancer activity. This 10 bp sequence was also in the *trpA1a* [-4136, -3517] sequence. Interestingly, TrpA1a is responsible for chemosensation in zebrafish larvae (Prober, 2008). Therefore, it is possible that this short sequence is a putative binding site for regulation of a subset of somatosensory neurons responsible for nociception.

TrkA knockout mice showed that TrkA/NGF signaling is required for survival of peripheral neurons during embryonic development. We designed multiple morpholinos aimed to knockdown TrkA in zebrafish. Two out of three morpholinos blocked splicing, as shown by RT-PCR, but did not affect over all number of RB neurons. At a glance, the central and peripheral axon morphologies also looked unaffected (data not shown). We attempted to verify TrkA knockdown by western blot (data not shown), however, no viable antibody was available for zebrafish TrkA.

Since *Fru.trkA*-expressing RB neurons seem to be predominantly non-Mauthner dendrite contacting, we wanted to test whether these two distinct central projection patterns elicit different behavioral responses. Using a transgene expressing ChR2-YFP, we used optogenetics to activate single RB neurons, recorded their behavior and imaged their central axon projection. Two of the three fish tested had RB neurons that did not contact the Mauthner cell dendrite, while one did.

In behavior studies where the Mauthner cells have either been ablated or lesions were introduced caudal to the hindbrain, touch response to the tail elicited an escape response with a longer latency compared to its untreated counterpart (Liu and Fetcho, 1999; Downes and Granato, 2006; Kohashi and Oda, 2008). Surprisingly, in our experiments, the RB neurons that did not contact the Mauthner cell dendrite resulted in a shorter latency of behavior (25.5 and 36 ms) than that of the RB neuron that contacted the Mauthner cell dendrite (39.5 ms). Furthermore, the average latency of any of the responses is much longer than that of a normal touch response. This could be attributed to the fact that a touch response would stimulate more than one RB neuron, possibly resulting in increased activation of the Mauthner cell.

In summary, we identified a subset of RB neurons with central axons that do not contact the Mauthner cell dendrite. We have also identified a 4 bp sequence that putatively regulates expression of genes required for nociception. It does not seem like knockdown of TrkA in zebrafish disrupts neuron survival or development, though verification of protein knockdown is required to validate this finding. Finally, there does not seem to be a significant difference between the behaviors elicited by RB neurons that contact the Mauthner cell dendrite and those that do not. However, a higher number of samples is needed to verify this claim. Also, it is possible that at an early stage (< 40 hpf), neuronal networks have yet to be established and therefore diverse behavior responses might not exist. Therefore, activation at later stages might provide better insight into the diversity of behavioral responses resulting from different subtypes of somatosensory neurons.

Acknowledgements

I would like to thank Dean Lee and Jett Lee for their work on identifying somatosensory neuron consensus sequences, Seanna Martin for performing laser ablations of *trkA*-expressing trigeminal neurons, Hillary McGraw for the *trkA in situ* probe, and Kevin Mouillesseaux for technical assistance on TrkA protein work.

References

- Boué-Grabot E, Akimenko MA, Séguéla P. 2000. Unique functional properties of a sensory neuronal P2X ATP-gated channel from zebrafish. *J Neurochem* 75:1600-1607.
- Downes GB, Granato M. 2006. Supraspinal input is dispensable to generate glycine-mediated locomotive behaviors in the zebrafish embryo. *J Neurobiol* 66:437-451.
- Fagan AM, Zhang H, Landis S, Smeyne RJ, Silos-Santiago I, Barbacid M. 1996. TrkA, but not TrkC, receptors are essential for survival of sympathetic neurons in vivo. *J Neurosci* 16:6208-6218.
- Kohashi T, Oda Y. 2008. Initiation of Mauthner- or non-Mauthner-mediated fast escape evoked by different modes of sensory input. *J Neurosci* 28:10641-10653.
- Kwan KM, Fujimoto E, Grabher C, Mangum BD, Hardy ME, Campbell DS, Parant JM, Yost HJ, Kanki JP, Chien CB. 2007. The Tol2kit: a multisite gateway-based construction kit for Tol2 transposon transgenesis constructs. *Dev Dyn* 236:3088-3099.
- Liu KS, Fetcho JR. 1999. Laser ablations reveal functional relationships of segmental hindbrain neurons in zebrafish. *Neuron* 23:325-335.
- Lumpkin EA, Caterina MJ. 2007. Mechanisms of sensory transduction in the skin. *Nature* 445:858-865.
- Martin SC, Marazzi G, Sandell JH, Heinrich G. 1995. Five Trk receptors in the zebrafish. *Dev Biol* 169:745-758.
- Palanca AM, Lee SL, Yee LE, Joe-Wong C, Trinh LA, Hiroyasu E, Husain M, Fraser SE, Pellegrini M, Sagasti A. 2012. New transgenic reporters identify somatosensory neuron subtypes in larval zebrafish. *Dev Neurobiol*.

- Pan YA, Choy M, Prober DA, Schier AF. 2012. Robo2 determines subtype-specific axonal projections of trigeminal sensory neurons. *Development* 139:591-600.
- Patapoutian A, Reichardt LF. 2001. Trk receptors: mediators of neurotrophin action. *Curr Opin Neurobiol* 11:272-280.
- Patel TD, Jackman A, Rice FL, Kucera J, Snider WD. 2000. Development of sensory neurons in the absence of NGF/TrkA signaling in vivo. *Neuron* 25:345-357.
- Silos-Santiago I, Molliver DC, Ozaki S, Smeyne RJ, Fagan AM, Barbacid M, Snider WD. 1995. Non-TrkA-expressing small DRG neurons are lost in TrkA deficient mice. *J Neurosci* 15:5929-5942.
- Slatter CA, Kanji H, Coutts CA, Ali DW. 2005. Expression of PKC in the developing zebrafish, *Danio rerio*. *J Neurobiol* 62:425-438.

Tables and Figures

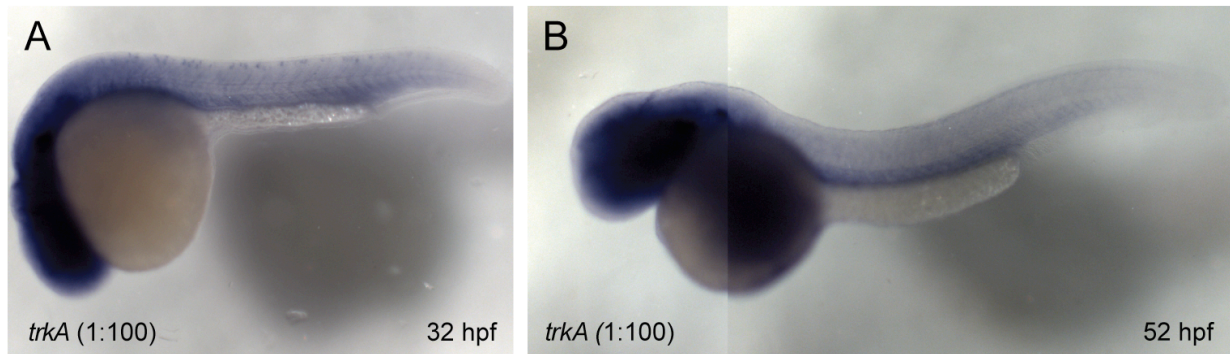


Figure 1. *TrkA* expression. *In situ* hybridization shows *trkA* mRNA expression at (A) 32 hpf and (B) 52 hpf. Larvae were embedded in 3.5 % methylcellulose and imaged using an upright Zeiss compound scope with an external light source. Images were taken with a 5x objective.

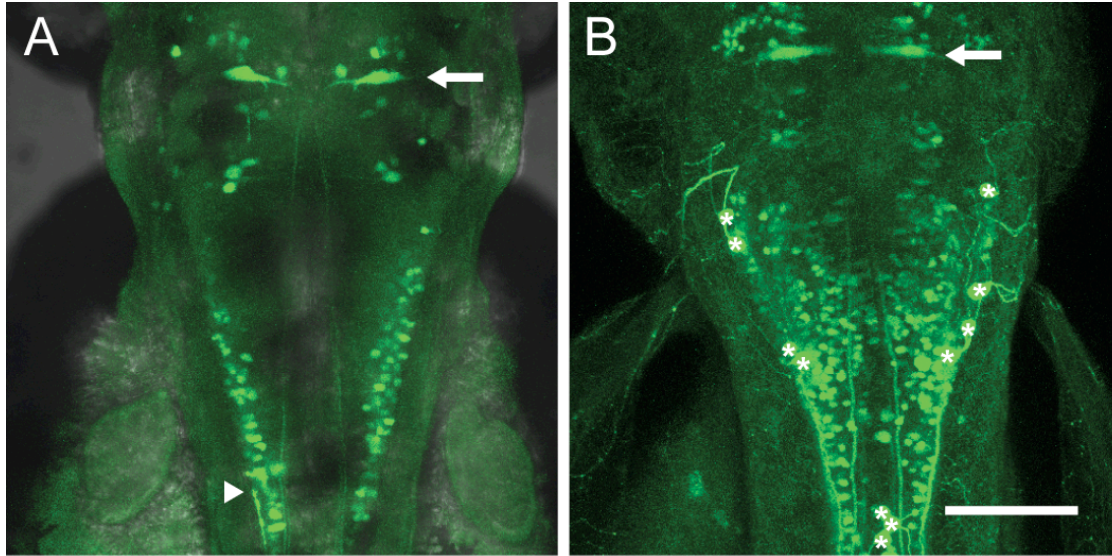


Figure 2. Central projections of *Fru.trkA* transgene-expressing neurons do not contact the Mauthner cell dendrite. (A) Transient expression of *Fru.trkA* [-996: -1]:*Gal4:GFP*. (B) Stable transgenic line expressing *Fru.trkA:Gal4:ChR2-YFP* with ablated trigeminal neurons. Dorsal confocal images taken at 72 hpf. Arrows indicate the Mauthner cell dendrite. Arrowhead in (A) points to an RB central axon terminal. Asterisks in (B) indicate RB cell bodies. All other cells are not RB neurons. Scale bar, 100 μ m.

Table 1. Six minimal regulatory regions share 18 consensus sequences. Six minimal regulatory sequences were compared in a pair-wise fashion to generate a list of consensus sequences. Only the eighteen sequences most likely to be enhancer elements are listed in this chart. The left-most column lists the consensus sequences. The top row lists the six minimal regulatory regions. Each appearance of a consensus sequence in a minimal regulatory region is indicated by a single “x.”

	<i>Fru.trkA</i> [-996,-814]	<i>Fru.trkA</i> [-238,-81]	<i>Fru.p2x3-2</i> [-946,-802]	<i>CREST3</i> (868 bp)	<i>trpA1a</i> [-4136,-3517]	<i>mtrkA</i> (457 bp)
ATAGCCT	x				x	
CTACTCC	x			x		
GGACAGATA	x			x		
GTTTCAGAT	x			xx		
ACATTTATT		x			x	
CATCACTC		x			x	
GGAACTTC		x			x	
TATTGATTTA		x			x	
AAAGCATG		x			x	
GCCGGA		x	x			
TCATCGT		x		x		
AAATCTGCTG				x	x	
CACTGTAAAT				x	x	
GAGACAG			x	x		
GGATGTG			x	x		
TCCCACT			x	x		x
TGACGGTG			x	x		
TGCTACAC			x	x		

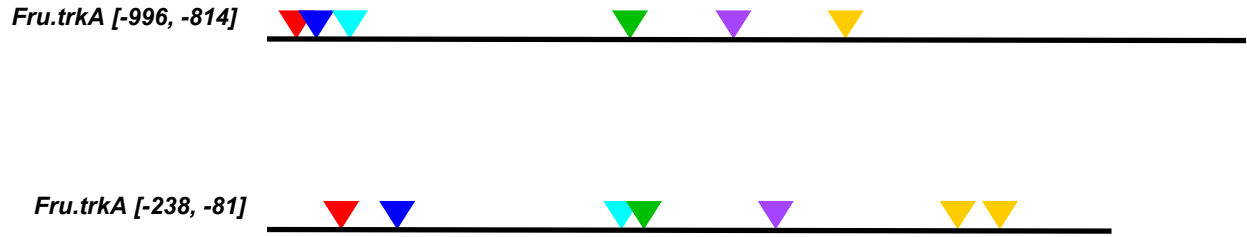


Figure 3. *Fru.trkA* [-996, -814] and *Fru.trkA* [-238, -81] show similar architecture. Six consensus sequences shared by *Fru.trkA* [-996, -814] and *Fru.trkA* [-238, -81] appear in the same order when mapped. Each consensus sequence is represented by a uniquely colored arrowhead.

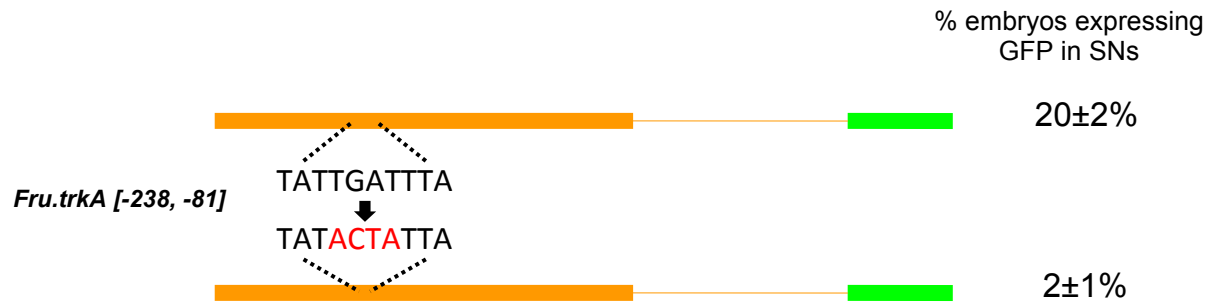


Figure 4. A 4 bp sequence, TGAT, is required for enhancer activity of *Fru.trkA* [-238, -81].

In *Fru.trkA* [-238, -81], TGAT was mutated to ACTA, with flanking sequences unchanged. The mutated *Fru.trkA* [-238, -81] was subjected to *in vivo* GFP expression analysis and was found to drive expression less strongly than the original *Fru.trkA* [-238, -81] fragment. Each construct was injected a minimum of three times; the average percentage for each construct is shown.

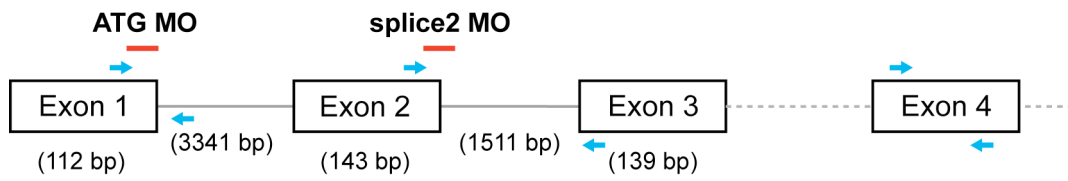


Figure 5. TrkA morpholino design. The ATG morpholino at the 3' end of Exon 1 acts as a splice morpholino, causing incorporation of Intron 1 into the transcript. The splice2 morpholino causes inclusion of Intron 2. Red lines represent morpholino position. Blue arrows represent primers.

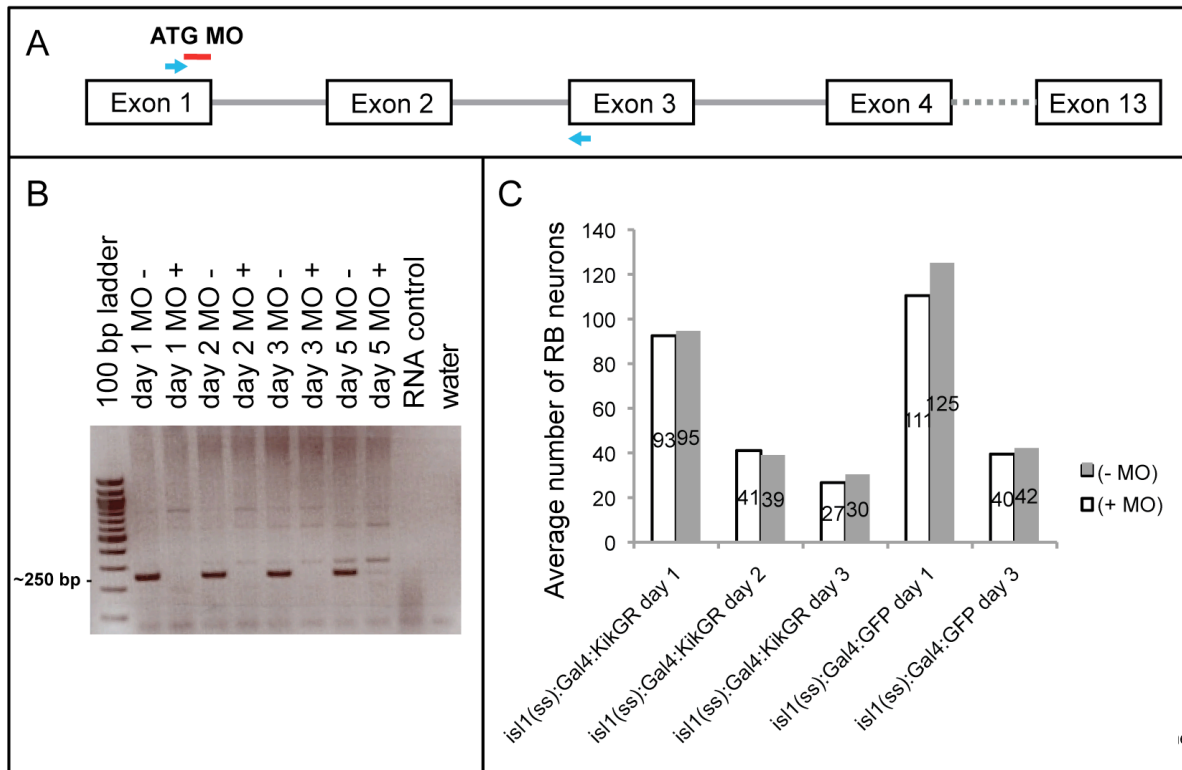


Figure 6. TrkA ATG morpholino does not affect RB cell number. (A) Location of TrkA ATG morpholino, red, and primers used to check morpholino function, blue. (B) RT-PCR using primers in Exon 1 and Exon 3. An ~250 bp band shows correct splicing from Exon 1 to Exon 3 in uninjected larvae. TrkA morphants lack a band due to inclusion of Intron 2, resulting in an additional ~3.3 kb, which is not amplified by the set PCR parameters. RT-PCR using primers for preproinsulin were used as a positive control (data not shown). (C) Quantification of RB cell body number in TrkA ATG morphants in *Tg(isl1(ss):Gal4:KikGR)* and *Tg(isl1(ss):Gal4:GFP)* lines show no change in cell number. All RB neurons were counted in day 1 larvae. Only a representative section over the yolk extension was quantified in day2 and older larvae. n = 10-12 fish for each data set.

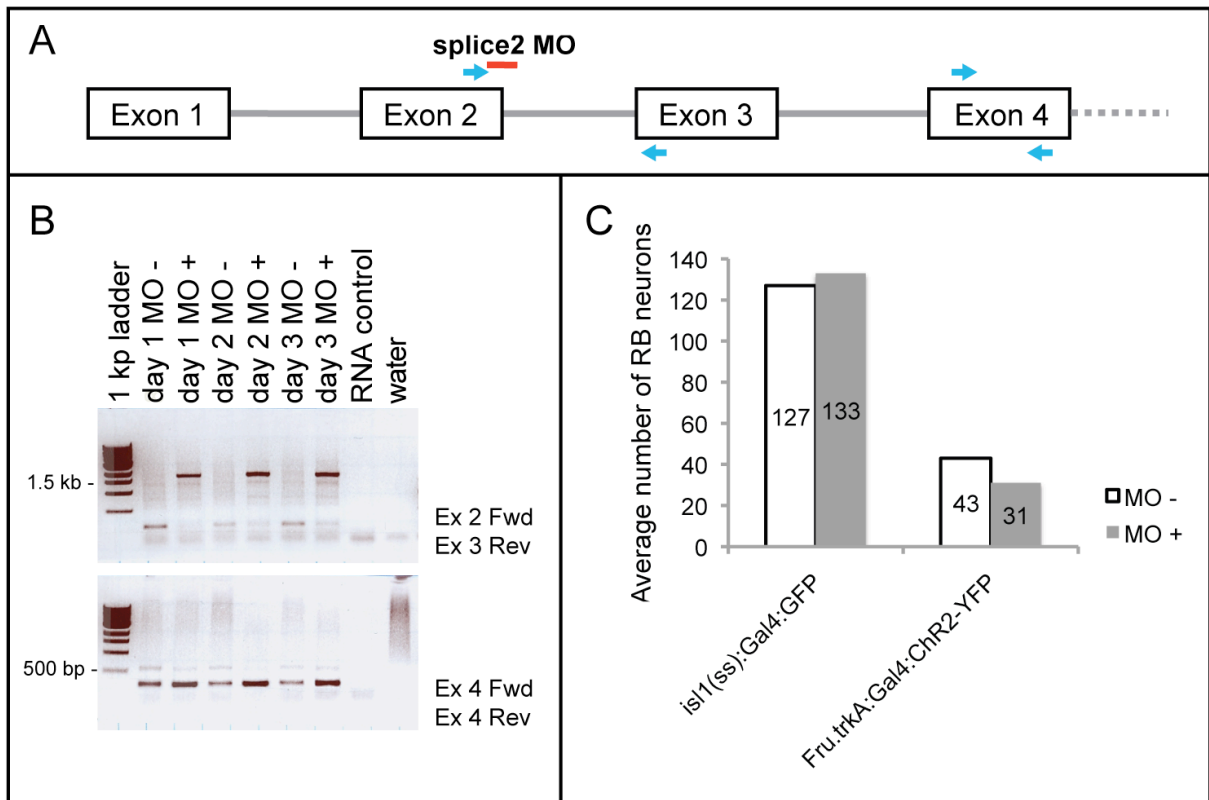


Figure 7. TrkA splice2 morpholino does not affect RB cell number. (A) Location of TrkA splice2 morpholino, red, and primers used to check morpholino function, blue. (B) RT-PCR using primers in Exon 2 and Exon 3, to verify block in splicing. Morphants result in a 1.5 kb band which includes Intron 2. Primers in Exon 4 were used as a positive control. (C) Quantification of RB cell body number in TrkA splice2 morphants. Quantification in *Tg(is1(ss):Gal4GFP)* and *Tg(Fru.trkA:Gal4:Chr2-YFP)* lines show no change in cell number. All RB neurons were counted in day 1 larvae.

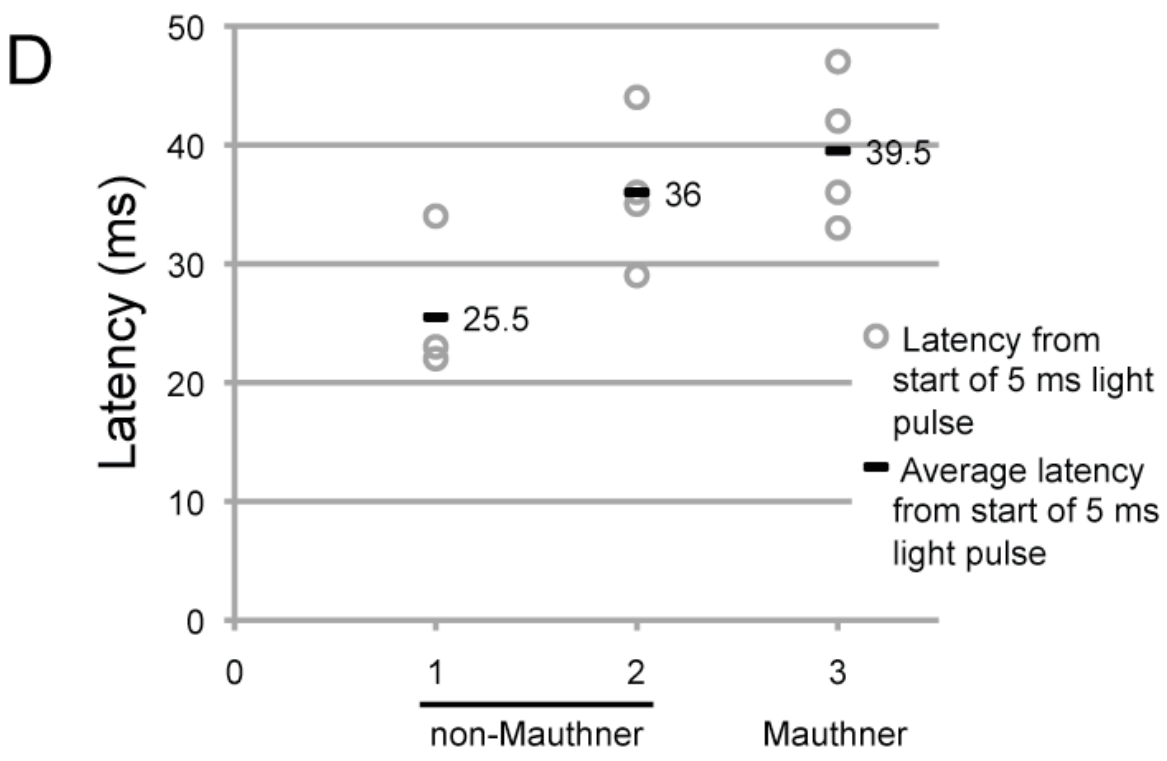
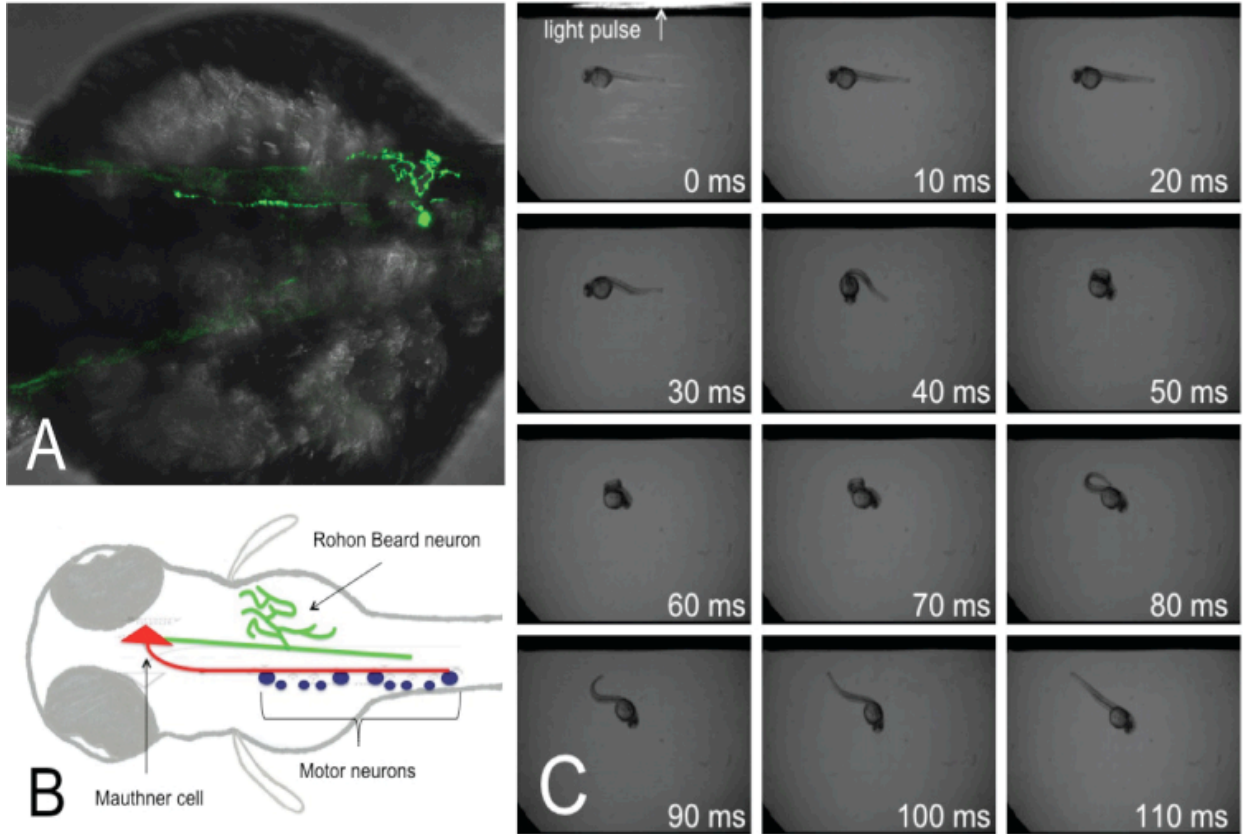


Figure 8. Activation of single neuron using a *Fru.trkA:Gal4-VP16:14xUAS:ChR2-YFP* transgene. (A) Single RB neurons expressing *Fru.trkA:Gal4-VP16:14xUAS:ChR2-YFP*. (B) Schematic diagram of the neural circuit involved in touch response. Activation of an RB neuron activates the Mauthner cell, which leads to contralateral muscle contractions resulting in a C-start escape away from the stimuli. (C) Still images of a 36 hpf larvae responding to the activation of a single RB neuron expressing ChR2-YFP following a 5 ms pulse of light from a 488 nm diode with a lens attachment. The behavior was recorded at 1000 frames per second with a high-speed camera. (D) Activation of both Mauthner dendrite contacting and non-Mauthner dendrite contacting RB neurons resulted in latency of behavior longer than previously published. Open circles indicate latency per response. Bars indicate average latency per fish.

Chapter 4

Optogenetic activation of zebrafish somatosensory neurons using ChEF-tdTomato

Introduction

The development of optogenetic methods for promoting or inhibiting neuronal excitability with defined wavelengths of light has made it possible to study the function of distinct populations of neurons in neural circuits controlling behavior. This technique is often used to activate groups of neurons, but it can also be used to activate individual neurons. Zebrafish larvae are particularly amenable to these methods since they are optically clear, their nervous system develops quickly, and creating transgenic animals is fast and routine. However, significant technical hurdles must be overcome to reliably achieve single neuron activation.

To optimize a procedure for optogenetic activation of single zebrafish neurons, we focused on somatosensory neurons. Zebrafish larvae detect a variety of somatosensory stimuli using two populations of neurons: trigeminal neurons, which innervate the head, and Rohon-Beard (RB) neurons, which innervate the rest of the body. Each trigeminal and RB neuron projects a peripheral axon that branches extensively in the skin to detect stimuli and a central axon that connects to downstream neural circuits. Animals respond to touch as early as 21 hours post-fertilization (hpf), indicating that coherent somatosensory circuits have formed (Saint-Amant and Drapeau, 1998; Drapeau et al., 2002). During larval development at least some trigeminal and RB neurons synapse onto the Mauthner cell to activate classic escape responses (Korn and Faber, 2005), but accumulating evidence suggests that there are multiple classes of somatosensory neurons with different patterns of connectivity that may elicit variations on the escape behavior (Liu and Fetcho, 1999; Downes and Granato, 2006; Kohashi and Oda, 2008; Burgess et al., 2009; Liu et al., 2012). Our motivation for developing this method was to characterize the behavioral function of different classes of somatosensory neurons, but this

approach could in principle be used to study the function of almost any neuron or population of neurons in larval zebrafish.

Douglass et al. previously described a method for activating Channelrhodopsin-2-expressing somatosensory neurons with blue light, eliciting escape behavior (Douglass et al., 2008). Their approach used an enhancer element from the *isll* gene to drive expression of ChR2-EYFP in somatosensory neurons. This transgene, however, was reported to display relatively weak fluorescence, requiring co-injection of a second reporter, *UAS::GFP*, to allow visualization of cells expressing ChR2-EYFP. This approach was used to elicit behavior responses between 24-48 hpf, but could never elicit a response past 72 hpf. Thus, while this method works for studying neural circuitry at very early larval stages (24-48 hpf), it is inadequate for characterizing neural circuits and behavioral responses in older larvae, when more diverse behavioral responses are apparent and neural circuits are more mature.

We sought to improve the sensitivity of this technique in order to characterize the function of subpopulations of larval RB neurons. To improve expression we used a somatosensory-specific enhancer (*CREST3*) (Uemura et al., 2005) to drive expression of LexA-VP16 and a stretch of LexA operator sequences (4xLexAop) (Lai and Lee, 2006) to amplify the expression of a fluorescently tagged light-activated channel. This configuration amplified expression of the channel, eliminating the need for co-expressing a second reporter and allowing us to directly determine the relative abundance of the channel in each neuron. Using the LexA/LexAop sequence had the additional advantage of allowing us to cross the transgene to zebrafish reporter lines that use the Gal4/UAS system. Transient expression of this transgene resulted in varying levels of expression, but was usually robust enough to visualize both the cell body and axonal projections of individual neurons over several days. To optimize sensitivity to

light we used the light activated channel ChEF, a channelrhodopsin variant consisting of a chimera of channelopsin-1 (Chop1) and channelopsin-2 (Chop2) with a crossover site at helix loop E-F (Lin et al., 2009). This channel is activated at the same wavelength as ChR2, but requires lower light intensity for activation. The ChEF protein was fused to the red fluorescent protein, tdTomato, enabling us to screen for protein expression without activating the channel. As a light source, we used a diode pumped solid-state (DPSS) laser coupled to a fiber optic cable to deliver a precise, high-powered pulse of blue light to a specific region of the larvae. This allowed us to focus laser light on individual neurons, eliminating the need for finding rare transgenic animals expressing the channel in a single neuron. Using this approach, we were able to activate single RB neurons, record behavioral responses with a high-speed video camera, and image the activated neurons at high resolution with confocal microscopy.

Procedure:

Prepare the following ahead of time

1) Prepare optic cable

- 1.1) Create a storage unit for the optic cable by melting the tapered neck of a glass Pasteur pipette over a Bunsen burner to create a $\sim 15^\circ$ angle.
- 1.2) Using a wire cutter, carefully cut the optic cable into two pieces. Each piece should have one end with a FC/PC adaptor and one exposed end. Store one piece as a reserve cable.
- 1.3) Strip the optic cable down to the cladding by removing the fiber jacket and strengthening fibers from $\sim 2''$ of cut end of the cable. (Figure 1)

- 1.4) Insert optic cable into prepared Pasteur pipette. Make sure cable can easily move in and out of the pipette tip.
- 1.5) With optic cable protruding from tip of Pasteur pipette, carefully cut and remove fiber cladding from around glass fiber, ~2mm from cut end.
- 1.6) Using a diamond pen/glass cutter, nick the glass fiber and break off the end to create a clean cut/surface at the end of the fiber.
- 1.7) Retract optic cable into Pasteur pipette for storage. Repeat step (1.6) if tip of optic fiber gets chipped or breaks unevenly.

Procedures 2-8 describe a method for injecting transgenes into embryos generally applicable to many zebrafish experiments. Variations on this method, like those described in other JoVE videos (Graeden and Sive, 2009; Kemp et al., 2009; Yuan and Sun, 2009; Kague et al., 2010; Eisenhoffer and Rosenblatt, 2011), are equally effective.

2) Pull injection needles

- 2.1) Using a needle puller, pull borosilicate glass tubing into two injection needles with a gradually tapered tip. Puller settings will vary. (On a Sutter Instruments needle puller we use settings: P = 500, Heat = 720, Pull = 50, Velocity = 70 and Time = 150). Every needle puller is different, so optimize puller settings empirically. For more tapered needles, increase the Heat and/or Pull. For less tapered needles, increase Time and/or decrease Pull.
- 2.2) Store needles in a secure container (i.e. a Petri dish with rolled tape, adhesive side out).

3) Pour injection molds

- 3.1) Melt 0.5 g agarose in 30 ml embryo/blue water, until agarose has completely dissolved.
- 3.2) Pour into bottom half of a Petri dish.
- 3.3) Place rectangular mold with mounting wells (Figure 2) into agarose, being careful to limit bubble formation around the wells.
- 3.4) Allow agarose to solidify.
- 3.5) Remove mold and fill Petri dish with blue/embryo water.
- 3.6) Store upright, filled with clean water, at room temp for same day use or at 4°C for future use.

4) Make plasmid DNA mix for injections

- 4.1) Dilute plasmid DNA to a concentration of 50 ng/μl with 1:10 phenol red in ddH₂O. For example:

1.0 μl	plasmid DNA (250 ng/μl)
0.5 μl	phenol red
3.5 μl	ddH ₂ O

- 4.2) DNA mix can be kept at room temperature if using immediately or stored at 4°C for several days.

5) Set up mating pairs. This should be done the evening before you plan to do injections.

- 5.1) Fill breeding tanks with system water and place male and female fish together. If injections cannot be performed as soon as lights turn on in the facility, separate male and female fish with a divider.

6) Prepare for injections (can be done while waiting for embryos)

- 6.1) Turn on pressure injector rig. Make sure the system is set to pulse. Start with the PULSE DURATION set to 1.
- 6.2) Turn on the AIR valve and adjust pressure injector to ~20 psi.
- 6.3) Using a dissecting scope at the highest magnification, break tip of needle with forceps or a poker to create a ~2 μm opening. (Figure 3)
- 6.4) Fill needles with DNA mix by: 1. Placing the needle, tip side up, into the DNA mix and letting the needle fill by capillary action or 2. Using a long-reach tip to pipet 1-2 μl of the DNA mix directly into the needle.
- 6.5) Place filled needle in a safe place until ready to inject.

7) Collect embryos

- 7.1) After facility lights have turned on remove dividers (if applicable). Collect embryos with a tea strainer and transfer them to a Petri dish with fresh blue/embryo water.

8) Inject embryos at the 1-2 cell stage

- 8.1) Transfer harvested embryos to injection molds using a plastic pipette.
- 8.2) Using a dissecting microscope, gently push embryos into wells with forceps or a blunt poker. (Figure 4)
- 8.3) Place loaded needle into a micromanipulator and position over embryos.
- 8.4) Calibrate injection volume by adjusting the PULSE DURATION in 1-step increments until you achieve the desired volume (~1 nl). This could be calibrated with a micrometer slide, as described in a previous JoVE videos (Yuan and Sun, 2009; Kague et al., 2010), but for

this experiment precision is not necessary, since a wide range of injection volumes will result in adequate expression.

- 8.5) Inject ~1 nl DNA mix directly into the cell and repeat for all embryos. DNA can also be injected into the yolk, but this tends to be less efficient. (Figure 5)
- 8.6) Remove injected embryos from mold using a gentle stream of blue/embryo water.
- 8.7) Store injected embryos at 28.5°C in the dark.
- 8.8) Remove unfertilized, damaged or dead embryos periodically.
- 8.9) Treat embryos with PTU between 18-24 hpf to prevent pigmentation.

9) Screen for transgene expression

- 9.1) Manually dechorionate 24-48 hpf embryos using forceps.
- 9.2) Anesthetize larvae using 0.02% tricaine.
- 9.3) Using a fluorescent dissecting microscope, identify larvae with RB or trigeminal neuron expression and transfer these to a new dish with fresh PTU blue/embryo water. Embryos with sparse expression in easily identifiable cells are optimal, but individual neurons will be targeted for activation with a fiber optic cable so a wide range of expression density is acceptable.
- 9.4) Store embryos at 28.5°C in the dark until desired experimental stage.

10) Mount larvae for behavior experiments

- 10.1) Make 1.5% agarose in ddH₂O water and store in a 42°C heat block to prevent it from solidifying.

- 10.2) Using a glass Pasteur pipette, transfer one of the pre-screened larvae into a tube of 1.5% agarose with as little blue/embryo water as possible.
- 10.3) Transfer larvae in a drop of agarose onto a small Petri dish.
- 10.4) Under a dissecting microscope, position larvae dorsal up.
- 10.5) When agarose has solidified, cut away the agarose with a thin razor blade (#11 scalpel), leaving a wedge of agar around the head.
- 10.6) Make two diagonal cuts at either side of the yolk; take care not to nick the larvae.
- 10.7) Fill the area surrounding the agarose with embryo/blue water.
- 10.8) Pull agarose away from the trunk and tail of the larva.

11) Prepare high-speed camera and imaging software

- 11.1) Mount high-speed camera onto dissecting scope.
- 11.2) Connect camera to computer.
- 11.3) Turn on computer.
- 11.4) Turn on high-speed camera.
- 11.5) Open video/imaging software (We use AOS imaging software and will describe procedures for using it here, but other imaging software is equally acceptable).
- 11.6) Adjust camera settings accordingly (i.e. 1000 frames per second (fps), 50% trigger buffer or other preferred settings).
- 11.7) Start recording.

12) Activate single neurons using a 473 nm laser

- 12.1) Attach stimulator, laser and optic cable.
- 12.2) Turn on stimulator.

- 12.3) Set stimulator to a maximum of 5 Volts and a pulse duration of 5 ms.
- 12.4) Turn on laser according to manufacturer's instructions.
- 12.5) Use fluorescent dissecting microscope to position tip of optic cable near cell body of a neuron with ChEF-tdTomato expression. (Figure 6A)
- 12.6) Deliver pulse of blue light to activate sensory neuron.
- 12.7) Record behavior using a high-speed camera set at 500 or 1000 frames per second.
- 12.8) Repeat experiment as desired, waiting 1 minute between each activation to avoid habituation. (We record a minimum of three responses for each neuron).
- 12.9) To release larvae, pry apart agarose with forceps, taking care not to injure the animal. This animal can be allowed to develop further and the procedure can be repeated at an older stage to characterize development of the behavior. The embryo can also be remounted for high-resolution confocal imaging of the activated cell to correlate behavior with cellular structure, as described below.
- 12.10) Transfer larvae to culture plate with fresh blue/embryo water. We use a 24-well plate to keep track of individual larvae.

13) Image neuron(s) with a confocal microscope

- 13.1) Anesthetize larvae with 0.02% tricaine
- 13.2) Mount larvae, dorsal side up, in 1.2% low melt agarose or in a dorsal mold
- 13.3) Image ChEF-tdTomato neurons with a 543 nm laser and appropriate filter and objective. We use a 20x objective.
- 13.4) Remove larvae from agarose and return to individual well with blue/embryo water.
- 13.5) Store at 28.5°C in the dark for further analysis.

Results/Discussion

We have described an approach for optogenetic activation of single RB neurons in live zebrafish. Our method employs transient transgenesis to express a fluorescently tagged channelrhodopsin variant, ChEF-tdTomato (Lin et al., 2009), in specific somatosensory neurons. This approach could easily be adapted for use in other larval zebrafish cell populations.

Using this approach we consistently elicited behavioral responses from 34-40 hpf larvae expressing ChEF-tdTomato. Using a 5 ms pulse of blue light at 5 V, we were able to activate single RB neurons (Figure 6). By positioning the optic fiber at different points along the animal, we found that it was necessary to aim the blue light directly at a cell body to elicit a behavioral response. Light pulses along the central axon or the peripheral axon never elicited a response, even in young larvae. This property was advantageous since we could confidently activate single neurons in animals in which multiple neurons were labeled, even if the central axons of other neurons passed near the targeted neuron's cell body.

To test the reliability of the approach for assessing kinematic parameters, we determined the latency of the escape response (the time from light activation to behavioral response) between 40 and 48 hpf, a parameter that is known to be highly stereotyped. To determine if the duration of light stimulus influences neuron activation, we illuminated target neurons for 5 or 10 ms (Figure 7A). Since the behavioral latency in both conditions were the same when calculated from the start of the light pulse, we concluded that the duration of the light pulse did not influence latency of behavior. However, we did find that reducing the voltage increased the latency of a behavior (Figure 7B). At 5 V, however, many responses (10 out of 16 fish) were 22.5 ± 6.5 ms, similar to the latency reported for natural escape responses (Figure 8). Thus, activating neurons with 5 V approaches maximal activation.

We analyzed 16 fish at approximately 35-40 hpf using the optimized parameters described above. While the majority of fish responded with a latency comparable to that reported for a natural escape response, 22.5 ± 6.5 ms, six of the sixteen fish responded within a range of 43-69 ms, and one sample resulted in an average latency of approximately 131 ms (Figure 8). Confocal images of these activated RB neurons showed that some fish had more than one RB neuron within the stimulated region. However, when we plotted the average behavior latency against the number of neurons within the stimulated region, we saw that both short (24.25 ± 8.25 ms) and long (60.5 ± 8.5 ms) latencies were evenly distributed between regions with single or multiple ChEF-tdTomato-expressing RB neurons (Figure 9). Due to the wide range in latencies that are independent of the number of RB neurons within the stimulated region, it is difficult to conclude whether or not two distinct behavior patterns exist that would correspond to the two central projection patterns we previously described. Furthermore, since we were unable to distinguish if individual RB neurons were Mauthner contacting or non-Mauthner contacting, it is still unknown whether these two distinct central axon projections elicit distinct behavior responses.

While we performed most of our analysis in younger larvae, we were also interested in characterizing behavioral responses in older animals. However, parameters for effectively eliciting behavioral responses from activating single RB neurons varied in older larvae. We successfully elicited behavioral responses from animals as old as 4.5 dpf, substantially later than was previously reported. But, while activation of single RB neurons with a 5 ms light pulse at 5 V consistently resulted in a behavioral response before 48 hpf, activation of older larvae (>60 hpf) was not as consistent. Longer pulses (10-100 ms) of light were often necessary to activate

neurons in 60 hpf larvae (Figure 10 and 11). Therefore, activation parameters may need to be optimized/calibrated based on experimental stage.

The approach we describe here could be used for many potential applications. We are using this method to define the behavioral responses elicited by different subtypes of neurons, but it could also be used to characterize the development of behavioral responses as the animal matures, the effects of drugs or mutants on behavior, or, in combination with physiology or imaging, to characterize downstream circuits activated by an identified neuron.

Acknowledgements

I would like to thank Fumi Kubo, Tod Thiele and Herwig Baier (UCSF/Max Planck Institute) for advice on behavior experiments and DPSS laser set up. Petronella Kettunen (University of Gothenburg) for initial collaboration on optogenetic experiments, Baljit Khakh, Eric Hudson, Mike Baca and John Milligan (UCLA) for technical advice, Roger Tsien (UCSD) for the ChEF-tdTomato construct, and Heesoo Kin and Chiara Cerri (Neurobiology course 2011, MBL) for their dedication to late night behavior movies.

References

- Burgess HA, Johnson SL, Granato M. 2009. Unidirectional startle responses and disrupted left-right co-ordination of motor behaviors in robo3 mutant zebrafish. *Genes Brain Behav* 8:500-511.
- Douglass AD, Kraves S, Deisseroth K, Schier AF, Engert F. 2008. Escape behavior elicited by single, channelrhodopsin-2-evoked spikes in zebrafish somatosensory neurons. *Curr Biol* 18:1133-1137.
- Downes GB, Granato M. 2006. Supraspinal input is dispensable to generate glycine-mediated locomotive behaviors in the zebrafish embryo. *J Neurobiol* 66:437-451.
- Drapeau P, Saint-Amant L, Buss RR, Chong M, McDearmid JR, Brustein E. 2002. Development of the locomotor network in zebrafish. *Prog Neurobiol* 68:85-111.
- Eisenhoffer GT, Rosenblatt J. 2011. Live imaging of cell extrusion from the epidermis of developing zebrafish. *J Vis Exp*.
- Graeden E, Sive H. 2009. Live imaging of the zebrafish embryonic brain by confocal microscopy. *J Vis Exp*.
- Kague E, Weber C, Fisher S. 2010. Mosaic zebrafish transgenesis for evaluating enhancer sequences. *J Vis Exp*.
- Kemp HA, Carmany-Rampey A, Moens C. 2009. Generating chimeric zebrafish embryos by transplantation. *J Vis Exp*.
- Kohashi T, Oda Y. 2008. Initiation of Mauthner- or non-Mauthner-mediated fast escape evoked by different modes of sensory input. *J Neurosci* 28:10641-10653.
- Korn H, Faber DS. 2005. The Mauthner cell half a century later: a neurobiological model for decision-making? *Neuron* 47:13-28.

- Lai SL, Lee T. 2006. Genetic mosaic with dual binary transcriptional systems in *Drosophila*. *Nat Neurosci* 9:703-709.
- Lin JY, Lin MZ, Steinbach P, Tsien RY. 2009. Characterization of engineered channelrhodopsin variants with improved properties and kinetics. *Biophys J* 96:1803-1814.
- Liu KS, Fetcho JR. 1999. Laser ablations reveal functional relationships of segmental hindbrain neurons in zebrafish. *Neuron* 23:325-335.
- Liu YC, Bailey I, Hale ME. 2012. Alternative startle motor patterns and behaviors in the larval zebrafish (*Danio rerio*). *J Comp Physiol A Neuroethol Sens Neural Behav Physiol* 198:11-24.
- Saint-Amant L, Drapeau P. 1998. Time course of the development of motor behaviors in the zebrafish embryo. *J Neurobiol* 37:622-632.
- Uemura O, Okada Y, Ando H, Guedj M, Higashijima S, Shimazaki T, Chino N, Okano H, Okamoto H. 2005. Comparative functional genomics revealed conservation and diversification of three enhancers of the *isl1* gene for motor and sensory neuron-specific expression. *Dev Biol* 278:587-606.
- Yuan S, Sun Z. 2009. Microinjection of mRNA and morpholino antisense oligonucleotides in zebrafish embryos. *J Vis Exp*.

Figures

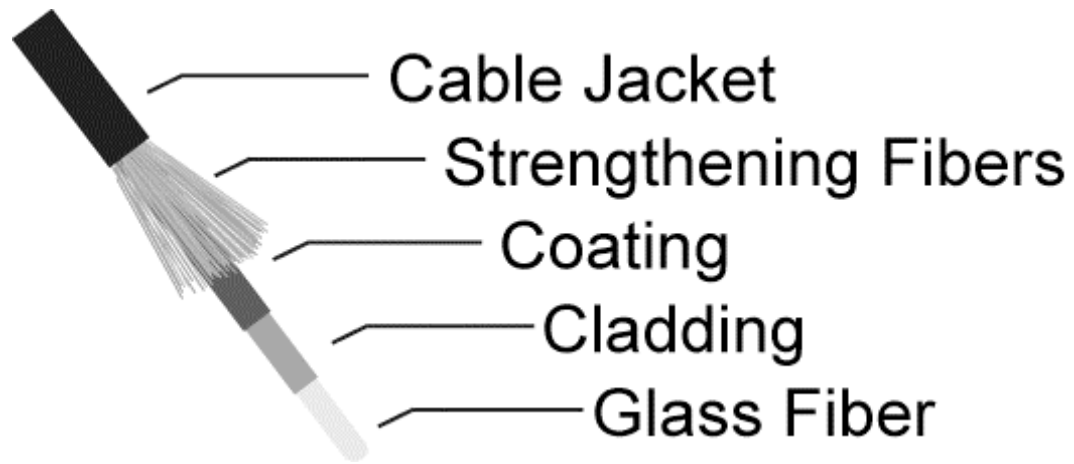


Figure 1. Layers of a fiber optic cable.

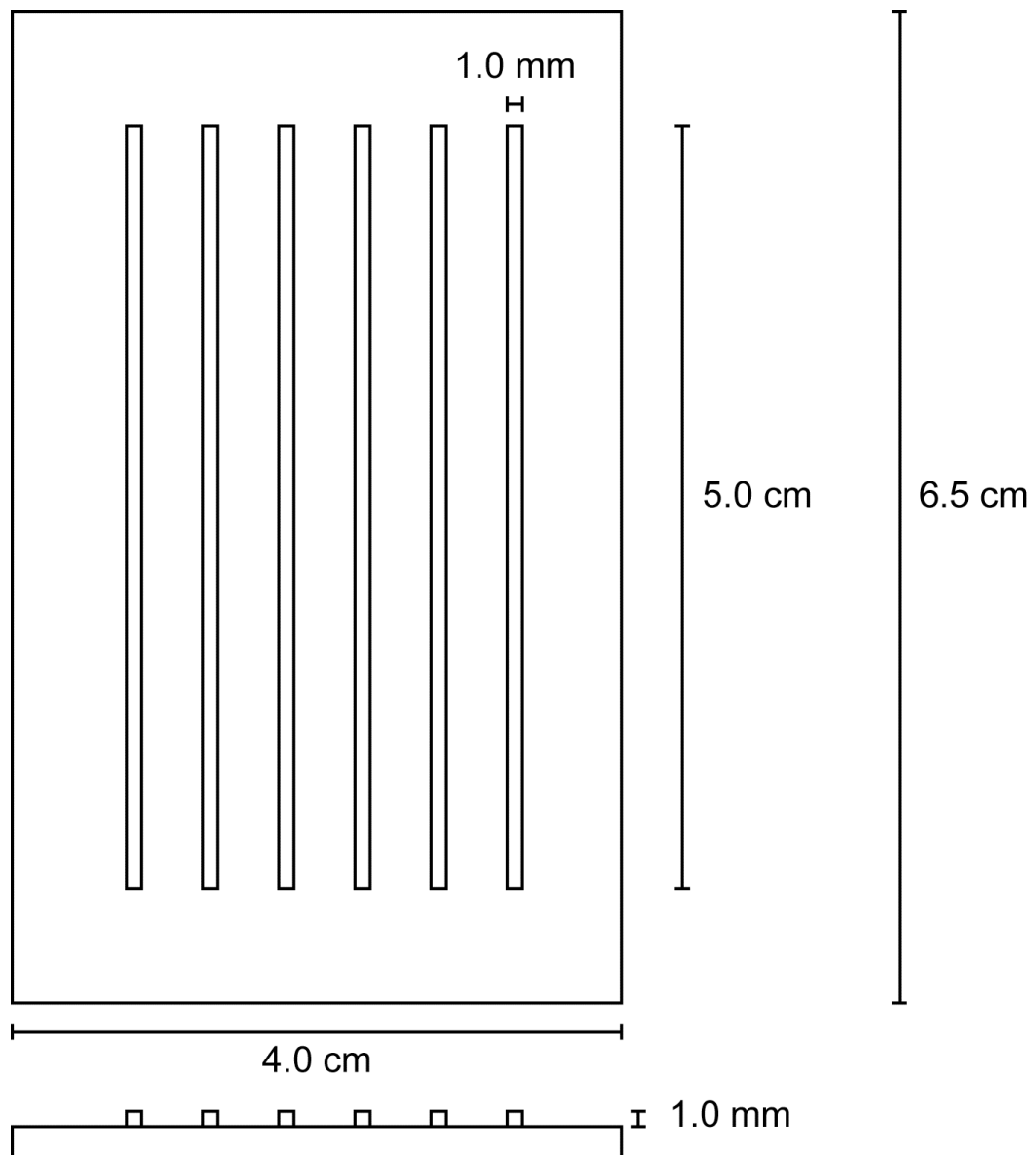


Figure 2. Injection mold template.

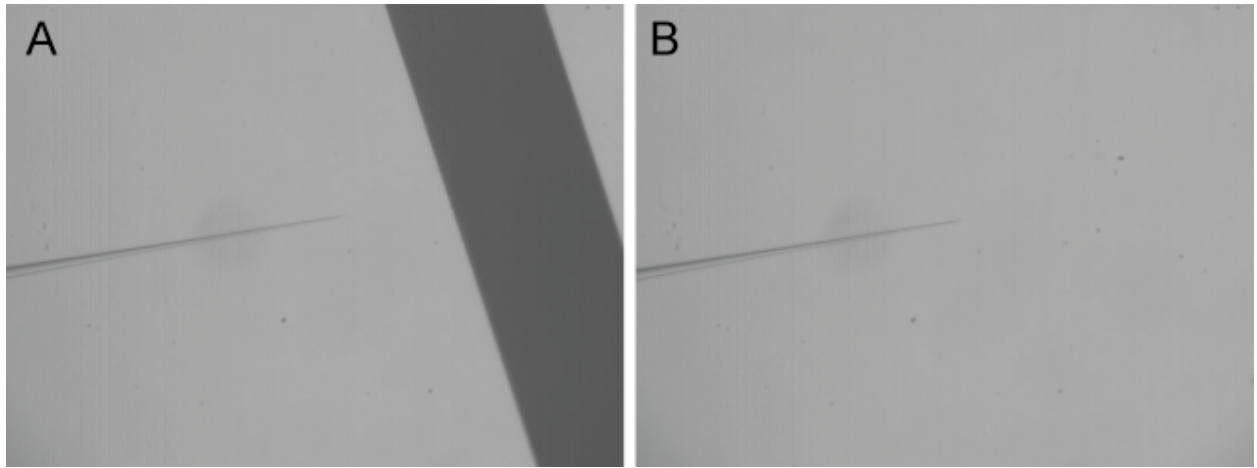


Figure 3. Breaking the needle.

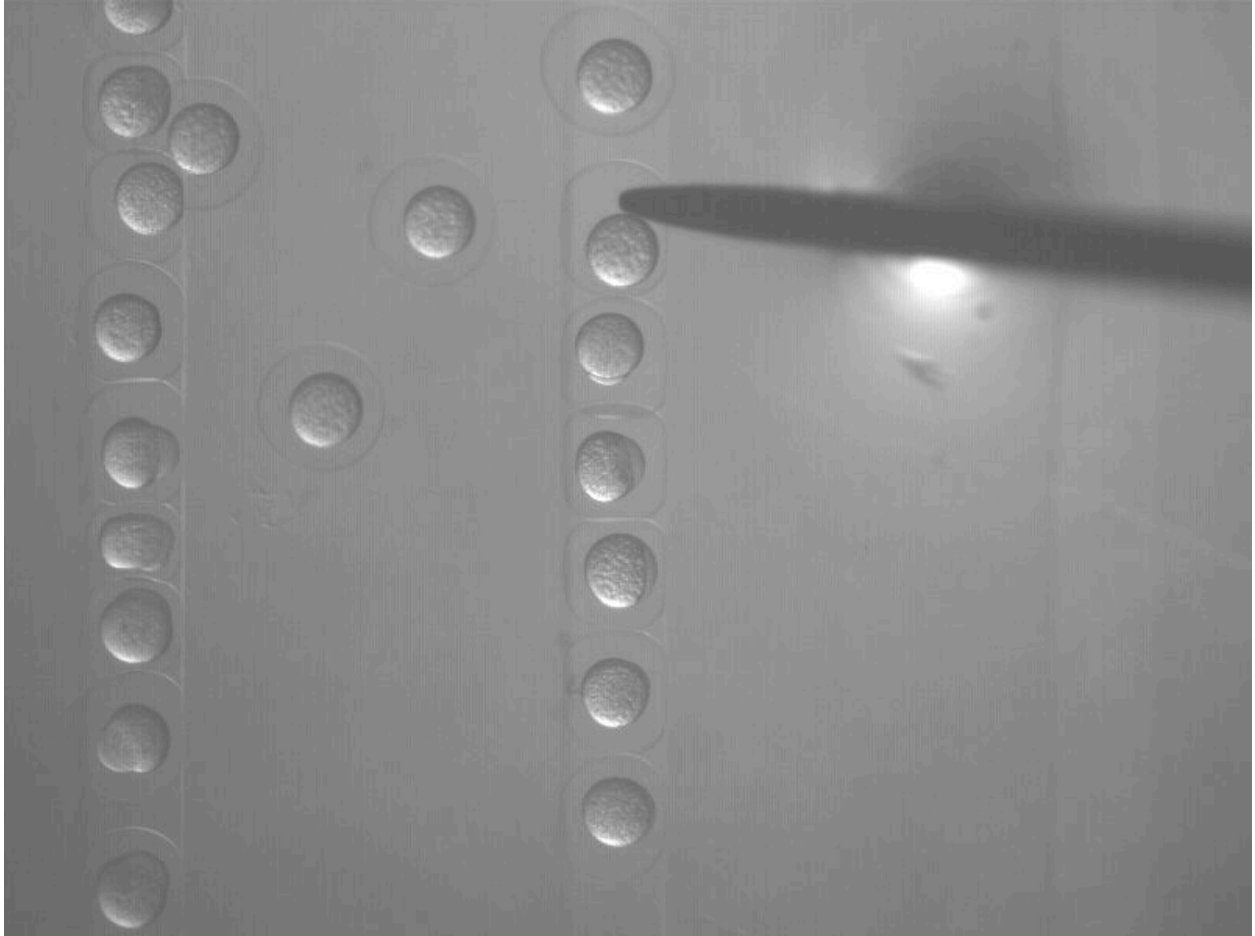


Figure 4. Placing embryos into the injection mold



Figure 5. Injecting 1 nl DNA mix into 1-cell stage embryo

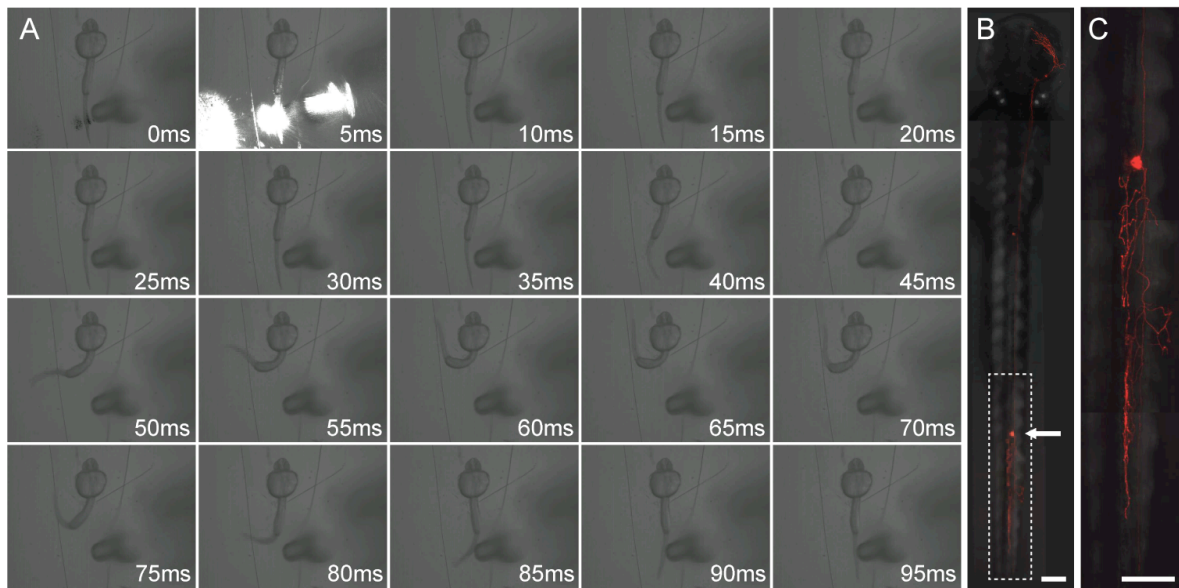


Figure 6. Activation of a single RB neuron expressing ChEF elicits a behavioral response.

(A) Still frames depicting activation of a single RB neuron expressing ChEF-tdTomato. Single neurons were activated by a 5 ms pulse from a 473 nm blue laser via a 200 μm fiber optic cable. Voltage driving the blue laser was set at a maximum of 5 volts. The resulting behavior was recorded at 1000 frames per second by a high-speed camera. (B) Confocal microscopy was used to image the activated RB neuron. Arrow shows region stimulated in behavior stills. (C) Magnified image of RB neuron indicated in (B). Scale bar, 100 μm .

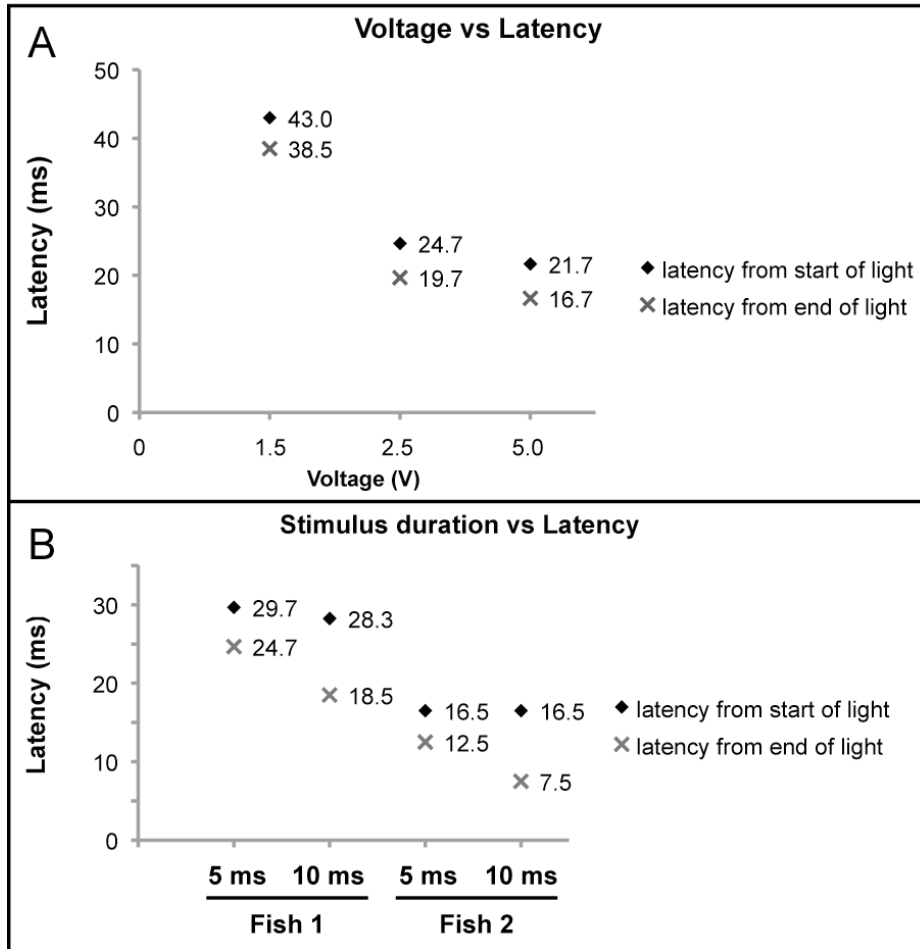


Figure 7. Latency of behavior under variable conditions. For most experiments we activated a single neuron in ~35 hpf larvae expressing ChEF-tdTomato with a 5 ms pulse from a 473 nm blue laser driven by a 5 V power source (Figure 6). To better understand the dynamics of ChEF activation, we varied parameters to determine their effect on behavior. (A) The duration of light stimulation (5 ms versus 10 ms) did not affect latency when quantified from start of light pulse. (B) At ~35 hpf, voltage inversely affects latency. Lower voltages resulted in an increase in latency of movement. For our experiments, we used the maximum voltage (5 V) permissible for our laser apparatus, which elicited reliably stereotyped behaviors from brightest-expressing RB neurons.

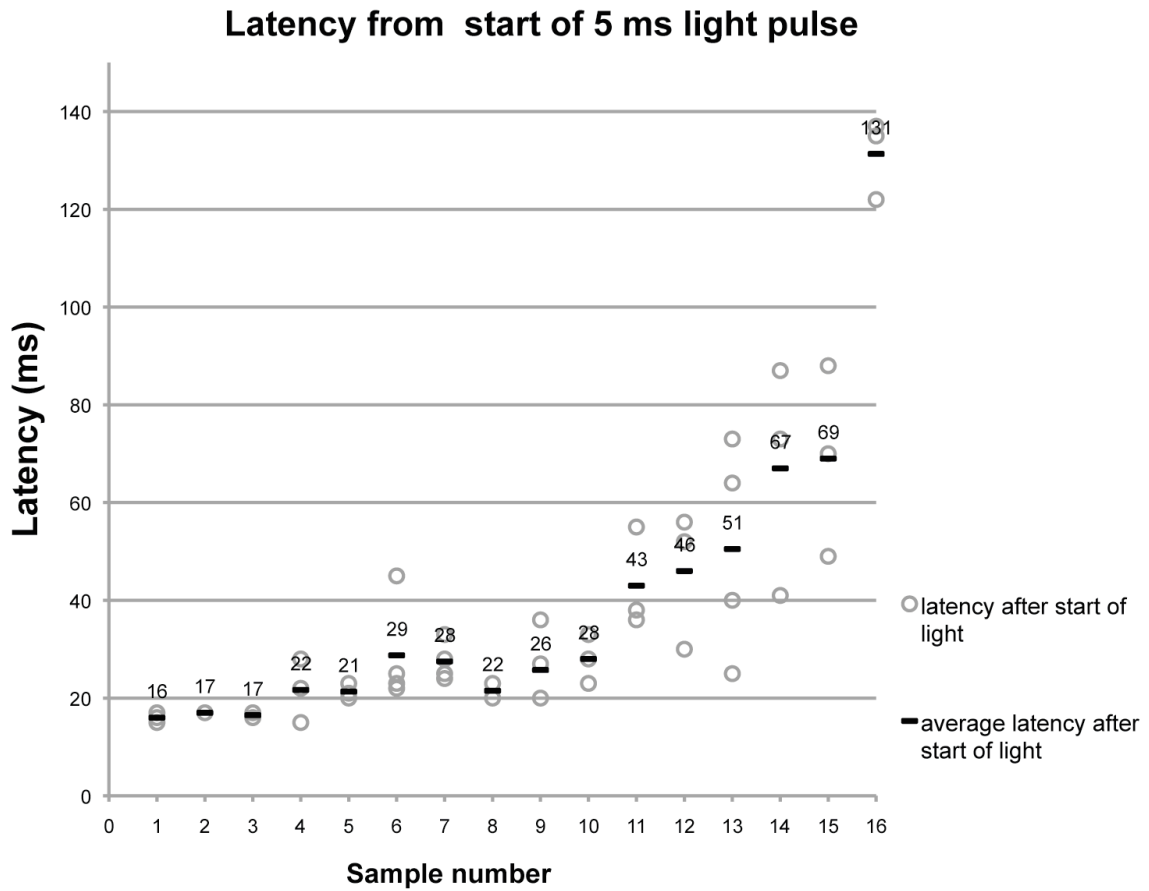


Figure 8. Latency of behavior in ~35 hpf larvae. Latency from each movie is plotted per fish (open circle). Average latency is indicated (bar). Samples with consistent latencies (samples 1-10) averaged $\sim 22.5 \pm 6.5$ ms. Less consistent samples (11-15) averaged $\sim 56 \pm 13$ ms. The longest latency ~ 131 ms, occurred least often.

Latency per number of neurons within stimulated region

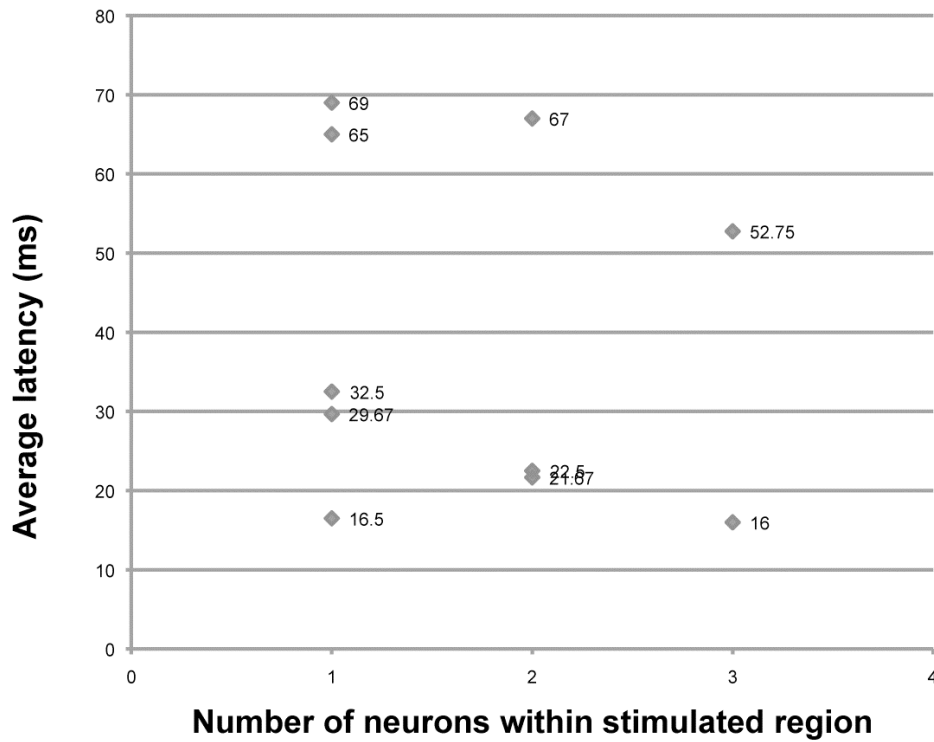


Figure 9. Average latency per number of neurons within stimulated region. Average behavior latency was plotted according to the number of RB cell bodies within the stimulated region, as visualized by confocal microscopy. Latency seemed to cluster into two groups, 24.25 ± 8.25 ms and 60.5 ± 8.5 ms, independent of the number of neurons within the stimulated region.

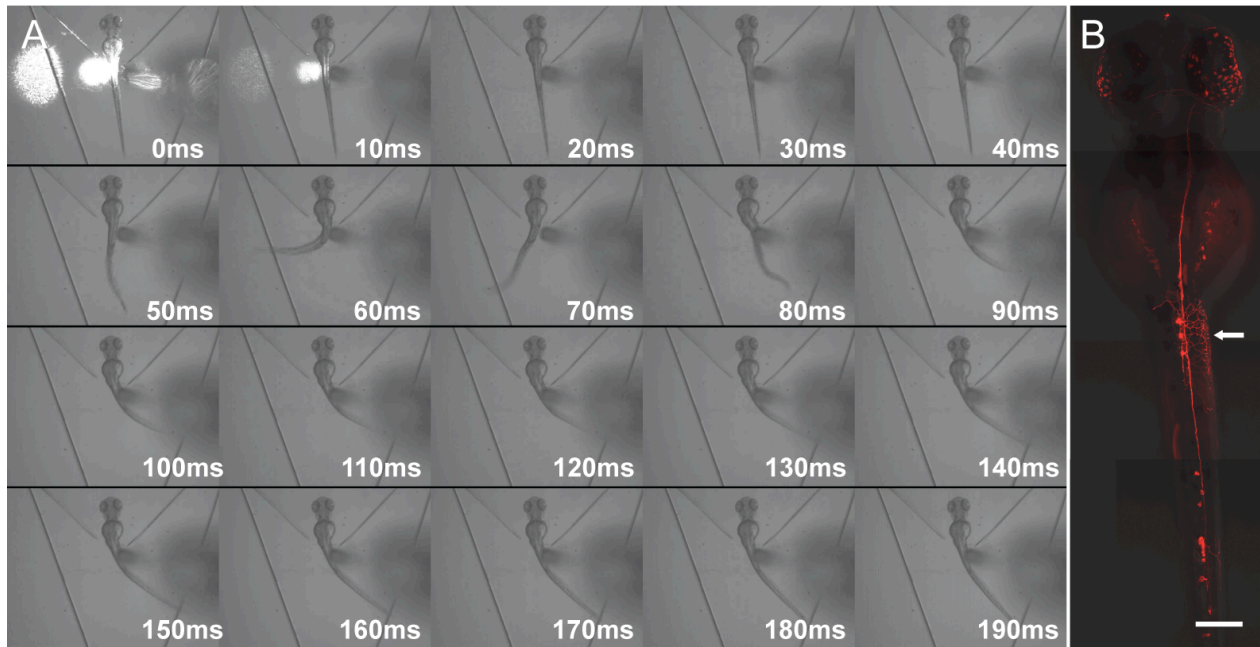


Figure 10. Activation of ChEF-tdTomato expressing RB neurons in 60 hpf larvae. (A) Still frames depicting activation of RB neurons expressing ChEF-tdTomato by a 10 ms pulse from a 473 nm blue laser via a 200 μm fiber optic cable. The resulting behavior was recorded at 1000 frames per second by a high-speed camera. (B) Confocal microscopy was used to image the activated RB neuron(s). Arrow shows region stimulated in behavior stills. Scale bar, 100 μm .

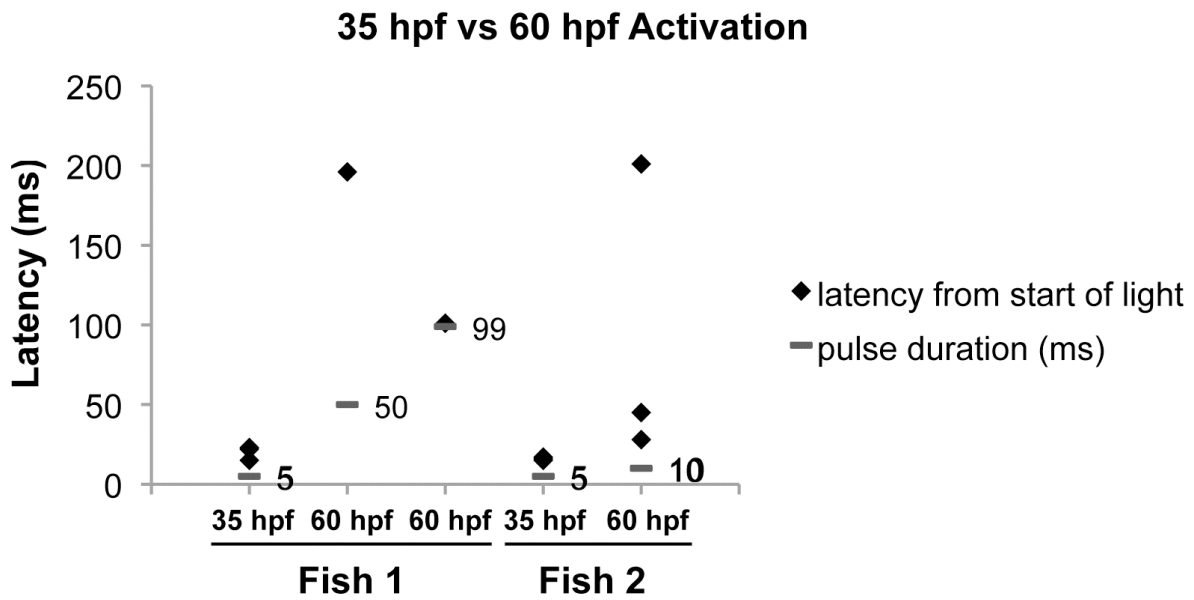


Figure 11. Activation of 60 hpf larvae required longer light stimuli compared to 35 hpf larvae. Activation of ChEF-expressing neurons at 60 hpf required a light stimulation of at least 10 ms and upwards of almost 100 ms.

Chapter 5
Concluding remarks

Identification and characterization of somatosensory neuron subtypes in larval zebrafish

Somatosensation is a vital aspect of life. The sense of touch plays an important role in basic survival mechanisms from humans to invertebrate animals (Anand, 1996; Julius and Basbaum, 2001; Tominaga and Caterina, 2004; Hwang and Oh, 2007; Tominaga, 2007). Behavioral responses and the neural circuitry involved in them have been studied over hundreds of years. From early classification of basic anatomy to the advent of optogenetics for studying neurons *in vivo* at a single cell level, great strides are being made in mapping specific neuronal networks. In zebrafish larvae trigeminal neurons in the head and Rohon-Beard neurons in the trunk and tail innervate the skin to detect various types of touch stimuli (Saint-Amant and Drapeau, 1998; Drapeau et al., 2002; O'Brien et al., 2012). Zebrafish respond to mechanical, thermal and chemical cues with a stereotyped escape response (O'Malley et al., 1996; Brustein et al., 2003; Kohashi and Oda, 2008; McHenry et al., 2009; Colwill and Creton, 2011). This behavior has long been described as a result of activating either of a pair of reticulospinal interneurons in the hindbrain called the Mauthner cells (Korn and Faber, 2005). In many organisms, somatosensory neurons can be categorized by their morphological, molecular as well as functional properties (Roberts, 1980; Blackshaw et al., 1982; Grueber et al., 2003; Lumpkin and Caterina, 2007; Marmigère and Ernfors, 2007). Advances in identifying molecular markers as well as improved optogenetic approaches (Douglass et al., 2008; Lin et al., 2009) are further improving our understanding of the mechanisms of somatosensation. In this study, we described a molecular subtype of somatosensory neurons, a morphological subtype, and an approach to further investigate the function of each of these subpopulations in zebrafish larvae.

Somatosensation is performed by a number of different types of neurons. Neurotrophin receptors and nociceptive channels are among the many genes expressed in various model

organisms (Lumpkin and Caterina, 2007). Using regions upstream of these specific genes, from either zebrafish or pufferfish, provided us with regulatory sequences that were used to drive expression of fluorescent transgenes in zebrafish somatosensory neurons. This method not only provided us with a transgenic tool for studying zebrafish neurons, but also demonstrated to us that these regulatory sequences are highly conserved from species to species and that the highly compact pufferfish genome serves as a useful source for future enhancer studies in zebrafish. Characterization of transgene activity revealed that these genomic sequences drove expression at various timepoints, hinting that these genes may have different regulatory mechanisms or highlight distinct populations of somatosensory neurons. Deletion analysis of several upstream regulatory regions identified minimal sequences necessary for expression in trigeminal and RB neurons. These minimal regulatory elements will not only be useful as a springboard for identifying putative transcription binding sites that might be involved in somatosensory specification, but also as more specific regulatory elements for driving temporal and cell-specific expression of any gene of interest.

PKC α , *p2rx3a* and *trpA1b* are expressed in a subset of somatosensory neurons in larval zebrafish (Slatter et al., 2005; Kucenas et al., 2006; Patten et al., 2007; Pan et al., 2012). *PKC α* is a kinase that functions in diverse signaling pathways, *P2rx3a* is an ATP-gated ion channel involved in nociception, and *TrpA1b* is a channel that is activated by pungent chemicals (Caron et al., 2008; Prober et al., 2008; Pan et al., 2012). From previous reports by Prober et. al., *trpA1b*-expressing neurons are required for detecting noxious chemical stimuli such as mustard oil, but may not be required for detection of thermal or mechanical stimuli. This study, however, used the lateral line system to determine the effects of *TrpA1a* and *TrpA1b* on mechanosensation, so *TrpA1a* and *TrpA1b* function in trigeminal and RB neurons has yet to be

determined. A more comprehensive functional characterization of this subtype can be performed by expressing GCaMP in somatosensory neurons and determining what stimuli activates neurons of the PKC α /*p2rx3a/trpA1b*-expressing neurons versus non-PKC α /*p2rx3a/trpA1b*-expressing neurons. Conversely, genetic/chemical or laser ablations of the PKC α /*p2rx3a/trpA1b* subset of neurons could be used for loss of function assays. The PKC α gene trap line was designed using a cassette that can be flipped to generate a fluorescently labeled mutant allele, ideally knocking out PKC α function completely in all PKC α -expressing neurons. This would help elucidate PKC α function in somatosensory neuron development. *Tg(Fru.p2x3-2:LexA:mCherry)* utilizes the LexA-LexAop binary expression system, therefore co-expression of a pro-drug dependent system, such as the nitroreductase enzyme *nsfB*, could be used to genetically/chemically ablate this specific population of sensory neurons. A quicker, though more laborious approach would be to perform 2-photon laser ablations of fluorescently labeled trigeminal and/or RB neurons labeled by any of the three transgenic lines, PKC α ^{ct7a}, *Tg(Fru.p2x3-2:LexA:mCherry)* or *Tg(trpA1b:EGFP)*. Any of these approaches could be used to identify the specific function of PKC α /*p2rx3a/trpA1b*-expressing versus non-PKC α /*p2rx3a/trpA1b*-expressing neurons.

Having identified different subsets of somatosensory neurons in zebrafish larvae, it would be interesting to perform a complete molecular and functional profile of each and to determine if distinct subtypes activate different neural networks. Recent advancements in our lab have enabled us to create an RNAseq profile on any fluorescently labeled population of cells in zebrafish. Initial studies using fluorescently labeled skin cells have provided us with an extensive list of genes expressed in that specific cell population. Using similar techniques, we have proposed to create a molecular profile of fluorescently labeled sensory neurons, in lines that label all sensory neurons, as well as lines that label only a subset of trigeminal and RB neurons.

Isolation of sensory neurons is a little more complicated than skin cells, since there are significantly less sensory neurons than skin cells in zebrafish. However, this could be easily overcome by proportionally increasing the number of larvae sampled. One complication with this experiment, however, is the expression of fluorescence in cell types that are neither trigeminal nor RB neurons. For example, in *Tg(Fru.p2x3-2:LexA:mCherry)*, fluorescence expression in the heart, muscle along the tail and in unidentified cells along the caudal fin, would result in false positive genes. In order to overcome this hurdle, it might be imperative to create molecular profiles for all of the transgenic lines we have characterized and compare them to each other. Genes from non-somatosensory cells within each line would theoretically cancel out.

Defining subtype specific neural networks

The zebrafish escape behavior has long been attributed to the activation of the Mauthner cells. Over the years, however, studies have described escape behaviors that are Mauthner-independent. Zebrafish larvae with laser-ablated Mauthner cells still respond to touch, though their latency of behavior is increased. This longer latency response has been attributed to activation of the Mauthner cell homologues (Liu and Fetcho, 1999). Further evidence of Mauthner-independent touch response came from analysis of lesioned larvae as well as in tail preps (Korn and Faber, 2005). In these cases, physical removal of contact with the Mauthner cell and its homologues, in addition to complete decapitation indicate that there must be a local circuit within the spinal cord that mediates this response (Liu and Fetcho, 1999; Downes and Granato, 2006; Kohashi and Oda, 2008; Burgess et al., 2009; Liu et al., 2012). In our study, we provide ample evidence that most RB neurons at early larval stages do not contact the Mauthner cell dendrite (Palanca et al., 2012). We also optimized a previously published optogenetic

approach to further investigate the role of non-Mauthner contacting RB neurons. Using this approach, we proposed to see if Mauthner dendrite-contacting and non-Mauthner dendrite-contacting RB neurons elicited distinct motor responses. From initial studies, there does not seem to be a distinction, however, analysis using a transgenic line that labels the Mauthner cells would need to be performed. This approach was also able to extend the activation time to well beyond that previously published (from less than 48 hpf to up to at least 4 dpf). Therefore, behavior responses can be monitored at later larval stages, when more sophisticated neural networks and motor behaviors have developed. Furthermore, by transgenically or retrogradely labeling interneurons with a calcium indicator, one could map the neuronal networks activated by individual RB neurons.

The findings and approaches described in these studies provide useful tools for further characterization and manipulation of somatosensory neurons subtypes in larval zebrafish. Furthermore, using subtype specific transgenes in combination with recently optimized optogenetics and calcium imaging techniques could provide a more comprehensive map of subtype-specific somatosensory neuron networks.

Ultimately, a thorough characterization of larval zebrafish somatosensation may provide insight into human fetal somatosensation as well as the development of peripheral neuropathies. Parallels between these organisms present a useful tool for understanding somatosensory circuits and how specific disruptions within the neural circuitry affect development, sensory recognition and processing. Identification and manipulation of specific somatosensory pathways in larval zebrafish would, therefore, provide an entry point for studying potential therapeutic reagents and treatments for complex peripheral neuropathies in humans.

References

- Anand P. 1996. Neurotrophins and peripheral neuropathy. *Philos Trans R Soc Lond B Biol Sci* 351:449-454.
- Blackshaw SE, Nicholls JG, Parnas I. 1982. Expanded receptive fields of cutaneous mechanoreceptor cells after single neurone deletion in leech central nervous system. *J Physiol* 326:261-268.
- Brustein E, Marandi N, Kovalchuk Y, Drapeau P, Konnerth A. 2003. "In vivo" monitoring of neuronal network activity in zebrafish by two-photon Ca(2+) imaging. *Pflugers Arch* 446:766-773.
- Burgess HA, Johnson SL, Granato M. 2009. Unidirectional startle responses and disrupted left-right co-ordination of motor behaviors in robo3 mutant zebrafish. *Genes Brain Behav* 8:500-511.
- Caron SJ, Prober D, Choy M, Schier AF. 2008. In vivo birthdating by BAPTISM reveals that trigeminal sensory neuron diversity depends on early neurogenesis. *Development* 135:3259-3269.
- Colwill RM, Creton R. 2011. Imaging escape and avoidance behavior in zebrafish larvae. *Rev Neurosci* 22:63-73.
- Douglass AD, Kraves S, Deisseroth K, Schier AF, Engert F. 2008. Escape behavior elicited by single, channelrhodopsin-2-evoked spikes in zebrafish somatosensory neurons. *Curr Biol* 18:1133-1137.
- Downes GB, Granato M. 2006. Supraspinal input is dispensable to generate glycine-mediated locomotive behaviors in the zebrafish embryo. *J Neurobiol* 66:437-451.

- Drapeau P, Saint-Amant L, Buss RR, Chong M, McDearmid JR, Brustein E. 2002. Development of the locomotor network in zebrafish. *Prog Neurobiol* 68:85-111.
- Grueber WB, Ye B, Moore AW, Jan LY, Jan YN. 2003. Dendrites of distinct classes of *Drosophila* sensory neurons show different capacities for homotypic repulsion. *Curr Biol* 13:618-626.
- Hwang SW, Oh U. 2007. Current concepts of nociception: nociceptive molecular sensors in sensory neurons. *Curr Opin Anaesthesiol* 20:427-434.
- Julius D, Basbaum AI. 2001. Molecular mechanisms of nociception. *Nature* 413:203-210.
- Kohashi T, Oda Y. 2008. Initiation of Mauthner- or non-Mauthner-mediated fast escape evoked by different modes of sensory input. *J Neurosci* 28:10641-10653.
- Korn H, Faber DS. 2005. The Mauthner cell half a century later: a neurobiological model for decision-making? *Neuron* 47:13-28.
- Kucenas S, Soto F, Cox JA, Voigt MM. 2006. Selective labeling of central and peripheral sensory neurons in the developing zebrafish using P2X(3) receptor subunit transgenes. *Neuroscience* 138:641-652.
- Lin JY, Lin MZ, Steinbach P, Tsien RY. 2009. Characterization of engineered channelrhodopsin variants with improved properties and kinetics. *Biophys J* 96:1803-1814.
- Liu KS, Fetcho JR. 1999. Laser ablations reveal functional relationships of segmental hindbrain neurons in zebrafish. *Neuron* 23:325-335.
- Liu YC, Bailey I, Hale ME. 2012. Alternative startle motor patterns and behaviors in the larval zebrafish (*Danio rerio*). *J Comp Physiol A Neuroethol Sens Neural Behav Physiol* 198:11-24.

- Lumpkin EA, Caterina MJ. 2007. Mechanisms of sensory transduction in the skin. *Nature* 445:858-865.
- Marmigère F, Ernfors P. 2007. Specification and connectivity of neuronal subtypes in the sensory lineage. *Nat Rev Neurosci* 8:114-127.
- McHenry MJ, Feitl KE, Strother JA, Van Trump WJ. 2009. Larval zebrafish rapidly sense the water flow of a predator's strike. *Biol Lett* 5:477-479.
- O'Brien GS, Rieger S, Wang F, Smolen GA, Gonzalez RE, Buchanan J, Sagasti A. 2012. Coordinate development of skin cells and cutaneous sensory axons in zebrafish. *J Comp Neurol* 520:816-831.
- O'Malley DM, Kao YH, Fetcho JR. 1996. Imaging the functional organization of zebrafish hindbrain segments during escape behaviors. *Neuron* 17:1145-1155.
- Palanca AM, Lee SL, Yee LE, Joe-Wong C, Trinh LA, Hiroyasu E, Husain M, Fraser SE, Pellegrini M, Sagasti A. 2012. New transgenic reporters identify somatosensory neuron subtypes in larval zebrafish. *Dev Neurobiol*.
- Pan YA, Choy M, Prober DA, Schier AF. 2012. Robo2 determines subtype-specific axonal projections of trigeminal sensory neurons. *Development* 139:591-600.
- Patten SA, Sihra RK, Dhimi KS, Coutts CA, Ali DW. 2007. Differential expression of PKC isoforms in developing zebrafish. *Int J Dev Neurosci* 25:155-164.
- Prober DA, Zimmerman S, Myers BR, McDermott BM, Kim SH, Caron S, Rihel J, Solnica-Krezel L, Julius D, Hudspeth AJ, Schier AF. 2008. Zebrafish TRPA1 channels are required for chemosensation but not for thermosensation or mechanosensory hair cell function. *J Neurosci* 28:10102-10110.

- Roberts A. 1980. The function and role of two types of mechanoreceptive "free" nerve endings in the head skin of amphibian embryos. *Journal of Comparative Physiology* 135:341-348.
- Saint-Amant L, Drapeau P. 1998. Time course of the development of motor behaviors in the zebrafish embryo. *J Neurobiol* 37:622-632.
- Slatter CA, Kanji H, Coutts CA, Ali DW. 2005. Expression of PKC in the developing zebrafish, *Danio rerio*. *J Neurobiol* 62:425-438.
- Tominaga M. 2007. Nociception and TRP channels. *Handb Exp Pharmacol*:489-505.
- Tominaga M, Caterina MJ. 2004. Thermosensation and pain. *J Neurobiol* 61:3-12.